Characterization of Molecular Systems and Monitoring of Chemical Reactions in Ionic Liquids by Nuclear Magnetic Resonance Spectroscopy

Valentine P. Ananikov*

Zelinsky Institute of Organic Chemistry, Russian Academy of Sciences, Leninsky Prospekt 47, Moscow 119991, Russia

Received February 18, 2009

Contents

1. Introduction

Recent development has shown that ionic liquids (ILs) have emerged as very attractive media for performing chemical reactions with a well-established potential in the context of Green Chemical synthesis. The widespread applications using ILs are governed by the unique combination of their physical properties: essentially no vapor pressure; excellent thermal stability; good solubility covering a wide range of inorganic, organic, organometallic, and polymeric substances in ILs; potential to be reused and recycled; high polarity; and weak coordination affinity.

Today the scope of applications involving ILs ranges far beyond the boundaries of being just a convenient "alternative" solvent. Their essential role in controlling both the direction and selectivity of chemical reactions as well as their important function in catalytic activity have all been demonstrated for numerous important reactions as well as industrially important processes. The most outstanding feature of ILs is highlighted by their ability to tune their physical and chemical properties by varying the structures of both the anion and cation. The structural diversity of potential cations and anions is further increased due to the variety of possible permutations and combinations. This proved an important prerequisite for the exponential growth in successful IL applications in recent years and ensures further future developments in this fascinating field.

Several excellent reviews have been published describing the preparation of ILs and their applications in modern chemistry.[1−7] Some of the special topics involving the role of ILs covered are as follows: catalysis,[8−11] Pd-catalyzed reactions,[12,13] hydroformylation,[14] heterocyclic chemistry,[15] chiral ILs,[16,17] chemical and biochemical transformations in

Valentine Ananikov received his Ph.D. degree in 1999 and his Habilitation in 2003, and in 2005 he was appointed Professor and Laboratory Head of the ND Zelinsky Institute of Organic Chemistry, The Russian Academy of Sciences. He was a recipient of the Russian State Prize for Outstanding Achievements in Science and Technology (2004), an Award of the Science Support Foundation (2005), and a Medal of the Russian Academy of Sciences (2000). His research has been supported by grants from the President of Russia (2004, 2007). He is a member of the International Advisory Boards of *Organometallics* and *Chemistry: An Asian Journal*. In 2008 he was elected as a Member of Russian Academy of Sciences. His scientific interests are focused on (i) transition metal catalyzed reactions, (ii) development of new NMR methods, and (iii) mechanistic studies of catalytic reactions.

* E-mail: val@ioc.ac.ru. Fax: +007 (499) 1355328

10.1021/cr9000644
Published on Web 10/25/2010

ILs,[18−22] enzyme catalysis in ILs,[23,24] molecular structure of ILs,[25,26] properties and applications of protic ILs,[27] electrochemical reactivity and voltammetry,[28−30] spectroscopy,[31,32] industrial chemistry and related applications,[33−36] macromolecules,[37,38] synthesis of nanomaterials,[39] inorganic complexes,[40] and chemistry of the f-elements.[41]

Despite the ongoing wide interest in ILs, some important unanswered questions remain regarding the mechanisms of chemical reactions in ILs, catalyst stability and decomposition pathways, and the nature of the solvent−solute interactions. In addition, the structural changes caused by solvation as well as the mechanism of in situ catalyst formation remain unclear. Mechanistic and structural studies carried out directly in ILs encounter significant difficulties due to the lack of general and efficient analytical techniques such as, for example, NMR spectroscopy in regular organic solvents. The unique properties of ILs highlight the urgent need for the development of such an analytical method for both the characterization of complex molecular systems and the direct monitoring of chemical reactions in ILs. Undoubtedly, the ability to access an appropriate analytical tool for in situ studies will greatly facilitate both the future research progress and their application in industry.

There is a common belief that NMR measurements in ILs are virtually impossible due to the dissipation of radiofrequency pulses caused by the strong ionic character of the media as well as the unacceptable resolution arising from the high viscosity and reduced molecular tumbling. However, as will be shown in this review, NMR spectra of acceptable quality can be recorded directly in ILs using routinely available hardware. Proton and heteronuclear spectra, as well as two-dimensional experiments, can be carried out in ILs after appropriate spectral parameters adjustment.

It should be noted that in the present review no attempt has been made to cover all aspects of spectroscopic studies in ILs. NMR studies of ILs performed in regular organic solvents, in dilute solutions (or with deuterium solvent additives), and in other non-native systems are beyond the scope of this review. These topics have been addressed in excellent reviews by Giernoth and co-workers.[31,32] Instead, discussion here will be limited to results achieved using NMR spectroscopy in *native* IL systems. As will be shown later, even a small dilution of ILs with regular organic solvents can dramatically change both their solvating and chemical properties. Therefore, structural and mechanistic studies must be performed in exactly the same media as that in which the actual chemical reaction occurs: no additives for the purpose of spectral measurements should be used. The present review provides the necessary information for understanding what NMR studies can be performed in *native* IL systems and what kinds of chemical information can be acquired. In this review, the application of NMR spectroscopy in ILs will be analyzed and discussed with an emphasis on the practical requirements needed to solve both structural and mechanistic problems.

2. Chemical Applications of NMR Spectroscopy in Native ILs Systems

The structures of the anions and cations of ILs, together with common abbreviations cited in the present review, are given in Figure 1. The summary of chemical applications of NMR spectroscopy in ILs is provided in this chapter, and the topics related to the high-performance NMR measurements in ILs will be discussed in sections 3 and 4.

2.1. Structure and Dynamics of Neat Ionic Liquids

In general, NMR measurements of ^{1}H, ^{11}B, ^{13}C, ^{19}F, and ^{31}P spectra are easy to carry out using commercially available NMR machines equipped with superconducting magnets from 200 to 750 MHz (in ^{1}H resonance). The spectra of neat ILs can be measured very rapidly for the above nuclei using a single scan in many cases. In the present section, ^{1}H NMR studies will be covered first, followed by heteronuclear spectroscopy, diffusion measurements, and relaxation studies. Finally, two-dimensional experiments carried out using neat ILs will be discussed with the view of the possible insights into the structure of ILs they might reveal.

A structural study of the [HMIM][HBr_2] moiety—the IL-containing protic cation [HMIM]$^+$—was carried out by Driver and Johnson using variable-temperature ^{1}H NMR. The results indicated that the ionic protic species were not chemically exchanged over the 24−94 °C temperature range studied.[42] At high temperatures, the N−H signal presented as a broad triplet in the ^{1}H NMR spectrum due to spin−spin coupling with the ^{14}N nucleus (spin = 1). The authors concluded that slow molecular motion and more efficient relaxation of the quadrupole moment/electric field gradient interaction leads to the disappearance of the triplet structure at lower temperatures. This was an important issue deserving some attention, since the presence of multiple lines may also be confused with chemical exchange. In contrast to the cation, where no chemical exchange was found, the authors reported the dynamic nature of the anionic part of the IL due to the following equilibrium:

$$Br^- + H_2Br_3^- = 2HB_2^-$$

The ^{1}H chemical shift observed for the acidic proton $\delta(^1H) = 5.44$ ppm in the neat IL had an intermediate value between the chemical shifts expected for the HBr_2^- and $H_2Br_3^-$ anions $\delta(^1H) = 10.2$ and 3.7 ppm, respectively.[42] Thus, a more correct representation of the IL at room temperature would involve an equilibrium mixture of the [HMIM]$^+$ cation and Br^-, as well as the HBr_2^- and $H_2Br_3^-$ anions.[42] Interestingly, the formation of dimeric and oligomeric anions such as $[(AcO)_xH_{x-1}]^-$ containing acetic acid molecules stabilized by hydrogen bonds was also observed and studied with ^{1}H NMR.[43]

The ^{1}H chemical shifts of the hydrogen atoms of the imidazolium cation measured in neat ILs were studied by Bagno, Chiappe, and co-workers in order to simplify the analysis of the cation−anion hydrogen bond interactions based on NMR data.[44] Under such conditions, the contributions of solvent and concentration effects were avoided, thus providing more reliable ^{1}H chemical shifts. A series of trihalide-based [HMIM][X] and [BMIM][X] ([X] = $[ICl_2]^-$, $[I_2Cl]^-$, $[Br_3]^-$, $[IBr_2]^-$) ILs were studied in a neat state, as well as in diluted solutions, and their relative hydrogen-bonding abilities were estimated.[44,45] An NMR study showed that addition of the halogens did not initiate any modifications in the cationic ring and it demonstrated a decrease in the basicity of the anion.

A combination of variable-temperature ^{1}H NMR and IR studies was used by Johnson and co-workers to determine the minimum values of the formation constants for the HCl_2^- and $H_2Cl_3^-$ species (10^4−10^5 and 5×10^2 L M^{-1}, respectively) in the IL [EMIM][HCl_2].[46] Analysis of the variable-temperature NMR data provided thermody-

Cations:

Type	Abbreviation	R_1	R_2	R_3
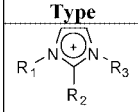	$[BEIM]^+$	C_4H_9	H	C_2H_5
	$[BMIM]^+$	C_4H_9	H	CH_3
	$[BMMIM]^+$	C_4H_9	CH_3	CH_3
	$[C_{10}MIM]^-$	$C_{10}H_{21}$	H	CH_3
	$[EMIM]^+$	C_2H_5	H	CH_3
	$[HBIM]^+$	H	H	C_4H_9
	$[HexMIM]^+$	C_6H_{13}	H	CH_3
	$[HIM]^+$	H	H	H
	$[HMIM]^+$	H	H	CH_3
	$[MBMIM]^+$	$CH_3CH_2CH(CH_3)CH_2$-	H	CH_3
	$[MMIM]^+$	CH_3	H	CH_3
	$[MNIM]^-$	CH_3	H	C_9H_{19}
	$[NpMIM]^+$	$(CH_3)_3CCH_2$-	H	CH_3
	$[OMIM]^+$	C_8H_{17}	H	CH_3
	$[PMIM]^+$	C_3H_7	H	CH_3
	$[(SiC_3)MIM]^+$	$(RO)_3Si(CH_2)_2CH_2$-	H	CH_3
	$[(SiC_3)BIM]^+$	$(RO)_3Si(CH_2)_2CH_2$-	H	C_4H_9
	$[SiMIM]^+$	$(CH_3)_3SiCH_2$-	H	CH_3
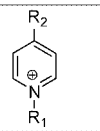	$[BMPy]^+$	C_4H_9	CH_3	-
	$[BPy]^+$	C_4H_9	H	-
	$[EPy]^+$	C_2H_5	H	-
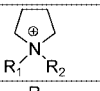	$[BMPyrr]^+$	C_4H_9	CH_3	-
	$[MPPyrr]^-$	C_3H_7	CH_3	-
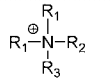	$[DEME]^+$	C_2H_5	CH_3	$CH_3OCH_2CH_2$-
	$[Me_3BuN]^+$	CH_3	C_4H_9	CH_3
	$[Me_4N]^+$	CH_3	CH_3	CH_3
	$[Et_3HN]^+$	C_2H_5	C_2H_5	H

Anions:

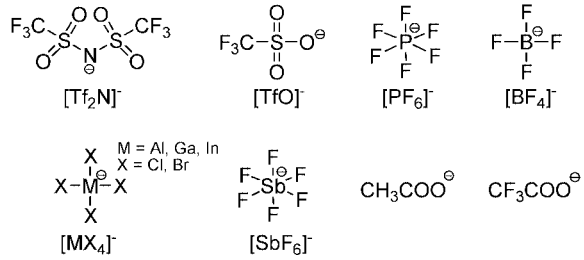

Figure 1. Structures of cations and anions of commonly used ILs.

namic parameters with good precision for the reaction below, $\Delta H = -22.8 \pm 1.0$ kJ mol^{-1} and $\Delta S = -31.8 \pm 2.9$ J K^{-1} mol^{-1}:

$$H_2Cl_3^- + Cl^- = 2HCl_2^-$$

Depending on the nature of intramolecular interactions they were involved in, a chemical shift change for the $[EMIM]^+$ protons was also reported by the authors. The same authors reported a ^{1}H NMR study that measured a stoichiometric equilibrium constant of 218 ± 25 for this reaction.[47]

An NMR observation of the species was used to construct a phase diagram for the ternary system HCl/[EMIM][Cl]/$AlCl_3$. ^{1}H NMR has proven to be a reliable tool for the estimation of the electronegativity of aluminum for the $[BMIM][AlEt_xCl_{4-x}]$ ($x = 1-3$) IL system[48] based on the modified Dailey−Shoolery equation[49] and ^{1}H chemical shifts. The method is also applicable for estimating the Lewis acidity of the $Al(Alk)_xCl_y$-based salts (Alk = alkyl group).

A ^{13}C NMR spectroscopy study was carried out by Wilkes, Frye, and Reynolds to characterize the cation−anion interactions in $[EMIM][AlCl_4]$.[50] Five possible environments of the cation were assumed to affect the ^{13}C chemical shifts; the greatest change was observed for the C-2 resonance of the carbon atom located between the nitrogens. It was reported that the observed chemical shift reflects an average value weighted by the mole fraction of each component. The chemical shifts attributed to each of the contributing species were estimated using a least-squares fit procedure. The ^{27}Al NMR spectrum for this IL showed the presence of two signals that were assigned to $[AlCl_4]^-$ and $[Al_2Cl_7]^-$. The effect of chemical exchange was observed between the aluminum species. It was characterized using variable-temperature NMR and a two-site chemical exchange simulation.[50] The composition dependence of the relaxation rates, the nature of the chemical exchange, and the relative concentrations of the $[AlCl_4]^-$, $[Al_2Cl_7]^-$, $[Al_3Cl_{10}]^-$, and Al_2Cl_6 species were also determined by ^{27}Al NMR.[51]

A combination of ^{1}H and ^{13}C NMR was utilized to establish the anion dependence of the cation−anion bond strength in neat ILs.[52] A linear correlation was observed between the ion-pair stabilization energies (calculated theoretically at the B3LYP/Lanl2DZp level) and ^{1}H and ^{13}C chemical shifts of the proton and carbon in position 2 of the imidazolium ring. The strongest and the weakest cation−anion interactions were found for the $[EMIM][Et_2PO_4]$ and $[EMIM][Tf_2N]$ ILs, respectively. Measurements were also

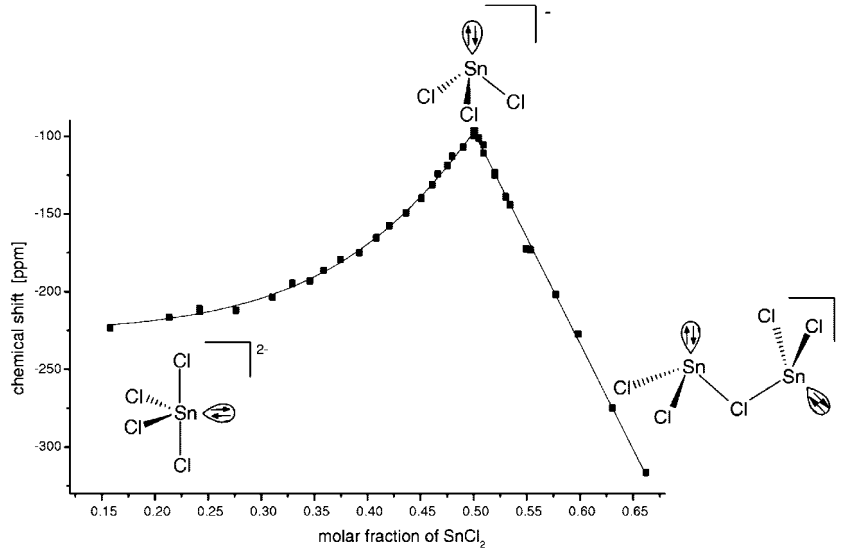

Figure 2. ^{119}Sn NMR chemical shifts as a function of molar fraction of SnCl2 ($\chi SnCl_2$) and plausible species in the [BMIM][Cl] IL. Reproduced with permission from ref 60. Copyright 2005 Elsevier.

carried out for a series of other [EMIM][X] ILs, where $[X]^-$ = $[CF_3COO]^-$, $[C_6H_{13}SO_4]^-$, $[EtSO_4]$, $[BuSO_4]^-$, $[SCN]^-$, $[BF_4]^-$, $[TfO]^-$, and $[N(CN)_2]^-$.[52]

The liquid structure of [EMIM][Tf_2N] was investigated by Ishiguro, Takamuku, and co-workers. They used a combination of large-angle X-ray scattering, neat NMR, and molecular dynamics simulation.[53] The study showed that the liquid structure is significantly different from the layered crystal structure observed for the solid state. The ^{13}C NMR proved of particular importance in observing the interaction of the imidazolium C2 proton of the $[EMIM]^+$ with the oxygen atom of the $-SO_2(CF_3)$ group of the $[Tf_2N]^-$.[53] It is noteworthy that this interaction was not assigned to hydrogen bonding; this is in contrast to several other studies.

The first systematic ^{15}N NMR study of neat ILs by Lyčka and co-workers included twelve 1,3-disubstituted imidazolium salts.[54] The measured chemical shifts for both nitrogen atoms were in a similar range: $\delta(^{15}N)_{N1}$ = 196.0−210.8 ppm and $\delta(^{15}N)_{N3}$ = 196.1−213.9 ppm. This therefore raises the question of correct signal assignment: obviously this cannot be done based on the chemical shift values alone. Unambiguous line assignment was carried out by the analysis of $^nJ(^{15}N,^1H)$ coupling constants mapped using a 2D $^1H-^{15}N$ gradient-selected HMBC experiment.[54] According to the NMR data measured, alkyl substituents influence the ^{15}N chemical shifts in a much more pronounced manner compared to the effect of the anion $[X]^-$. The data measured should prove useful for further analysis using theoretical methods, since ^{15}N NMR is known to reflect valuable structural parameters and electronic properties of molecular systems.[55,56]

The potential of ^{14}N NMR spectroscopy for studying neat ILs was investigated by Blümel and co-workers.[57] In addition to the neat samples, the authors also used ^{1}H and ^{13}C NMR spectroscopy to study ILs immobilized on silica because this is closely related to their application in heterogeneous catalysis.[57]

Deuterium isotope effects on the proton $\Delta^1H(H,D)$ and chloride ion $\Delta^{35/37}Cl(H,D)$ as well as NMR chemical shifts upon deuteration of the imidazolium C-2 and C-2,4,5 positions were measured by Moyna and co-workers to characterize interionic hydrogen bonds in [BMIM][Cl].[58] These Δ values stand for variations of ^{1}H and $^{35/37}$Cl resonances upon H/D substitution. However, the $\Delta^1H(H,D)$ values were below the statistically acceptable barrier and did not provide useful structural information. In contrast, the $\Delta^{35/37}Cl(H,D)$ values were ca. 1−2 ppm, and their measurements were carried out with good precision (standard deviation < 0.12 ppm). Thus, the NMR study made it possible to identify the Cl···H hydrogen bonds of the chloride anion with all imidazolium protons. According to the $\Delta^{35/37}Cl(H,D)$ values determined, the hydrogen bond involving the imidazolium proton at the C-2 position was stronger than the hydrogen bonds involving protons at the C-4 and C-5 positions. The results of the NMR study are in good agreement with crystallographic and ab initio studies.[58] The results of the ^{35}Cl and ^{13}C NMR study of the [BMMIM][$ZnCl_3$] IL at 100−110 °C indicated an evolution toward the dissociated structure [BMMIM···Cl···$ZnCl_2$].[59]

A ^{119}Sn NMR study has been carried out by van Eldik and co-workers to investigate the nature of the [BMIM]-[$SnCl_3$] anion and to characterize the dependence of the ^{119}Sn chemical shifts from the molar composition of the IL (Figure 2).[60] The maximum value of the ^{119}Sn chemical shift was observed for a 1:1 ratio of the [BMIM][Cl]/$SnCl_2$. This suggests the formation of the $[SnCl_3]^-$ anion. A linear dependence of an observed chemical shift versus an increasing molar fraction of $SnCl_2$ on the right side of the curve ($\chi SnCl_2 > 0.5$) suggested the formation of the $[Sn_2Cl_5]^-$ dimer. Nonlinear behavior on the left side of the curve ($\chi SnCl_2 < 0.5$) was evidence of an equilibrium involving the $[SnCl_4]^{2-}$ species. The presence of a single ^{119}Sn signal over the whole concentration range indicated a rapid exchange on the NMR time scale. The authors also reported a dependence of the ^{1}H chemical shifts on the H-2 signal as a function of the $SnCl_2$ molar ratio. In addition to interconversion of the $[Sn_xCl_y]^{n-}$ species, ^{1}H chemical shifts were also influenced by hydrogen bonding with the anionic species.[60]

Several studies have been published dealing with the application of self-diffusion measurement experiments in studying the structure and dynamics of various ILs. For [MEIM][$EtAlCl_3$], the diffusion coefficients of the cation $[MEIM]^+$ and anion $[EtAlCl_3]^-$ were measured simulta-

neously by ^{1}H NMR.[61] Direct correlation of self-diffusion coefficients and viscosity with ^{13}C and ^{1}H correlation times indicated that the transport properties of the IL are determined by the molar quantities of the salt rather than the individual properties of the ions in the IL.[61] Similar conclusions have been made in the ^{1}H diffusion and ^{13}C NMR relaxation study of the [MEIM][$AlCl_4$] IL.[62,63] Using NMR data and ab initio calculations, the appropriate model was developed to describe the movement of the $[MEIM]^+$ cation in the IL.[62]

Independent measurements of the self-diffusion coefficients of the anions (^{19}F NMR) and cations (^{1}H NMR) for a series of ILs were carried out by Watanabe and co-workers.[64−66] It was found that the cations diffuse almost equally compared to the anions in [EMIM][BF_4] and [BPy][BF_4], whereas the cations diffuse faster than the anions in [EMIM][Tf_2N] and [BPy][Tf_2N].[64] A summation of the cationic and anionic diffusion coefficients was used to estimate ionic transport properties for each IL, resulting in the following order: [EMIM][Tf_2N] > [EMIM][BF_4] > [BPy][Tf_2N] > [BPy]-[BF_4].[64] For ILs of the general type [RMIM][Tf_2N] (R = methyl, ethyl, butyl, hexyl, and octyl), diffusion measurements revealed higher self-diffusion coefficients for the cations compared to the anions. This was true even if the cation radius was larger than that of the anion.[65] On the basis of these studies, the authors have introduced an ionic diffusion parameter to characterize several important IL properties.[65]

The effect of mixing ILs was the subject of a diffusion-measurements study carried out for mixtures of [MPPyrr]-[Tf_2N] and [BMPyrr][Tf_2N].[67] The larger cation $[BMPyrr]^+$ was found to diffuse more slowly in mixtures where $[MPPyrr]^+$ was the dominant component, whereas the $[MPPyrr]^+$ cation was moving slightly faster.

A promising approach for estimating the ionic nature of ILs was developed by Watanabe and co-workers in order to answer the question of "how ionic" are these ILs.[68−70] In the methodology they developed, the ionic nature of the IL was defined as the molar conductivity ratio $\Lambda_{imp}/\Lambda_{NMR}$, where Λ_{imp} is the molar conductivity measured by the electrochemical impedance method and Λ_{NMR} was estimated from the pulsed-field-gradient spin−echo NMR self-diffusion coefficients. An extensive study of the $\Lambda_{imp}/\Lambda_{NMR}$ correlation with the solvatochromic polarity scales of ILs was reported. This study was of particular help in understanding the effect of the ionic properties of the ILs on the intermolecular interactions and also in illustrating their degree of aggregation.[69] Another successful application includes the characterization of the anionic[68] and cationic[70] effects on ion dynamics and ionicity. The $\Lambda_{imp}/\Lambda_{NMR}$ and effective ionic concentration values (C_{eff}, the product of $\Lambda_{imp}/\Lambda_{NMR}$ and molar concentration) can be considered as useful parameters for the estimation of IL physical properties and, possibly, even chemical reactivity in this media.

Variable-temperature diffusion measurements for [EMIM][BF_4] indicated that a phase change took place at 333 K.[71] The phase change was caused by a structural rearrangement of the [EMIM][BF_4] ion pair into individual ions $[EMIM]^+$ and $[BF_4]^-$.[71]

Alkyl side chain effect on the transport properties of a series of ILs was investigated by Kanakubo and co-workers. They carried out independent measurements of the self-diffusion coefficients of both the cations (^{1}H NMR of the 3-methyl group) and anions (^{19}F NMR of the $[PF_6]^-$) of the following series [BMIM][PF_6], [HexMIM][PF_6], and [OMIM][PF_6].[72] In this comparative study, ILs with longer alkyl chains were found to have stronger interionic interactions. Other examples of self-diffusion measurements in ILs include the studies of proton transport[66] and hydrogen bonding.[71]

Relaxation measurements are another source of valuable information about the structure and dynamics of ILs. A ^{13}C relaxation study, combined with NOE (nuclear Overhauser effect) measurements, has been used to study molecular structure and rotational motion of the [BMIM][PF_6] system.[73,74] The analysis of the spin−lattice relaxation times (T_1) of the $[BMIM]^+$ cation revealed the relative motion of each carbon atom in the cation.[73] These rotational motions are particularly sensitive to some important IL properties such as hydrogen bonding, phase changes, and viscosity.[61,73,75,76] The phase change of [EMIM][BF_4] at 333 K observed by self-diffusion measurements was confirmed by ^{11}B quadrupolar relaxation rate measurements.[71]

The intrinsic structure and the microdynamics of the [EMIM][$AlCl_4$] chloroaluminate IL were studied using ^{13}C NMR relaxation methods as a function of IL composition and temperature.[77,78] The studies reported an NMR approach, which can be useful for probing cation−anion interactions.

NMR measurements of ^{1}H and ^{19}F spin−lattice relaxation times (T_1) and self-diffusion coefficients at various temperatures have been carried out by Chung and co-workers for trimethylsilylmethyl-substituted ILs [SiMIM][X]. They compared these to the isostructural neopentyl- substituted ILs [NpMIM][X] where [X] = $[Tf_2N]^-$ or $[BF_4]^-$ (see Figure 1 for abbreviations).[79] Observed differences in the measured NMR properties were correlated with reported viscosity changes in order to understand Si-substitution effects on the IL viscosity. In fact, lower room-temperature viscosities have been found for both [SiMIM][Tf_2N] and [SiMIM][BF_4]; values are smaller by factors of 1.6 and 7.4, respectively, compared to the neopentyl analogues [NpMIM][X], [X] = $[Tf_2N]^-$ and $[BF_4]^-$.[79]

Both the ^{13}C spectra and ^{13}C−T_1 relaxation times as a function of temperature were measured to investigate [BMIM]-[Br] IL in the supercooled state.[80] The measurements revealed discrete segmental motions of the $[BMIM]^+$ cation. The motion of the imidazole ring was extremely restricted at low temperatures, while the signal of the methyl group in the butyl chain was active even after a phase change into the solid state.[80]

Although two-dimensional NMR spectroscopy can be quite challenging to carry out in neat ILs, it is undoubtedly considered a superior source of unique structural information. The first NMR evidence for the presence of short intermolecular contacts (<5 Å) between imidazolium rings was reported in the pioneering study of basic [EMIM]-[$AlCl_4$] IL by Osteryoung and co-workers.[81] 2D ROESY spectra with the cross-peaks corresponding to NOE transfers were recorded at 500 MHz and 25 °C. In the NMR spectra, the intermolecular contacts were clearly resolved and provided independent evidence for the structure of the hydrogen-bonding network in the IL. Cation−cation distances in [BMIM][BF_4] and [BMMIM][BF_4] were estimated by Mele and co-workers by analysis of 2D NOESY data (Figure 3).[82] The measurements of the quantitative NOE interactions network made it possible to construct possible aggregation motives in the studied IL (Figure 3). Averaged intermolecular

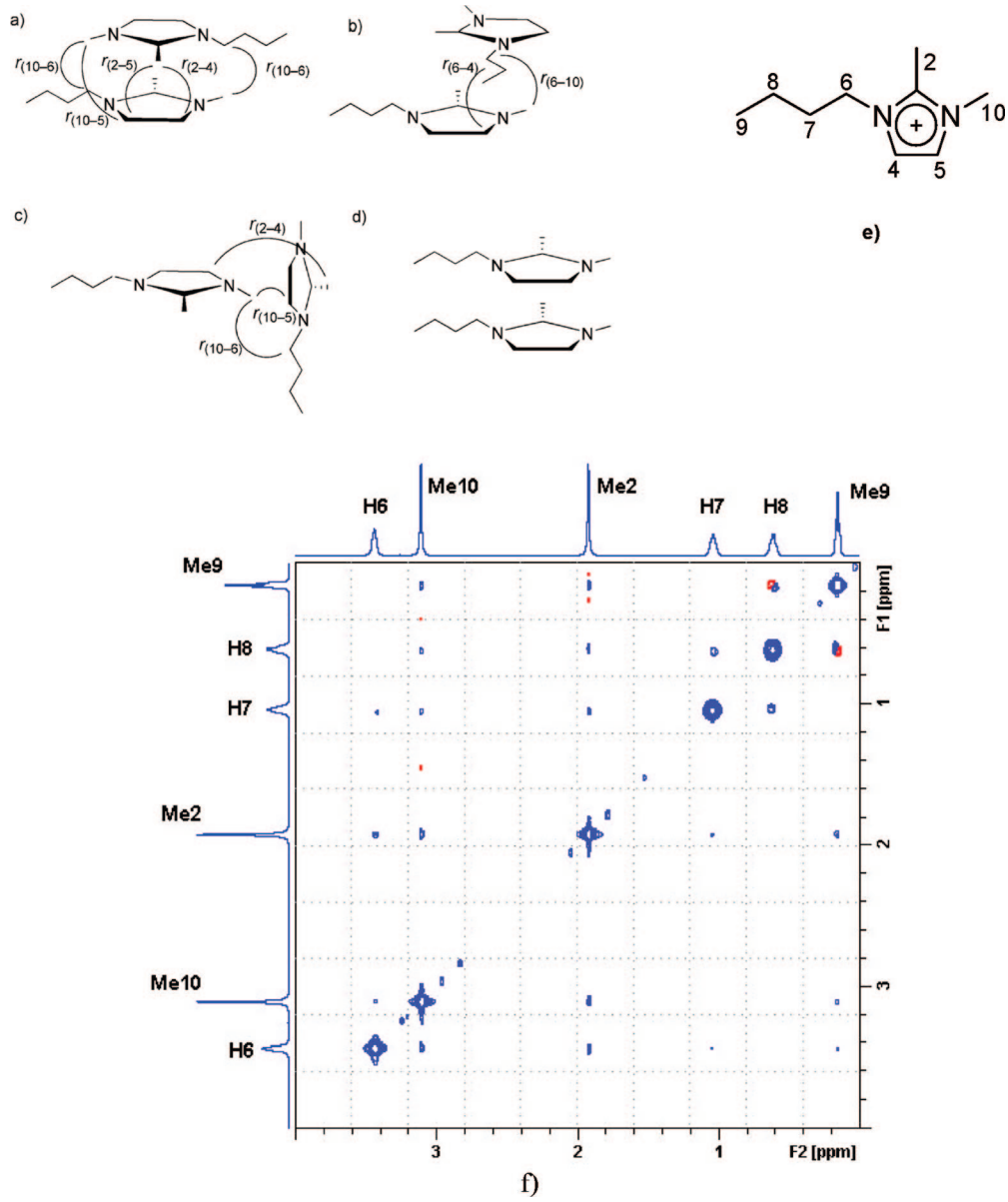

Figure 3. Possible aggregation motives of [BMMIM][BF_4]: sandwich-type (a, b) and T-shaped (c) interactions were consistent with distances, while parallel arrangement (d) was not; (e) denotes atoms numbering; (f) a high-field part of the 2D NOESY spectrum (mixing time = 50 ms, 500 MHz, 315 K; positive levels in blue, negative levels in red). Reproduced with permission from ref 82. Copyright 2006 Wiley-VCH Verlag GmbH & Co. KgaA.

distances for [BMMIM][BF_4] (in Å), $r(5-10)_{H-Me} = 3.1(9)$, $r(5-2)_{H-Me} = 3.1(7)$, $r(4-2)_{H-Me} = 3.2(2)$, $r(6-4)_{CH_2-H} = 3.2(9)$, and $r(6-10)_{CH_2-Me} = 3.0(9)$, showed reasonable agreement with the structural data obtained by X-ray studies (r denotes intermolecular distance, atom numbering is shown in Figure 3e, and the type of the interacting groups is indicated in the subscript). It is noteworthy that the presence of the bulky and noncoordinating $[Tf_2N]^-$ anion increased the actual distances: corresponding intermolecular contacts were not observed in the NOESY spectrum.[82]

Judeinstein and co-workers carried out an excellent comparative NMR study of the structure and local organization of proton-conducting ILs consisting of triethyl amine and a series of organic acids (acetic acid, trifluoroacetic acid, and bis(trifluoromethanesulfonyl)imide acid).[83] A carefully selected set of NMR experiments was chosen to characterize the ILs (Figure 4). Determination of the ^1H and ^{19}F self-diffusion coefficients revealed interesting features of the different transport properties for the components of each IL. For example, similar values for H^+, $[Et_3HN]^+$, and acidic anion were observed in [Et_3HN][CF_3COO], whereas they were noticeably different in [Et_3HN][CH_3COO]. The ^{15}N NMR was characteristic of the nature of the nitrogen group: a doublet if hydrogen is attached to the nitrogen atom (due to spin−spin coupling) and otherwise a singlet. The relative acidic properties of the ILs were further studied by analyzing the ^1H and ^{15}N chemical shifts. Finally, a combination of $^{15}N-^1H$ and $^{13}C-^1H$ HOESY experiments was carried out in order to reveal the structural properties of the ILs. A complementary set of NMR experiments provided sufficient information to suggest a plausible structure for the ILs studied (Figure 4).[83] It should be pointed out that this study concerned protic ILs, which have different properties, especially for ^1H resonance, compared to the widely used aprotic ILs (see also section 3.1).

	TFA-TEA	TFSi-TEA	AA-TEA
Diffusion coefficients at 340K ($x10^6$ cm^2s^{-1})	D_{H+} = 1.90 D_A = 1.97 D_{TFA} = 1.94 $D_{H+} = D_A = D_{TFA}$	D_{H+} = 1.29 D_A = 1.27 D_{TFSi} = 0.97 $D_{H+} = D_A > D_{TFSi}$	D_{H+} = 3.54 D_A = 2.51 D_{AA} = 2.95 $D_{H+} > D_{AA} > D_A$
^{15}N NMR N-H coupling	Yes	Yes	No
HOESY $^{15}N\ldots^{1}H$	N…H interaction	N…H interaction	N…H interaction
HOESY $^{13}C\ldots^{1}H$	Interactions between anion, amine, H^+	Intermolecular interactions	Interaction of H^+ with CH_3COO^-
Dissociation scheme	mostly associated as ion-pair	ammonium and TFSi anion dissociated	proton fully dissociated

Figure 4. Summary of NMR results and proposed structures of the ILs (TFA = $[CF_3COO]^-$, TEA = $[Et_3HN]^+$, AA = $[CH_3COO]^-$, TFSI = $[Tf_2N]^-$). Reproduced with permission from ref 83. Copyright 2008 American Chemical Society.

2.2. Water and Impurities Effects on Ionic Liquids

Water is one of the most commonly occurring impurities in ILs, which may dramatically influence the yield, selectivity, and reproducibility of chemical reactions carried out in the ILs. The potential of native-state NMR for studying IL/water system interactions is obvious, since the addition of a deuterium-containing cosolvent introduces the risk of also adding an uncontrolled amount of water, the effects of which would be rather difficult to rationalize and eliminate.

Water molecules change the IL structure by introducing water−cation interactions in addition to the cation−anion interactions already present. Water−anion interactions, although not expected to be strong for weakly basic anions, also cannot be ignored. The nature of the water−cation interactions as well as the sites of water binding to [BMIM][BF_4] were determined using ^1H NMR and $^1H\{^{19}F\}$ NOE experiments.[84] At a very low water content, the interaction of water with the IL was highly specific and was localized at the C_{sp2}−H protons (H2, H4, and H5 protons of the imidazolium ring). Increasing the amount of water led to nonselective solvation.[84] The degree of IL hydration was found to depend significantly on the strength of cation−anion interactions and the self-aggregation of the IL.[85−87] ^1H NMR combined with fluorescence spectroscopy was successfully utilized to investigate IL/water systems and to determine critical aggregation concentrations, standard free energies of aggregation, and the aggregation numbers of several ILs.[88]

When [BMIM][PF_6] was exposed to moisture, two types of PF_2X_n species were detected by ^{31}P NMR.[89] The formation of one of the species was facilitated by the presence of $SnCl_2$ and water. A probable explanation for the formation of the PF_2 moiety was based on the assumption that the equatorial F ligands of PF_5 are relatively easily substituted compared to the apical F ligands.[89] Although the study did not explicitly identify the nature of the X groups, X = Cl or OH may be proposed. The decomposition of the $[PF_6]^-$ counterion in the presence of water (and $SnCl_2$) indicates that the aqueous workup of reaction mixtures in some cases might lead to a damage of the IL system.

^{17}O NMR studies in [EMIM][$AlCl_4$] IL have shown that, under acidic conditions, reaction with water leads to two different types of the oxygen-containing species: (1) hydroxochloroaluminate and (2) O-bridged oxochloroaluminates (two forms).[90] Under basic conditions, rapid exchange between oxochloroaluminate and hydroxochloroaluminate took place. In both cases, even a small amount of water (∼50 mM) produced significant changes in the IL properties.[90] The nature of the chemical interactions involving water in chloroaluminate ILs was revealed by analysis of the ^{17}O NMR spectra.[91] Evidence for the involvement of the oxy species $[Al_3OCl_8]^-$, $[Al_3O_2Cl_6]^-$, and $[Al_2OCl_5]^-$, as well as hydroxy species $[Al_3Cl_9(OH)]^-$ and $[Al_2Cl_6(OH)]^-$, was reported.

The ^1H (^2H) NMR spectra of protons (deuterons) recorded in oxide-free basic [EMIM][$AlCl_4$] ILs showed a single line.[92] An in-depth NMR study revealed the complicated nature of this signal resulting from the fast exchange between the HCl, HCl_2^- anion, and the $Cl(HCl)_n^-$ anions. The effect of Cl^- concentration on the ^2H NMR chemical shifts was measured using a 0.1 M solution in the IL. Both ^1H and ^2H NMR spectra were utilized to determine the DCl_2^-/DCl and HCl_2^-/HCl equilibrium constants with sufficient accuracy under variable-temperature conditions (30−90 °C). The thermodynamic parameters of the equilibrium were determined from the variable-temperature experiments, $\Delta H = -9.8 \pm 0.8$ kJ mol^{-1} and $\Delta S = 4.8 \pm 2.5$ J mol^{-1} K^{-1}:

$$HCl + Cl^- = HCl_2^-$$

The NMR study suggested that an IL surrounding interacts more strongly with the chloride ion than with the hydrogen dichloride ion compared to the other solvents studied.[92]

Interestingly, the theoretical study by Palomar and coworkers at the GIAO-B3LYP/6-31++G** level highlighted a rather complicated influence of the water molecules on the chemical shifts of 1,3-dialkylimidazolium ILs.[93] In fact, they found that specific interactions of the cation with the water molecules change the ^1H chemical shifts to higher values, while nonspecific interactions with water (as the solvent) affect the chemical shifts in the opposite manner. The study reports a computational approach to dealing with solvent−solute interaction problems.[93] The influence of ion pairs and cluster formation on the ^1H and ^{13}C NMR chemical shifts was investigated at the theoretical level by a combined molecular dynamics and quantum mechanics/molecular mechanics (QM/MM) methods approach.[94] Experimental measurements and theoretical GIAO−DFT calculations of ^1H chemical shifts were carried out to study water effects in trihexyl(tetradecyl)phosphonium chloride IL.[95] The study suggested that cation−anion−water configurations at low water concentrations were transformed into cation−water−water configurations at higher water concentrations.[95]

A combined NMR and IR study by Firestone and coworkers has shown that water molecules disrupt the hydrogen-bonding network between the anion and imidazolium ring in the IL.[96,97] The addition of an appropriate concentration of water to [C_{10}MIM][Br] and [C_{10}MIM][NO_3] was found to change the native structural motif of the IL and resulted in the formation of an "ionogel" composition. For mixtures with high (≥0.8) or low (≤0.16) ratios of water to IL, satisfactory ^1H NMR spectra were obtained in the native

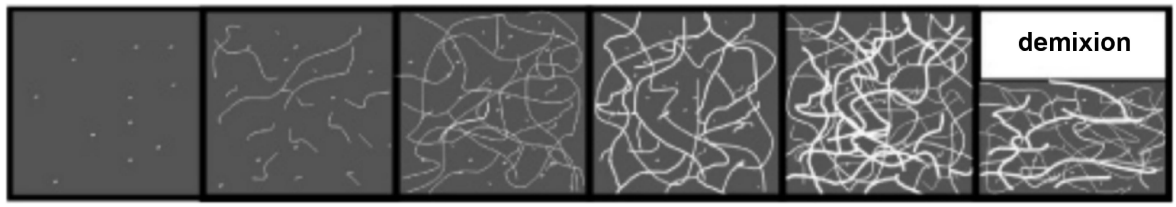

Figure 5. Plausible view of the microstructure of the [BMIM][Tf_2N]/water system with increasing amount of water from left to right (the IL is shown in gray and water is shown in white). Reproduced with permission from ref 100. Copyright 2007 American Chemical Society.

mixtures, whereas for intermediate water/IL ratios, investigations using acetonitrile solutions were found to be a better choice.[96,97] Disruption of the hydrogen bonding between the anion and cation upon mixing with water was also reported for [HBet][Tf_2N] (Hbet = $Me_3N^+CH_2COOH$, betainium cation).[98] Temperature-dependent phase changes caused by rearrangement of the IL structure were monitored using ^1H NMR.[98]

Characteristic water concentrations in [BMIM][Cl] were determined by Nakahara and co-workers utilizing kinetic measurements and ^2H NMR.[99] If the concentration of water was above the characteristic point, water molecules were able to participate in reactions as reactants. Below this concentration point, the water molecules interacted with the IL and they were deactivated as reactants. The characteristic water concentration was established in terms of the coordination number of the chloride anion, which was found to be 1.6 for [BMIM][Cl].[99]

Rollet and co-workers studied the self-diffusion properties of cations, anions, and water molecules in the [BMIM][Tf_2N]/water system (0.3−30 mol % of water) using ^1H and ^{19}F NMR.[100] The measured self-diffusion coefficients of all species were found to increase with water content. However, the water molecules did show anomalous diffusion properties. The evolution of the diffusion coefficient of water was completely out of step with that of the IL ions: it increased 25 times quicker. The authors suggested that increased amounts of water led to phase separation on a microscopic scale, resulting in the formation of a network of water-rich channels (Figure 5). NMR measurements were used to estimate the ratio of linked and bulk water (a factor of 10 at 30 mol % of water) and to characterize the size of the water pores (~5 μm). This study emphasized that water molecules not only disturb the molecular structure of the IL via direct interaction with the cations and anions of the IL but also change the supramolecular organization via the formation of a partially segregated biphasic system.[100] Weiss and co-workers observed that very small amounts of an alcohol or water can induce critical changes into the supramolecular structure of ILs.[101] The transformation of the IL into the liquid-crystalline phases was monitored by ^1H and ^2H NMR spectroscopy in the native state. The authors observed a "molecular lubrication" effect of water or alcohol additives: cation−anion electrostatic interactions were sufficiently attenuated by complexing with hydroxyl groups, thus leading to increased fluidity. This effect initiated both conformational and structural changes and resulted in mesophase induction.[101,102]

A combined ^1H NMR and molecular dynamics study also showed that different IL/water interaction regimes are possible depending on the amount of water present.[103] At low water content, the ions of the [BMIM][BF_4] IL are selectively coordinated by the water molecules and the overall ionic network is not perturbed, whereas at high water content, the network is disrupted and the ions are solvated by water clusters in a nonspecific way.[103]

Mixing−demixing behavior of the [choline][Tf_2N]/water system ([choline]$^+$ = (2-hydroxyethylammonium)trimethylammonium) was shown to be strongly temperature dependent.[104] ^1H NMR spectrum of the [choline][Tf_2N]/water mixture at 25 °C was found to be nearly identical to the spectrum recorded in the absence of water, thus indicating the absence of interactions between two phases. Heating at 100 °C resulted in the formation of a single phase and disappearance of the water signal in ^1H NMR. Formation of single phase with water was suggested to involve breakage of the hydrogen bonds between anion and cation of the IL. A similar behavior is known for some other IL/water mixtures as well.[104]

Self-diffusion measurements were used as a sensitive test for determining the purity of various ILs. It was reported that even a small amount of impurity significantly affected transport phenomena in the IL.[105] Of particular note is the fact that ca. 3% of impurities in commercially available [BMIM][PF_6] led to a ~25% change in the self-diffusion coefficients of the anion and cation. Although the authors did not determine the exact nature of the impurities, they showed that the impurities can be removed in a well-known two-stage purification procedure: (1) removal of colored impurities with activated charcoal and (2) drying under vacuum.[105]

The water impurity effect on the reaction rate and selectivity was addressed using ^1H and ^{19}F NMR in [BMIM][Tf_2N].[106] An unusually large rate effect on the reaction of adamantyl mesylate induced by only small amounts of water in the IL was found. The reaction rate increased from $k = 1 \times 10^{-6}$ to 17×10^{-6} s^{-1} on changing the water content from 0.11% to 1.00%.[106] In another reaction, the solvolysis of cumyl trifluoroacetate, the formation of 24% of a minor product was observed if the IL contained even 0.5% of water.[106]

2.3. Water/Proton Removal

The discussion in the previous section has clearly shown the importance of controlling the amount of water in IL samples. Water/proton removal techniques based on native-state NMR as the analytical method of choice are discussed here.

^2H NMR was used to study proton removal from chloroaluminate ILs using a model system with added DCl.[107] $EtAlCl_2$ was used to remove acidic impurities according to the reaction:

$$EtAlCl_2 + HCl(\text{or } DCl) \rightarrow C_2H_6^{gas}(\text{or } C_2H_5D^{gas}) + AlCl_3$$

Scheme 1. NMR Monitoring of Water Removal Process

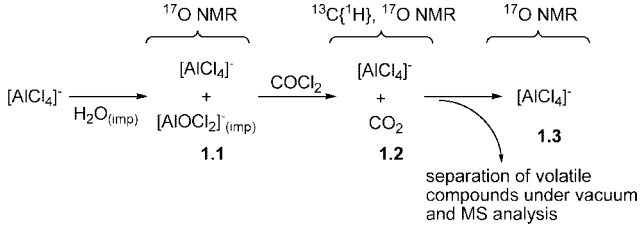

The reaction was monitored using ^{1}H, ^{2}H, and ^{27}Al NMR spectroscopic techniques. Deuterium NMR proved the most convenient tool for monitoring the study, and complete removal of the acidic impurities was confirmed by this method. Even at small concentrations, DCl gave the largest peak in the ^{2}H NMR spectrum and it was easy to monitor disappearance of this peak. Neither the product of the above reaction ($AlCl_3$) nor the initial reagent ($EtAlCl_2$) was found to introduce any noticeable changes into the normal composition of the IL.[107]

Another approach for promoting water removal from chloroaluminate IL utilized the reaction of oxide contamination with phosgene.[108−110] Seddon, Welton, and co-workers used step-by-step multinuclear NMR monitoring to follow the process (Scheme 1).[109] The $^{13}C\{^{1}H\}$ NMR spectrum of the IL with added phosgene showed two peaks attributed to $COCl_2$ (144.6 ppm) and CO_2 (124.3 ppm). Both these species were also detected by ^{17}O NMR with $\delta(^{17}O) = 497.5$ and 84.0 ppm for $COCl_2$ and CO_2, respectively. Despite only a small amount of CO_2 (0.04 equiv to IL) present, it was clearly visible using a 360 MHz NMR spectrometer operating at 90.55 and 48.82 MHz for ^{13}C and ^{17}O, respectively.[109] The presence of the species was independently confirmed by MS analysis. Detection of phosgene and carbon dioxide in step **1.2** was found to be more informative and much more sensitive for monitoring oxide species removal due to the fact that comparison of the ^{17}O spectra of the aluminum species in steps **1.1** and **1.3** is more complicated (Scheme 1).

The quantitative efficiency of proton removal under vacuum was successfully monitored using NMR.[110] The smallest detectable proton concentration using ^{2}H NMR was reported as 1.92×10^{-4} M as measured by a 400 MHz spectrometer operating at 61 MHz for ^{2}H. More modern NMR equipment with improved sensitivity[111] should ensure improvement of the smallest detectable concentration of ~1 order of magnitude. This may come close to the limit of 5.5 μM reported for electrochemical measurements.[110] Evacuation of the [EMIM][AlC_4] sample to a pressure less than 5×10^{-6} Torr for 5 h resulted in complete disappearance of proton signals (Figure 6). After the evacuation, only those signals corresponding to natural-abundance ^{2}H of the imidazolium cation were observed. The authors also discussed a possible algorithm for monitoring proton/water removal from ILs using ^{2}H and ^{17}O NMR and compared the results with electrochemical measurements.[110]

The high sensitivity of the ^{1}H chemical shifts of water to the presence of acid was used in an elegant approach by Nakahara and co-workers for an in situ NMR spectroscopic study to detect acid impurities in ILs.[112] A detection limit below 10^{-3} mol kg^{-1} was successfully achieved using a 400 MHz NMR spectrometer. The efficiency of the recrystallization purification procedure for the commonly used imidazolium ILs was analyzed using this approach.[112]

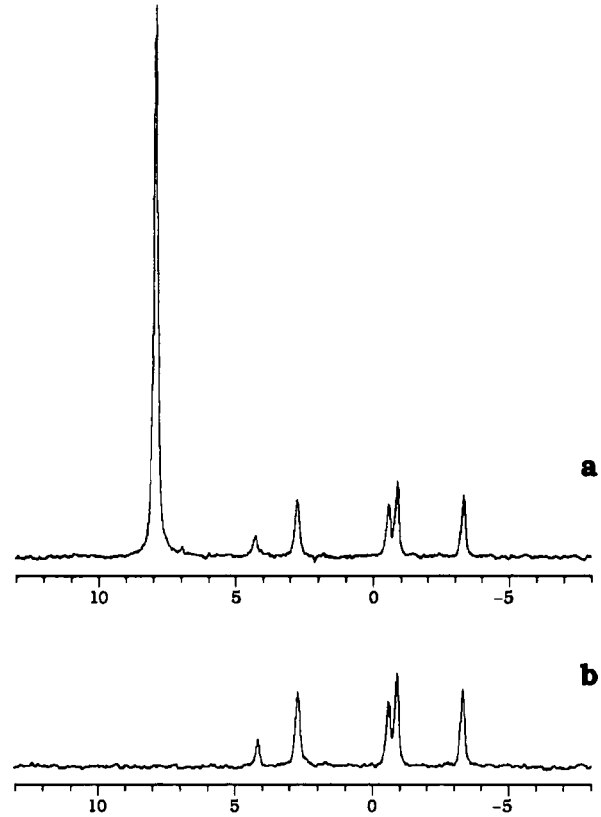

Figure 6. (Top) ^{2}H NMR spectrum of the initial [EMIM][AlC_4] sample containing 19.8 mM protons (δ = 8 ppm); (Bottom) the sample after 5 h under vacuum (61 MHz (400 MHz for ^{1}H), 90 °C). Reproduced with permission from ref 110. Copyright 1991 American Chemical Society.

2.4. Solubility of Gases

Gas solubility is a very important property related to the performance of several catalytic reactions of industrial importance. For instance, knowledge of the solubilities of CO and H_2 are critical for designing carbonylation, hydroformylation, and hydrogenation processes.

It should be noted that high-pressure NMR spectroscopy provides an easy and convenient tool for determining the solubility of gases in ILs and is particularly important for gases such as hydrogen, which cannot be determined using gravimetric measurements.[86,113,114]

The solubility of molecular hydrogen in several ILs has been determined by Dyson and co-workers using high-pressure ^{1}H NMR (at 101.3 bar H_2 pressure).[114,115] For most of the ILs studied, H_2 solubility ($[H_2] = 0.47-0.98$ mM) was significantly lower compared to that in organic solvents ($[H_2] = 2.54-3.75$ mM) and close to the solubility of hydrogen in water ($[H_2] = 0.81$ mM).[114,115] The only exception was reported for the IL $[P(C_6H_{13})_3(C_{14}H_{29})][PF_3(C_2F_5)_3]$, which had a hydrogen solubility of $[H_2] = 1.84$ mM.[114]

Using high-pressure NMR experiments, the concentration of hydrogen in [EMIM][Tf_2N] was estimated to be $[H_2] < 0.01$ M (297 K, 30 bar).[116] However, after addition of CO_2 to the system, the ^{1}H NMR signal for the molecular hydrogen was observed at $\delta(^{1}H) = 4.3$ ppm, and the estimated concentration of hydrogen in this system was found to be $[H_2] < 0.14$ M (297 K, 120 bar). Releasing the pressure of CO_2 resulted in the disappearance of the corresponding H_2 signal from the ^{1}H spectrum. This clearly demonstrates

that the presence of CO_2 led to an order of magnitude increase in the H_2 solubility in the IL. Leitner and co-workers carried out a systematic study of hydrogen solubility enhancement with respect to CO_2 pressure and described the application of a multiphase IL/CO_2 system for the Ir-catalyzed enantioselective hydrogenation of imines.[116]

The solubility of carbon monoxide in 37 ILs and in selected organic solvents was measured using high-pressure ^{13}C NMR by Laurenczy and co-workers.[117] The solubility of CO in the ILs ([CO] = 0.66−4.20 mM) was significantly lower compared to common organic solvents ([CO] = 7−17 mM).[117] Although the effect was small, it was also found that CO solubility in the ILs decreased with increasing temperature. The solubility of CO ([CO] = 0.66−4.20 mM)[117] showed a larger dependence on the nature of the IL than the solubility of H_2 ([H_2] = 0.62−0.98 mM).[114] This is most likely due to the presence of the dipole moment and higher polarizability.[117] On the basis of ^{13}C and ^{19}F NMR chemical shifts, a simple empirical model has been developed to predict the solubility of CO in ILs.[117]

The solubilities of C_2 hydrocarbons, as determined by ^1H and ^{13}C NMR, in the supported [BMIM][PF_6] IL at 1 bar pressure showed significant differences depending on the nature of the gas (mole fraction χ at 25 °C is given):[118]

$$\text{acetylene } (74 \pm 7) \times 10^{-3} \gg \text{ethylene } (6.5 \pm 2) \times 10^{-3} > \text{ethane } (3.5 \pm 1) \times 10^{-3}$$

The solubilities of all the C_2 hydrocarbons studied were found to decrease with increasing temperature (exothermic solvation process).[118]

A joint theoretical and experimental study by Tempel and co-workers has shown that ILs may be utilized for selective storing of a large quantity of PH_3 and BF_3 gases in a small volume.[119] The observed values of a 1.92 molar ratio for PH_3/[BMIM][Cu_2Cl_3] (15 °C, 1.1 bar) and ~0.9 for BF_3/[BMIM][BF_4] provide strong evidence for their high gas storage capacity. The $^{31}P\{^1H\}$ NMR spectrum of PH_3/[BMIM][Cu_2Cl_3] exhibited a singlet at $\delta(^{31}P) = -171.9$ ppm ($\delta(^{31}P) = -252.6$ ppm for pure PH_3 gas). The ^{19}F NMR spectrum of the BF_3/[BMIM][BF_4] system contained a single sharp peak at $\delta(^{19}F) = -142.5$ ppm ($\delta(^{19}F) = -134.3$ ppm for pure BF_3 gas and $\delta(^{19}F) = -150.6$ ppm for the anion of pure IL). Thus, the NMR study has shown that chemical complexation between the solute species and the selected IL was the key feature responsible for the observed reversible binding of PH_3 and BF_3.[119]

The solubility of H_2S in various ILs and their ability to establish specific intermolecular interactions have been studied by Pomelli, Dyson, and co-workers using both high-pressure NMR (14 bar) and theoretical ab initio calculations.[120] Dissolution of H_2S induced noticeable changes in the ^1H NMR spectrum of the IL, but no significant changes were observed in any of the ^{11}B, ^{13}C, ^{19}F, and ^{31}P NMR spectra. Although the difference in solubilities was not large, the relative solubility of hydrogen sulfide in a series of [BMIM][X] ILs changed according to the order X = $[Cl]^-$ > $[BF_4]^-$ > $[TfO]^-$ > $[Tf_2N]^-$ ≫ $[PF_6]^-$. The solubility of H_2S (molar fraction) was found to be in the range of 0.72−0.86. Theoretical calculations have shown a tight interaction between the H_2S molecule and the anions, with the estimated interaction energy of 7−14 kcal mol^{-1} at B3LYP and MP2 levels. It is worth noting that the stability of the H_2S−$[PF_6]^-$ complex was lower than the stability of the other H_2S−$[X]^-$ complexes, which is in agreement with experimental data. This spectral study confirmed the potential of ILs for H_2S removal and storage.[120]

2.5. Extraction and Separation

NMR spectroscopy has been successfully applied to the investigation of separation ability and the selectivity of ILs toward possible applications in the area of extraction. The extraction and separation are closely related to industrial purification as well as to environmental protection issues. The analytical investigation of a native biphase or multiphase system in a native state is an example of the use of this convenient and reliable technique because the addition of deuterium-containing cosolvents to the mixture has the potential to change the equilibrium and lead to a wrong distribution of components between the phases. Of course, another possible option is to analyze the composition of each phase separately using either solution NMR in deuterated solvents or another appropriate analytical method.

Zhang and Zhang addressed the problem of the selective removal of sulfur from fuels.[121] Using ^1H and ^{13}C NMR, it was found that S-containing five-membered aromatic ring compounds are favorably absorbed over six-membered aromatics. S-containing nonaromatic compounds are poorly absorbed. The absorption capacity was determined by measuring the molar ratio of thiophene to IL after performing the extraction procedure. The highest absorption capacity was found for [BMIM][PF_6] (3.5:1) with somewhat smaller values reported for [BMIM][BF_4] and [EMIM][BF_4] (2.2:1 and 0.86:1, respectively).[122] NMR analysis was also used to monitor IL regeneration as well as recovery of the absorbed S-containing compounds.

A ^1H NMR study confirmed that [BMIM][OTf] and [OMIM][Cl] were good extraction agents for ethanol from mixtures with *tert*-amylethyl ether: the extraction is needed for ether purification in an industrial process.[123,124] NMR (750 MHz) was utilized for the determination of the solute distribution ratio and the selectivity of the solvent. A more recent study has shown that [EMIM][$EtSO_4$] was an even better choice with the highest purity of *tert*-amylethyl ether recovery of all the IL systems considered.[125]

Liquid−liquid equilibrium data for a system containing limonen, linalool, and [EMIM][$EtSO_4$] were measured by Arce and co-workers using direct ^1H NMR analysis of the different phases at equilibrium.[126] This method allows quantitative analysis of the contents of the three components as well as construction of corresponding tie-line diagrams with good accuracy (Figure 7). Because separation of linalool from the binary mixture is an important challenge in the food and cosmetic industry, the study focused on the determination of the linalool distribution ratios and selectivities, as well as the effect of temperature.[126] A comparative analysis of the extraction performance of [EMIM][$MeSO_3$] as well as regular organic solvents indicated that the IL provides the highest linalool purity.[127]

The liquid−liquid equilibrium at various temperatures of the ternary hexane−benzene−[EMIM][Tf_2N] system was determined using ^1H NMR.[128] It was demonstrated that the IL can be an excellent solvent for liquid extraction processes aimed at the separation of aromatic and aliphatic hydrocarbons. Separation of toluene from the toluene/heptane mixtures using ILs was studied by GC and NMR analytical methods; ^1H NMR spectroscopy was reported as being

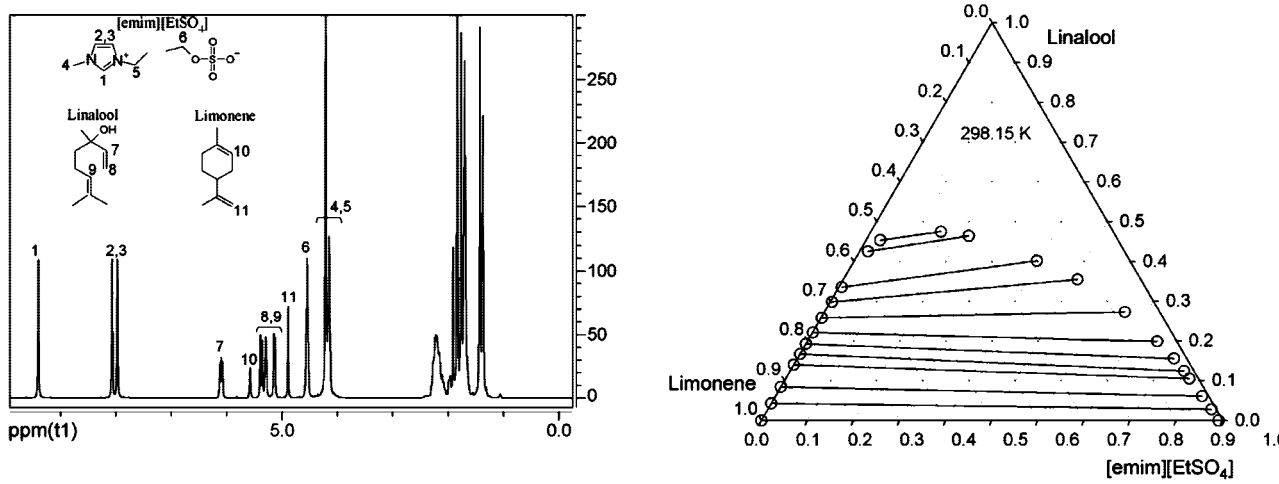

Figure 7. (Left) An example of a 500 MHz ^{1}H NMR spectrum of the mixture with signal assignment; (Right) experimental tie-lines (298 K). Reproduced with permission from ref 126. Copyright 2007 Elsevier.

necessary because ILs did not elute from a gas chromatography column.[129]

The liquid−liquid phase-separation phenomenon with lower critical solution temperature (LCST) in the binary mixture of poly(ethylglycidyl ether) and [EMIM][Tf_2N] was studied with variable-temperature ^{1}H NMR (65−105 °C) using a double-tube technique.[130] The hydrogen bonds between the protons of the [EMIM]$^+$ cation and the oxygen atoms of the poly(ethylglycidyl ether) chain were found to be the primary driving force for the LCST-type phase behavior.[130]

The stability constants of cesium complexes with the 18-crown-6 ether were measured using ^{133}Cs NMR in the [BPy][CH_3SO_4], [BMPy][BF_4], and [BMIM][Tf_2N] systems.[131] Interestingly, it was found that a 1:1 complex of Cs^+/18-crown-6 was formed in [BPy][CH_3SO_4], whereas both 1:1 and 1:2 species were formed in [BMPy][BF_4]. Variable-temperature NMR (30−50 °C) was used to estimate the thermodynamic parameters of the second 18-crown-6 molecule complexation to the 1:1 complex in [BMPy][BF_4]: $\Delta H = 47$ kJ mol^{-1} and $\Delta S = 131$ J mol^{-1} K^{-1}. Thus, it can be concluded that the enthalpy change is favorable for the formation of the 1:2 complex, whereas the entropy change hinders the complexation.[131] The study was further extended to investigate the influence of the nature of cation and anion of ILs on the stability of cesium complexes with 18-crown-6.[132]

Lithium complexes with several different crown ethers were studied by ^{7}Li NMR in [EMIM][$AlCl_4$].[133] The stability of the 1:1 complexes was found to change in the order: 18-crown-6 < 12-crown-4 < benzo-15-crown-5 < 15-crown-5. Variable-temperature NMR (5−84 °C) was applied to determine the stability constants at different temperatures as well as to calculate the ΔH and ΔS values.[133]

As reported by Wang and co-workers, nanosized copper pollutants in environmental contamination sources can be extracted using ILs with high efficiency (80−95%) and a short contact time (~2 min).[134] A ^{1}H NMR study revealed that the key interaction of Cu(II) and the nitrogen atoms of the IL enhanced dissolution and the extraction properties.[134]

2.6. Solvent−Solute Interactions

Solvent−solute interaction studies address a broad range of topics involving IL solutions of inorganic species, organic molecules, and even large biomolecular compounds such as carbohydrates and proteins. The discussion in this section is organized according to the increasing size of the solute molecules. Because questions related to the water−IL, gas−IL systems, and extraction have been considered earlier (see sections 2.2, 2.4, and 2.5, respectively), they will not be repeated here.

NMR spectroscopy in native IL systems made an important contribution to the studies dealing with the solvation and transport properties of the Li^+ ion in connection with the development of high-performance lithium batteries. Hayamizu and co-workers carried out a multinuclear ^{1}H, ^{7}Li, and ^{19}F NMR study of the quaternary ammonium room-temperature IL, [DEME][Tf_2N]. They obtained measurements for self-diffusion coefficients and spin−lattice relaxation times.[135] A similar study was also carried out for the [MMPIM][Tf_2N] IL ([MMPIM]$^+$−1,2-dimethyl-3-propylimidazolium) system.[136] In the study, the reorientational motion of the cation and lithium ion jump distances were estimated to characterize the ion transport properties of this particular IL in view of its possible application as an electrolyte for lithium batteries.[135] Lee and co-workers investigated the origins of potential difficulties associated with the possible application of ILs as an electrolyte component in lithium ion batteries.[137] Using ^{1}H, ^{31}P, and ^{7}Li NMR diffusion measurements, the authors carried out a quantitative investigation of the transport properties of IL-modified electrolytes. This suggested that the faster movement of the [BMMIM]$^+$ cation versus Li^+ was the main reason a barrier layer for lithium ion transport developed.[137] Faster diffusion of [EMIM]$^+$ cation was also observed in the ^{1}H, ^{19}F, and ^{7}Li NMR study of self-diffusion of the individual components of the [Li]$^+$/[EMIM]$^+$/[BF_4]$^-$ system.[138,139] By varying the $LiBF_4$ concentration in [EMIM][BF_4], it has been shown that Li^+ and BF_4^- form an ion complex and diffuse together. Formation of the ion complex increases the number of active [EMIM]$^+$species. Thus, the ion conductivity of this particular system was governed mainly by diffusion of the [EMIM]$^+$cation.[138] Saito

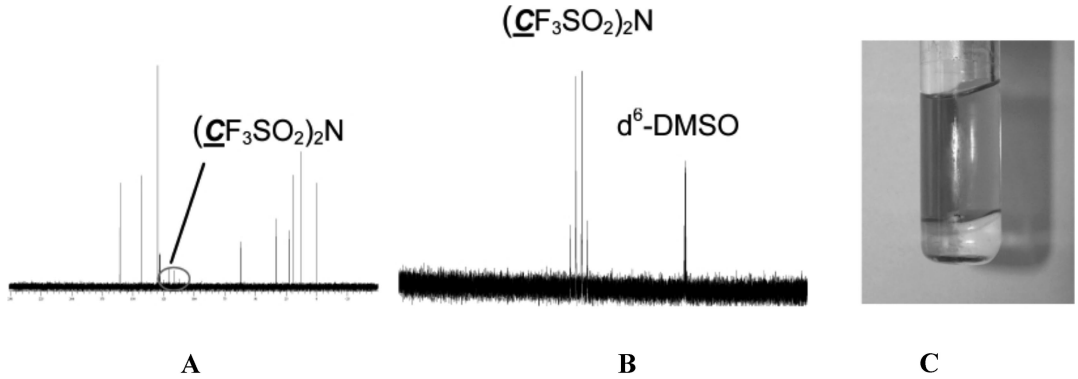

Figure 8. ^{13}C NMR spectra of the upper (A) and lower (B) phases of the biphasic system [BMPy][Tf_2N]−$AlCl_3$ = 1:2.2 (C); DMSO-d_6 was used as external standard (75 MHz (300 MHz for ^1H), 298 K). Reproduced with permission from ref 149. Copyright 2004 The Royal Society of Chemistry.

and co-workers have shown that the lithium species in lithium IL electrolytes have a solvated form $Li(Tf_2N)_{n+1}^{n-}$, with the solvation number (n + 1) being ∼3−4 in the $LiTf_2N$/[BMMIM][Tf_2N] system.[140] As a result, solvated lithium species are negatively charged, and their motion to the anode for lithium deposition is restricted. Apparently, the solvation bonds between Li^+ and Tf_2N^- need to be released for better performance.[140] Passerini and co-workers carried out a detailed NMR study of the interactions of [MPPyrr][TF_2N] with $LiTf_2N$ and correlated the spectral data with a phase diagram and other measurements.[141] A combined multinuclear NMR and ac impedance spectroscopy study was carried out by Roling and co-workers for $LiTf_2N$ solutions in [BMPyrr][Tf_2N] to develop a strategy for further improving the lithium transfer number.[142] Two-dimensional $^1H-^7Li$ and $^{19}F-^7Li$ HOESY NMR was successfully applied for the analysis of structure-properties analysis of lithium electrolytes based on ILs containing aliphatic quaternary ammonium cations.[143] The ^1H NMR chemical shifts and ^1H and ^{19}F self-diffusion coefficients of the anion and cation were used to characterize a novel type of protic IL consisting of bis(trifluoromethanesulfonyl)imide and benzimidazole.[144] The measured characteristics, combined with other IL physical properties, were used to rationalize the electroactivities for H_2 oxidation and O_2 reduction on a Pt electrode and showed a favorable potential of these ILs as fuel cell electrolites.[144]

Solid-state NMR spectroscopy was successfully utilized to investigate a binary organic/inorganic crystalline electrolyte consisting of the phosphotungstic acid $H_3PW_{12}O_{40}\cdot nH_2O$ and the IL [BMIM][Tf_2N].[145] The ^1H and ^{31}P spectral analysis revealed that coordination of $[BMIM]^+$ and $PW_{12}O_{40}^{3-}$ resulted in restricted motion of the ions. It was concluded that the ion jump in this system occurs during the melting and solidification of the hybrid material.[145]

^{27}Al NMR spectroscopy has been used to study an $AlCl_3$ solution in 1:1 [BPy][$AlCl_4$] IL.[146] The formation of $[AlCl_4]^-$ and $[Al_2Cl_7]^-$ was detected directly in the IL using ^{27}Al NMR. The study showed that the IL was not a static solution; rather it can be better described as a series of equilibria.[146] Possible interaction modes of the $[Al_2Cl_7]^-$ anion with the nitrogen atoms of the cation were discussed by comparing ^{13}C NMR data for the [BPy][$AlCl_4$] and [BDMAP][$AlCl_4$] ILs,[147] as well as for the interaction of *N,N*-dimethylaniline with [EMIM][$AlCl_4$].[148]

^1H, ^{13}C, and ^{19}F NMR spectroscopy were all utilized to study phase transitions when $AlCl_3$ was dissolved in [BMPy][Tf_2N] and with a view to designing a new IL system.[149] Wasserscheid and co-workers observed a surprisingly high solubility of $AlCl_3$ in the IL. Depending on the structure of the cation, as high as 5 mol of $AlCl_3$ may dissolve in 1 mol of IL. A remarkable feature of the system, which showed biphasic behavior in some specific composition ranges, was directly characterized by NMR spectroscopy (Figure 8). For example, at an IL/$AlCl_3$ ratio of 1:2.2, the upper phase was found to contain a mixture of cation and chloro−[Tf_2N]−aluminate ions, while the lower phase was composed of a mixture of neutral chloro−[Tf_2N]−aluminum species.[149] Both phases were clearly distinguishable by NMR analysis in the native state.

D'Anna, Noto, and co-workers have found that the addition of a small amount of organic solvent may significantly change the structure of neat ILs.[150] An amount even as small as 75 μL of dioxane added to 0.5 mL of [BMIM][BF_4] induced noticeable changes in the ^1H NMR spectrum. The H-2 signal of the IL was split into a couple of signals of varying intensity (similar changes were also observed for some other IL signals). The spectral data suggested formation of different ion-pairs in the mixture. Remarkably, very slow reorganization of the IL molecules has been mentioned in the study (i.e., several days as monitored using ^1H NMR).[150] The interaction of IL with cosolvents (dioxane, ethylacetate, MeOH, amines) led to chemical shift changes of the H-2 proton $\Delta\delta$ up to ∼0.1−0.5 ppm, depending on the content.[151,152] The degree of disorder induced by the cosolvent depended on the nature of the IL: [BMIM][BF_4] was more sensitive than [BMIM][Tf_2N].[150,151] The reorganization of the IL observed by ^1H NMR was independently confirmed by a UV−vis spectral study as well as conductivity measurements.[150−152]

An in-depth study of the effects of a cosolvent on the structure of ILs was carried out by Pregosin and co-workers using ^1H chemical shifts and diffusion measurements on a 400 MHz NMR instrument.[153] In addition, a series of two-dimensional $^1H-^{19}F$ HOESY and ^1H NOESY NMR experiments were measured on neat and binary IL systems. The $^1H-^{19}F$ HOESY spectrum of the neat IL as well as binary mixtures with CD_3OD or CD_2Cl_2 as cosolvents (Figure 9), together with the 2D NOESY data, revealed several unusual features. In the neat IL, there are strong interaction contacts from $[BF_4]^-$ to all the ring protons without noticeable selectivity. This observation challenges the commonly accepted picture of hydrogen bonding being the primary interaction between cation and anion, because if this were the case more selective interactions would be expected. The

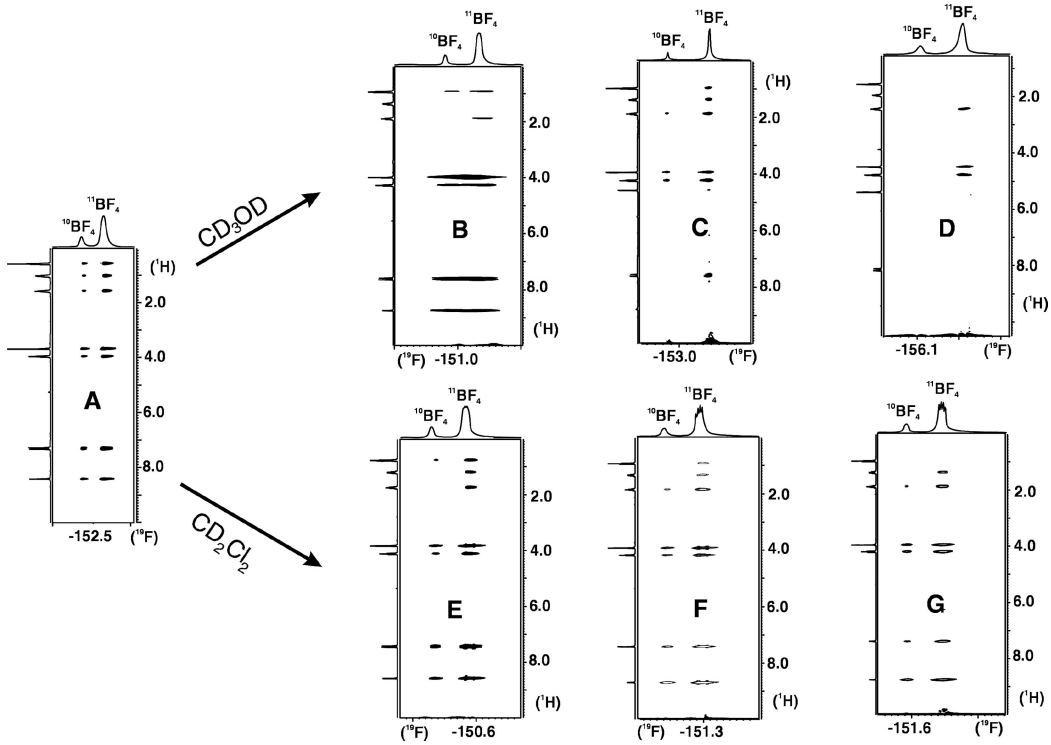

Figure 9. Series of ^{1}H, ^{9}F-HOESY spectra under different conditions: (A) neat IL (IL) [BMIM][BF_4], (B) 0.55 mL IL + 0.05 mL CD_3OD, (C) 0.1 mL IL + 0.5 mL CD_3OD, (D) 0.01 mL IL + 0.59 mL CD_3OD, (E) 0.55 mL IL + 0.05 mL CD_2Cl_2, (F) 0.1 mL IL + 0.5 mL CD_2Cl_2, and (G) 0.01 mL IL + 0.59 mL CD_2Cl_2 (400 MHz, 300 K). Reproduced with permission from ref 153. Copyright Elsevier 2006.

study of such binary systems revealed that even a small amount of cosolvent dramatically reduces potential aggregation within the IL (i.e., 0.05 mL of organic solvent added to 0.55 mL of IL). Methanol additives were found to significantly reduce the intensity of the cross-peaks (Figure 9). This observation indicates strong solvation by the methanol, which in turn reduces anion−cation contact. Dichloromethane additives, in contrast, do not eliminate cross-peaks, which suggests strong ion pairing in this system (Figure 9).[153]

The nature of the interactions of aluminum halide−alkylpyridinium halide molten salts with benzene has also been studied using ^{1}H and ^{13}C NMR.[154,155] The addition of benzene to the IL resulted in a decrease in the dielectric constant of the medium and initiated ion pair formation between the alkylpyridinium cations and the anions.[154] Liquid clathrate formation between 1-alkyl-3-methylimidazolium-containing ILs and aromatic hydrocarbons was investigated using ^{1}H NMR.[156] Interaction of the π-system of toluene and the IL imidazolium ring was investigated by a combined NMR study and molecular dynamics simulations.[157] The solvent−solute interactions and the site−site distances between toluene and the IL were found to be strongly dependent on the substitution at the C_2 position of the imidazolium ring as determined by ^{1}H NMR and 2D ROESY experiments. Toluene was found to penetrate into the bonding network of the IL [BMMIM][Tf_2N], and the π-system of toluene was oriented in a plane parallel to the $[BMMIM]^+$ cation. In contrast, the presence of hydrogen bonding between the C_2−H and the anion in [BMIM][Tf_2N] (calculated association energy > 20 kJ mol^{-1}) stabilized the IL aggregates and toluene penetration did not take place.[157]

The superacidic properties of a 2:1 melt of $AlCl_3$/TMSuBr and $AlCl_3$/TMSuBr with added HBr were studied by ^{1}H NMR ($[TMSu]^+$−trimethylsulfonium).[158] It was shown that both melts exhibit properties of a Brønsted superacid, since *m*-xylene, toluene, and benzene were all found to be either partially or completely protonated. A comparative study of toluene and benzene protonation in the $AlCl_3$−[TMSu][Br]−HBr and $AlCl_3$−[EMIM][Cl]−HCl systems revealed the same degree of protonation, thus suggesting that both melt systems have similar acidities.[158,159]

^{13}C NMR was used by Srinivasan and co-workers to evaluate the Brønsted acidity of [HBIM][BF_4] through observing the interaction of the IL with the carbonyl group of selected aldehydes and β-keto esters.[160−162] The interactions resulted in a ~3 ppm change in the chemical shift of the carbonyl group. Recording ^{1}H NMR spectra of neat [HBIM][X] ([X] = $[BF_4]^-$, $[Cl]^-$, $[Br]^-$, $[ClO_4]^-$) made it possible to find out the correlation of chemical shifts of N−H protons with acidity and chemical reactivity.[163]

The Brønsted acidity of the ILs formed by combining [BMIM][Cl] and 2 equiv of the group IIIA metal chlorides ($AlCl_3$, $GaCl_3$, $InCl_3$) was characterized by ^{13}C NMR. The results were compared with sulfuric and triflic acids.[164] The measurements were carried out for the neat ILs and then repeated after HCl(gas) adsorption. To estimate the Hammet acidity, the authors carried out a careful analysis of the NMR spectra and discussed possible ways of signal assignment. Good correlations between the Hammet acidity function estimated from the ^{13}C NMR chemical shifts in the ILs and toluene carbonylation ability were reported. The authors suggested that, in these ILs, up to three separate environments of Brønsted acidity may be available, some of them with superacidity properties after the addition of HCl.[164]

The interaction of thiophene with ILs has been studied in detail using ^{1}H, ^{11}B, ^{19}F, and ^{31}P NMR spectroscopy.[122] Thiophene dissolution in the IL resulted in pronounced changes into the NMR chemical shifts of the protons of the

imidazolium cation as well as in the boron, phosphorus, and fluorine atoms of the anions. For each of the ILs studied, at the maximum absorption of the thiophene, the NMR results suggested that relatively ordered stacking structures of 4/1, 2/1, and 1/1 were formed for the thiophene/[BMIM][PF_6], thiophene/[BMIM][BF_4], and thiophene/[EMIM][BF_4] species, respectively. The results from this structural study were in agreement with the measured highest absorption capacity for these ILs.[122]

The aggregation behavior of the solute molecules was found to be strongly dependent on the nature of the IL. Using a fluorinated surfactant as model solute compound, it was found that traditional micelles formed in [BMIM][BF_4], whereas, as evidenced by ^{1}H NMR, formation of segregated nanodroplets of the solute was observed in [BMIM][PF_6].[165] Interaction of [BMIM][BF_4] with *p*-xylene in the presence of a surfactant led to the formation of a microemulsion, which was characterized by ^{1}H NMR.[166] The 2D ROESY experiment was found to be an efficient method for studying the microstructure of micelles in [BMIM][BF_4] and [BMIM]-[PF_6] ILs[167] and "oil-in-IL" micelles in [BMIM][BF_4].[168] Formation of the "oil-in-water" micelles was reported in the presence of the [BMIM][BF_4] according to a combined study using optical microscopy, small angle X-ray diffraction, and ^{1}H, ^{19}F, ^{23}Na diffusion NMR.[169] The analysis of the sodium bis(2-ethylhexyl)sulfosuccinate/water/[BMIM][BF_4] ternary system showed that the IL was strongly adsorbed at the interface and initiated substantial modification of the interfacial geometry, resulting in establishing of the micellar phase.[169] Thermodynamic parameters, determined by variable-temperature ^{1}H NMR (25−50 °C), have shown that micelle formation of polyoxyethylene surfactants in [BMIM][BF_4] is entropy-driven at low temperature, whereas the process becomes enthalpy-driven at high temperature.[170] The ^{1}H NMR analysis of the hydrogen-bond interactions has shown that solvophilicity of the polyoxyethylene surfactants is much higher in [BMIM][PF_6] compared to [BMIM]-[BF_4].[171]

It is interesting to point out that the reverse "IL-in-oil" microemulsions studied by diffusion NMR and other methods were used as nanoreactors to perform the Matsuda−Heck reaction in the presence of Pd catalyst.[172] The product yield in the microemulsions (67%) was significantly larger compared to the reaction in bulk IL (33%), and a correlation between the reaction yield and the amount of IL was observed.[172] This study highlights a possible strong effect of confinement inside the IL microemulsions on the structure and properties of dissolved species.

A complex methodology, based on ^{1}H NMR, Fourier transform−Raman (FT-Raman), and conductivity measurements, was developed by Riisager, Wasserscheid, and coworkers for analysis of the IL/1-hexanol binary model system.[173] The liquid−liquid equilibrium phase diagram showed good consistency between the complementary measurements using the different techniques. The approach was useful for obtaining information about miscibility and for determining critical solution temperatures. Analysis of $\Delta\delta(^1H)_{OH}$ values for the hydroxyl group of the alcohol provided information concerning the hydrogen-bond redistribution on transition from pure organic liquid to the binary IL system.[173] Specific interactions and solvation of the IL [OMIM][BF_4] with ethylene glycol derivatives were addressed by Singh and Kumar using a combination of ^{1}H NMR, UV−vis, and FT-IR techniques.[174] Analysis of the chemical shift values was carried out to reveal different packing effects in the binary mixture.

A structural and chemical investigation of the interaction of the model IL tetramethylammonium fluoride tetrahydrate, $[(CH_3)_4N]F\cdot 4H_2O$, with supercritical/subcritical CO_2 and methanol has been reported by Yonker and Linehan.[175] The formation of methylcarbonate and ethylcarbonate were observed in situ under typical conditions used for supercritical CO_2 methodology.

The ^{1}H NMR study of the solutions of ferrocene and cobaltocenium cation in the [BMIM][BF_4] and [BMIM][PF_6] ILs has shown that the solute molecules in a small concentration did not change the ILs aggregation in significant manner.[176] Rather, the interaction of the solute species with the surfaces of the aggregates was proposed. The study indicated that even subtle structure changes in the system may play an important role in modifying the mass transport and dynamic properties.[176]

A high-resolution ^{13}C NMR study of cellulose and cellulose oligomers was performed in [BMIM][Cl] solution.[177] According to the ^{13}C chemical shifts, the interaction of the solute with the IL leads to a disordered oligomer structure. It was suggested that the IL could be used as a versatile nonderivatizing/nondegrading solvent for studying cellulose materials.[177] Brendler and co-workers used 1D and 2D NMR experiments involving ^{1}H and ^{13}C nuclei to provide important data about dissolving abilities and interactions of molten salt hydrates and cellulose. In addition, ^{7}Li NMR in the presence of $LiClO_4$ or LiSCN salts proved a useful technique.[178] The ^{1}H and ^{13}C NMR spectra confirmed that neither decomposition of the IL nor derivatization of microcrystalline cellulose takes place during dissolution in [EMIM][(MeO)RPO_2] (R = H, Me, MeO).[179] The mechanism of cellulose dissolution in [BMIM][Cl] was studied using ^{13}C and $^{35/37}$Cl NMR and model systems. The important role of hydrogen bonding between the hydroxyl protons of solutes and chloride ions of IL (1:1 stoichiometry) was revealed.[180] A multinuclear NMR study of the solvation of carbohydrates in the [RMIM][X] ionic liquids series (R = methyl, ethyl, butyl, and allyl; X = Cl, OAc) has shown that the process is governed by the interactions between the IL anion and the carbohydrate.[181,182] The interactions of the IL cation and the solute was found to be relatively weak[182] or at least too weak to play a significant role in solvation.[181] The importance of cellulose treatments using new advanced methods prompted several investigations on the subject that involved MAS NMR.[183]

Recently, it was reported that proteins can dissolve in ILs. A surprisingly high thermodynamic stabilization of proteins by the IL media was reported.[184−186] Byrne and Angell have shown that easily adjustable proton acidity suggests ILs can function as a convenient media to study the protein folding/unfolding process.[187] The ^{1}H NMR chemical shifts of the N−H group of the ammonium cation (7.05−9.15 ppm range) provided the necessary information about the acidic properties of ILs. The study involving [BMIM][ClO_4] IL[187] and various ammonium cations was applied to two proteins—hen egg white lysozyme and ribonuclease A.[184−188] The authors noticed that solutions of the proteins in ILs can show several surprising properties such as stability to hydrolysis and aggregation, ability for multiple folding/unfolding cycles, etc. It appears that this novel application of ILs is worth further investigation by NMR spectroscopy.

Scheme 2. Diels−Alder [4 + 2]-Cycloaddition Reaction[189]

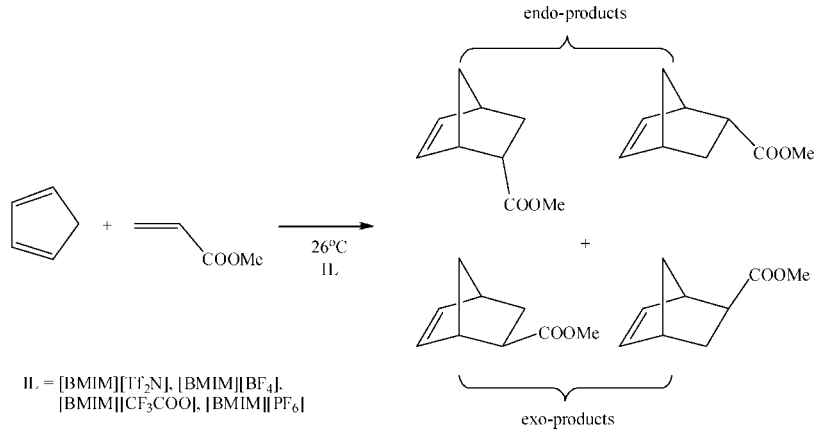

Scheme 3. Interaction of Acetyl Chloride with $AlCl_3$ Based on NMR Study[191]

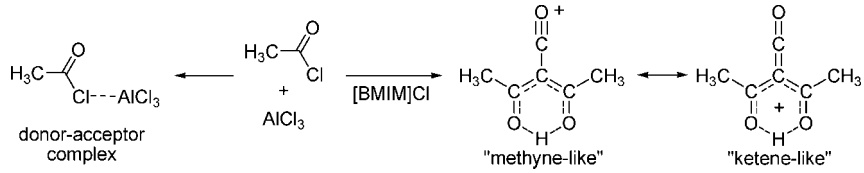

2.7. Monitoring of Chemical Reactions

Direct NMR investigation of chemical reactions being carried out in ILs is one of the most powerful analytical applications of the method, resulting in a great impact on our knowledge about the mechanistic nature of the observed transformations. The results of published NMR studies of chemical reactions, including NMR monitoring in ILs, are discussed in this section.

The Diels−Alder reaction between cyclopentadiene and methyl acrylate was investigated in situ by using ^1H and ^{13}C NMR in different ILs (Scheme 2).[189] The NMR study indicated that the rate of formation of the *exo*-products was unaffected by the presence of the IL, whereas the rate of formation of the *endo*-products was increased. This lead to an overall higher selectivity. It was shown that the lowering of transition state energies was related to the interactions between the transition state and the solvent, rather than to highly specific structure-dependent interactions.

An empirical solvent parameter scale, based on NMR spectroscopy data ("the Δ scale"), was developed to predict the selectivity of Diels−Alder reactions in ILs (a similar NMR approach was used to predict carbon monoxide solubility in ILs; see section 2.4).[189]

A ^1H NMR study of the mechanism of a Friedel−Crafts reaction in the IL [EMIM][$AlCl_4$] suggested a stoichiometric reaction between the CH_3OH and $[Al_2Cl_7]^-$, which may lead either to the 1-oxoethylium electrophile (CH_3CO^+) or to the undissociative reactive complex $CH_3COCl\cdots[Al_2Cl_7]^-$.[190] Thus, the IL was found to be acting both as solvent and catalyst. The anionic $[Al_2Cl_7]^-$ species was proposed as the plausible catalytic center in the IL.

A comparative in situ NMR study by Horváth and co-workers was carried out in order to understand the differences of acetyl chloride interactions with $AlCl_3$ in both regular organic solvents and an IL.[191] In contrast to a regular donor−acceptor complex, the formation of the diacetylacetylium tetrachloroaluminate, $[(CH_3CO)_2CHCO]^+[AlCl_4]^-$, via trimerization of the acetyl chloride was observed in the IL (Scheme 3). Understanding the differences between these reactions played an important role in shedding light on the mechanism of the Friedel−Crafts acylation reaction. Another important question concerns the nature of the trimer, since the contribution from "methyne-like" and "ketene-like" resonance forms could be expected (Scheme 3).

An in situ NMR study in an IL clearly detected the formation of the $[(CH_3CO)_2CHCO]^+$ cation (^1H, ^{13}C, and DEPT) and the $[AlCl_4]^-$ anion (^{27}Al). A two-dimensional $^{13}C-^{13}C\{^1H\}$ COSY experiment involving a labeled $CH_3{}^{13}COCl$ substrate was used to confirm the proposed structure of the trimer (Figure 10). Analysis of the $^{13}C-^{13}C$ coupling constants provided further structural information and made it possible to assign a "ketene-like" structure in agreement with the observed NMR signals (Figure 10).[191]

Several carbocation-forming reactions in native IL systems were investigated by Creary and co-workers using both ^1H and ^{19}F NMR.[106] The ionization of trifluoroacetates, mesylates, and triflates leading to carbocationic intermediates has been studied in [BMIM][Tf_2N]. For example, the NMR measurements were successfully utilized to measure the solvolysis rate constants of substituted cumyl trifluoroacetates in the range $k = 2.93 \times 10^{-7}$ to 3.67×10^{-4} s^{-1}. The kinetic study was carried out for substrates with different electronic character of the substituents, and the corresponding Hammett parameters were obtained. The study showed that carbocation chemistry in ILs is somewhat different from the chemistry expected in regular solvents.[106]

The Ru-complex catalyzed hydrogenation reaction of benzene to give cyclohexane was studied in a range of ILs (Scheme 4).[114] It was concluded that for this reaction the solubility of H_2 in the IL has little influence on the reaction rate.[114] Interestingly, an order of magnitude difference in solubility of acetylene and ethylene played a key role in designing highly selective Pd nanoparticles system for the catalytic hydrogenation of acetylene in the [BMIM][PF_6]-supported ionic liquid phase.[118] Low ethylene solubility increased the selectivity of the process, because further hydrogenation to give ethane was greatly suppressed under these conditions.

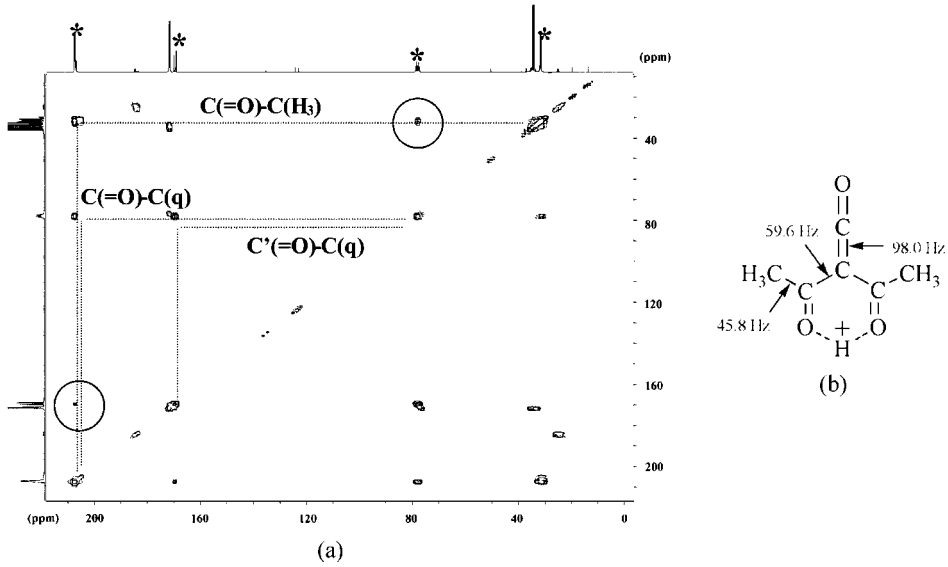

Figure 10. (a) $^{13}C-^{13}C\{^1H\}$ COSY spectrum at 125 MHz (500 MHz for ^1H) and 298 K of the $CH_3{}^{13}COCl/AlCl_3$/[BMIM][Cl] mixture and the structure assignment based on coupling constants (resonances due to structure (b) are marked with asterisks); (b) the structure with coupling constants shown. Reproduced with permission from ref 191. Copyright 2002 The Royal Society of Chemistry.

Scheme 4. Ru-Catalyzed Hydrogenation of Benzene[114]

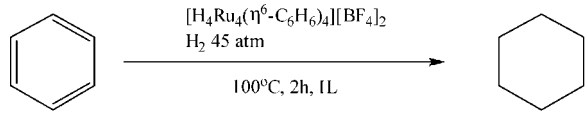

IL = [BMIM][CF_3COO], [BMIM][PF_6], [BMIM][Tf_2N], [BMIM][SbF_6], [OMIM][BF_4], [BPy][Tf_2N], [BMPyrr][Tf_2N], etc.

Scheme 5. Ru-Catalyzed Hydroformylation of an IL[117]

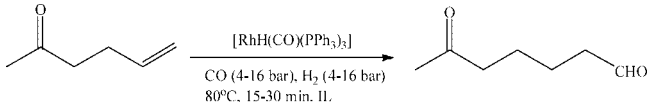

IL = [BMIM][BF_4], [BMIM][PF_6], [BMIM][Tf_2N], [HexMIM][BF_4], etc.

The investigation of the Rh-catalyzed hydroformylation of 5-hexen-2-one was performed in several ILs (Scheme 5).[117] Surprisingly, the turnover frequency (TOF) did not correlate to either the carbon monoxide solubility or the viscosity of the IL. Increasing the partial pressure of H_2 relative to CO led to an increased TOF, therefore suggesting that the oxidative addition of H_2 could be the rate-determining step. Increasing the partial pressure of CO relative to H_2 decreased the TOF. This is most likely due to formation of stable carbonyl complexes.[117]

The mechanism of Rh-catalyzed hydroformylation in an IL was studied using NMR spectroscopy by Agbossou-Niedercorn and co-workers.[192] Analysis of the 2D ROESY spectrum revealed the interaction between the ligand (a sulfonated derivative of triphenylphosphine) and the protons of the imidazolium ring of [MBMIM][Tf_2N]. The observed NMR patterns are evidence of the existence of π-stacking interactions and allowed deduction of the possible structure of the [MBMIM]−ligand complex (Figure 11). The study indicated that the catalytic properties of the Rh system with the sulfonated triphenylphosphine ligand can be altered in the IL. On the other hand, for the neutral triphenylphosphine ligand, the properties of the catalyst are mostly preserved with respect to those observed in pure organic solvents.[192]

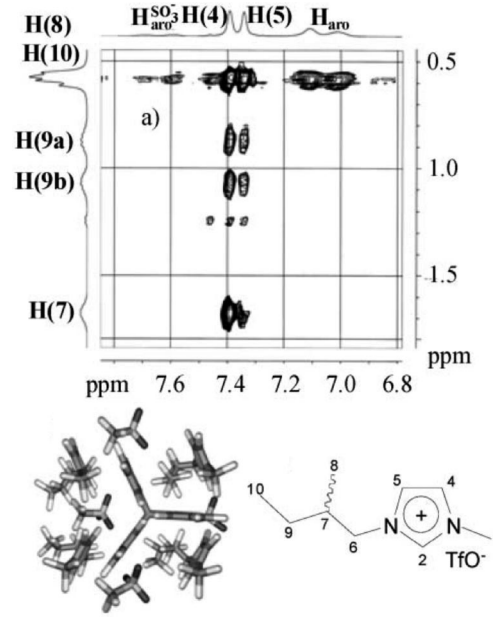

Figure 11. Partial plot of the 2D ROESY spectrum of the [MBMIM][Tf_2N]−ligand mixture and the proposed structure of the corresponding complex (300 MHz, 300 K). Reproduced with permission from ref 192. Copyright 2008 The Royal Society of Chemistry.

The formation of N-heterocyclic carbenes in biphasic hydroformylation reactions promoted by Rh complexes in [BMIM][Tf_2N] was evident from ^1H and ^{13}C NMR data.[193] This study also highlighted the role of the phosphine ligand in the reaction.

The mechanism of methyltrioxorhenium-catalyzed olefin epoxidation was studied by Abu-Omar and co-workers using ^2H NMR spectroscopy (Scheme 6).[194] Two different approaches were utilized to obtain kinetic information for the reaction. First, the oxidation of deuterated substrates (styrene-d_8, cyclohexane-d_{10}) was monitored by ^2H NMR. The signals of the substrates and products (epoxide or diol) were well resolved in the ^2H NMR spectra. Second, the nondeuterated alkenes (styrene, 2-fluorostyrene, 2,6-difluorostyrene) were

Scheme 6. Re-Catalyzed Olefin Epoxidation in ILs Based on the ^{2}H NMR Study[194]

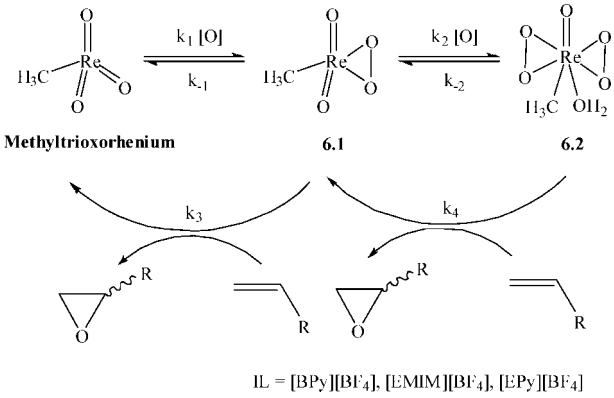

Scheme 7. Re-Catalyzed Dihydroxylation of C=C Bond[196]

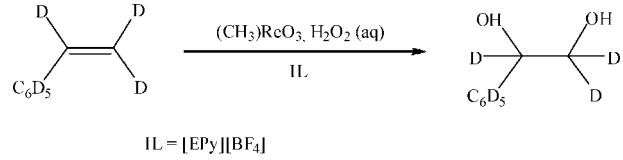

Scheme 8. Main Product and Side Products in the Oxidation of Benzyl Alcohol by Ceric Ammonium Nitrate (CAN) in [EMIM][TfO][197]

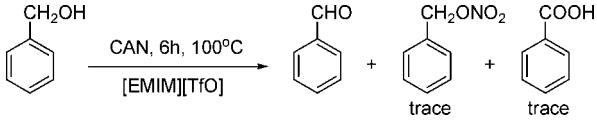

reacted with the deuterated rhenium complex CD_3ReO_3. On the basis of kinetic measurements, the fast step was assigned to the reaction of the olefin with **6.2** (k_4) whereas the reaction with **6.1** (k_3) was shown to be slow (Scheme 6). For the ILs studied, the following rate ratio was determined: $k_4 = 4.5k_3$. It should be noted that in regular solvents the opposite relationship was observed, where **6.1** was more reactive than **6.2**. The rate constants k_4 and k_3 were sensitive to the structure of the IL anion but not sensitive to the structure of the cation.[194]

The electrochemical oxidation of anthracene-d_{10} and the H/D exchange reaction was monitored by ^{2}H NMR in [EMIM][$AlCl_4$].[195] ^{2}H NMR monitoring of the catalytic styrene-d_8 oxidation by aqueous H_2O_2 leading to styrene-d_8−1,2-diol (Scheme 7) revealed a steady-state intermediate. This was assigned as being the η^2-diolato complex of a Re(VII) peroxo species.[196]

The oxidation of benzyl alcohol by ceric ammonium nitrate in the IL [EMIM][TfO] was studied by Binnemans and co-workers, using ^{13}C NMR (Scheme 8).[197] The formation of benzyl nitrate and benzoic acid as side products during the oxidation reaction was detected by NMR monitoring (Figure 12). An interesting feature of the recorded NMR spectra was the presence of a broad signal of benzyl alcohol, which can be an evidence for a rapid exchange of free and cerium-coordinated substrate.[197]

The performance of the [BMIM][X] IL series, where ([X] = $[Cl]^-$, $[Br]^-$, $[ClO_4]^-$, $[BF_4]^-$, $[PF_6]^-$), used to promote sonochemical acetylation was correlated to the nature of the anion by considering the relationship between the ^{1}H chemical shifts of the most deshielded imidazolium proton and the reaction time needed for complete conversion.[198] The chemical shifts of the imidazolium protons ($\delta(^1H)$ = 8.9−10.6 ppm) were used as an indicator of the Lewis/

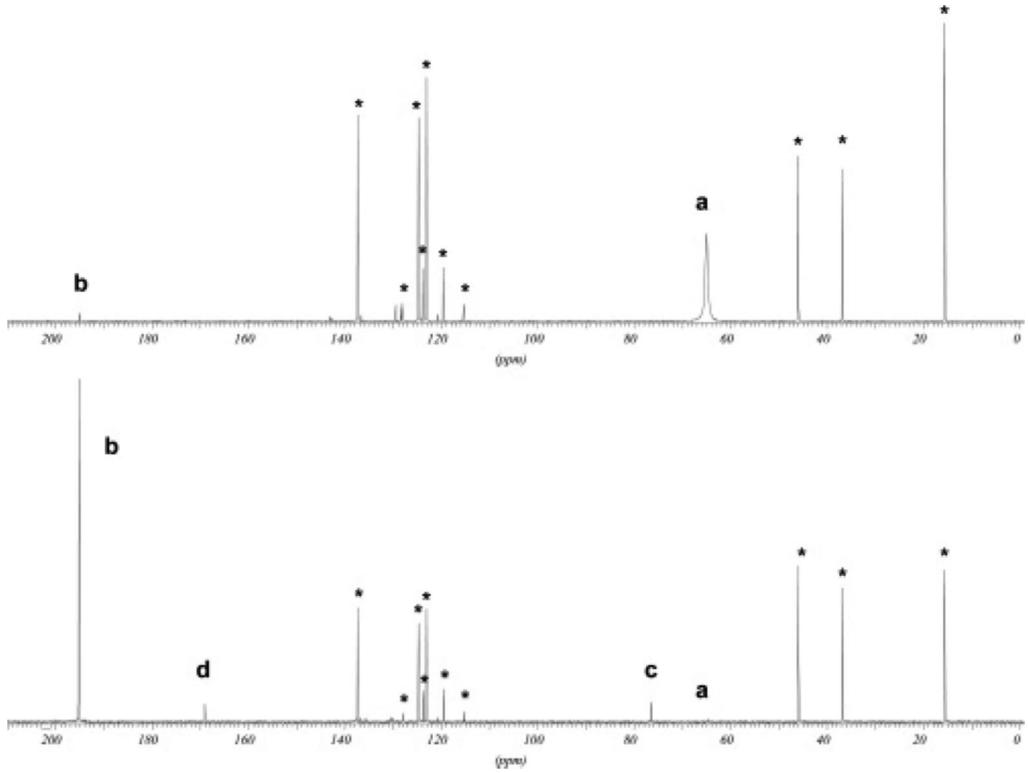

Figure 12. $^{13}C\{^1H\}$ NMR monitoring of the oxidation of ^{13}C labeled $Ph^{13}CH_2OH$ by $(NH_4)_2(Ce(NO_3)_6)$ in [EMIM][TfO] after 5 min (top) and 6 h (bottom) of reaction (75 MHz (300 MHz for ^{1}H), 298 K). Peak labels are as follows: (a) benzyl alcohol, (b) benzaldehyde, (c) benzyl nitrate, and (d) benzoic acid. The resonances marked by an asterisk (*) are due to the [EMIM][TfO] IL. Reproduced with permission from ref 197. Copyright 2005 American Chemical Society.

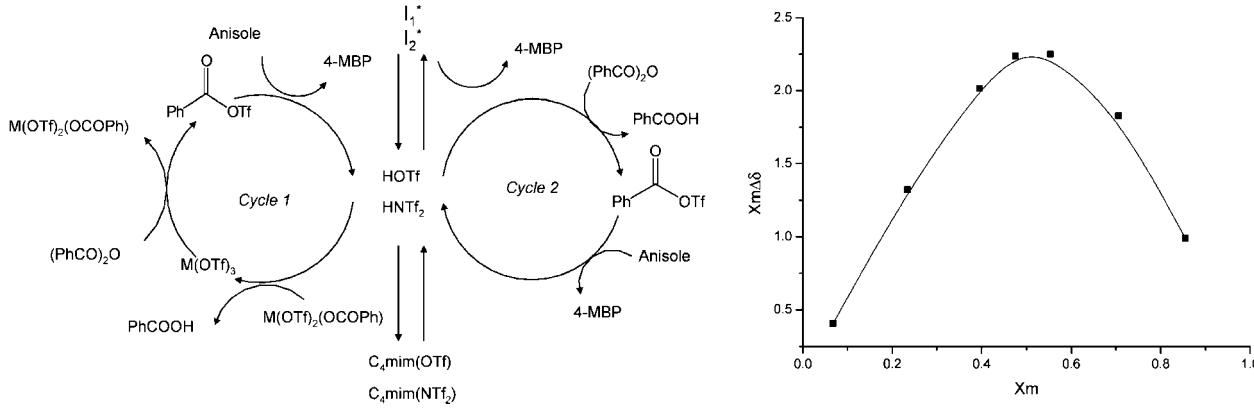

Figure 13. Proposed mechanism of the catalytic reaction (left) and Job's plot of the $\Delta\delta$ chemical shift change of the carbonyl group vs mole fraction for 4-MBP in solution (right); I^*_1 and I^*_2 are the inactive complexes formed by complexation of the HOTf and $HNTf_2$ acids with the 4-MBP. Reproduced with permission from ref 200. Copyright 2006 American Chemical Society.

Brønsted acidities of the different ILs, the key factor for the reaction studied.

^{1}H NMR monitoring of the alkylation of aniline by MeI and EtI in [EMIM][Tf_2N] was utilized by Chiappe and co-workers to understand the origin of chemoselectivity observed in this IL.[199] The registration of spectra at regular time intervals showed that MeI was considerably more reactive than EtI. Respectively, 10 min and 1 h reaction periods were needed to reach ca. 25−30% conversion. Broadening of the ^{1}H NMR signals due to decreased resolution was evidence of the precipitation of the alkylation products directly in the NMR tube. The different solubilities of the products were suggested as being a key factor in the observed chemoselectivity.[199]

The metal salt-catalyzed benzoylation of anisole to yield 4-methoxybenzophenone (4-MBP) was studied by Rooney and co-workers by applying complementary kinetic and ^{13}C NMR techniques.[200] A rather complicated reaction mechanism was proposed for this catalytic system (Figure 13). A ^{13}C NMR examination of the reaction mixture was used for studying the interactions of $In(OTf)_3$ and triflic acid with 4-MBP in [BMIM][Tf_2N]. Evidence for the involvement of the carbonyl group in the interaction was the 6 ppm downfield chemical shift change. The stoichiometry of the interaction between 4-MBP and triflic acid was determined from ^{13}C NMR using Job's method of continuous variations. The maximum on the Job's plot at ∼0.5 confirms the 1:1 stoichiometry of the complex (Figure 13). The temperature dependence of the equilibrium constant and corresponding thermodynamic parameters of the reaction were established from variable-temperature ^{13}C NMR (20−80 °C) data.[200]

NMR monitoring was successfully used to investigate an ether cleavage reaction in the IL [HMIM][HBr_2].[42] The reaction was followed using ^{13}C{^{1}H} NMR by observing the disappearance of the substrate signals and the appearance of new product signals. This approach, which is widely used in NMR studies of chemical reactions in regular solvents, is clearly also a powerful approach for estimating reaction rates in ILs under various conditions (temperature, concentrations, etc.).

The application of ^{2}H NMR to the direct investigation of different chemical reactions in ILs has also been reported.[196] This technique was also successfully applied to the oxidation of DMSO-d_6, cyclohexene epoxidation, and dihydroxylation as well as the addition of methyl iodide to the dimethylsulfide-d_6 (Scheme 9).[196]

Scheme 9. Monitoring of Chemical Reactions Directly in IL Using NMR Spectroscopy[196]

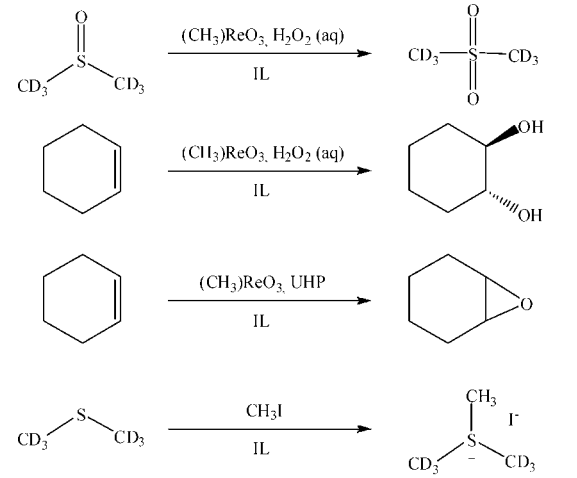

The catalytic active sites responsible for the observed selectivity in the disproportionation of light paraffins were determined in [Me_3NH][$AlCl_4$] using variable-temperature ^{1}H and ^{27}Al NMR.[201] It was found that the disproprotionation reactions begin to yield the product at a temperature of ∼80 °C: this corresponds to a phase change in the IL and to preferential formation of the $[Al_xCl_y]^-$ species.

The formation of the polyimide nanoparticles was monitored by ^{1}H and ^{19}F NMR in [EMIM][Tf_2N].[202] Polyimide nanoparticles were prepared by the heterophase polycondensation of diamines and aromatic tetracarboxylic acids. The nature of the produced polyimide was easily controlled by NMR: mobile (dissolved) polymer chains gave relatively sharp signals, while the particles (solid) resulted in very broad signals. In fact, analysis of the NMR data has shown that 30% of the polymer was represented as mobile chains and 70% of the polymer was consumed by nanoparticles formation.[202]

An interesting application of NMR spectroscopy deals with the monitoring of chemical reactions on the surface of solid particles. Reactions of [BMIM][$AlCl_4$] and [(SiC_3)MIM][Cl] with silanol groups (R_3Si-OH) on the surface of silica were monitored with ^{29}Si MAS NMR.[203] Surface coverage and the amount of residual silanol groups were both studied. ^{27}Al NMR spectral data were used to confirm partial removal of

Scheme 10. NMR Monitoring of Chemical Transformations Involving Pt Complexes[89]

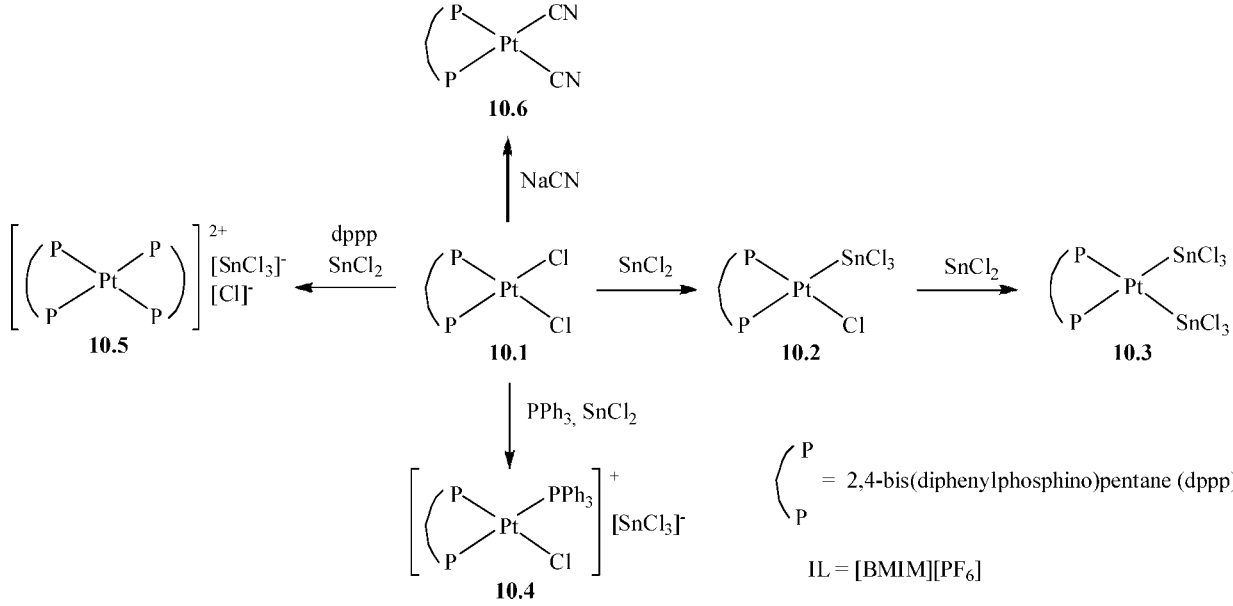

the $AlCl_3$ from the surface.[203] Solid-state ^{29}Si NMR was used to characterize the formation of a silica-supported ionic liquid via the reaction of benzyl chloride-functionalized silica with N-substituted imidazoles, followed by reaction with CuI to form supported Cu−NHC−SiO_2 catalysts.[204] The microenvironments of the solvent cages of IL ion pairs in a silica-supported Pd hydroamination catalyst and in the thin−film Rh hydrogenation catalyst were characterized with the help of multinuclear MAS NMR.[205,206] Solid-state ^{13}C, ^{19}F, and ^{31}P NMR were all successfully utilized to monitor the intercalation of phosphonium ionic liquids into polypyrrole films.[207]

Solid-state ^{11}B NMR in [BMIM][Cl] IL in a combination with solution-state ^{11}B NMR in [MMIM][$MeSO_4$] was applied to study hydrogen release from ammonia borane initiated by bis(dimethylamino)naphthalene proton sponge.[208] Formation of intermediate species was successfully detected with ^{11}B NMR, and different reaction pathways were examined. ILs were proved more favorable for efficient hydrogen release compared to other solvents.

2.8. Transition Metal Complexes

Investigation of the chemical transformation of transition metal complexes in ILs is a topic worthy of special attention. In addition to a general interest in transition metal chemistry, these reactions very often represent (or model) formation of an active form of the catalyst from the catalyst precursor. Establishing the active form of the catalyst and the structure of the catalyst active center is a problem of primary importance in catalysis. NMR studies involving Pt, Pd, Rh, Ir, Os, and Ag complexes in native IL systems are discussed in this section.

The usefulness of NMR spectroscopy in studying the reactions of transition metal complexes directly in ILs was systematically investigated using model platinum diphosphine complexes by Kollár and co-workers.[89] Using both ^{13}C and ^{31}P NMR spectroscopy, the formation of platinum complexes of catalytic importance was monitored directly in [BMIM][PF_6] (Scheme 10). Insertion of $SnCl_2$ into the Pt−Cl bond gave the trischlorostannato complexes **10.2** and **10.3**. Ligand exchange reaction with monodentate (PPh_3) or bidentate (dppp) phosphines leads to the cationic and dicationic complexes **10.4** and **10.5**, respectively. A chloride ligand exchange giving **10.6** was observed after the reaction of **10.1** with 2 equiv of NaCN. This study confirmed some similarities between the reactions of platinum complexes in ILs and conventional organic solvents.[89] On the other hand, a ^{31}P NMR study of the reaction of $PtCl_2$(dppe) with dppb =1,4-bis(diphenylphosphino)butane (dppb) and $SnCl_2$ in the same IL [BMIM][PF_6] revealed formation of the unusual cationic mononuclear $[PtCl(L^A)(\eta^1\text{-}L^B)]^+$ and dinuclear $[Pt_2Cl_2(L^A)_2(\eta^1,\eta^1\text{-}L^B)]^{2+}$ complexes (L^A and L^B denote bidentate diphosphine ligands bis(diphenylphosphino)ethane (dppe) and dppb).[209] It appears, therefore, that quite different products may be expected in ligand-substitution reactions in ILs depending on the nature of the metal complex and the ligands.

The novel ILs—bis(*N*-2-ethylhexylethylenediamine)silver(I) nitrate, [Ag(eth-hex-en)$_2$][NO_3], and bis(*N*-hexylethylenediamine)silver(I) hexafluorophosphate, [Ag(hex-en)$_2$][PF_6],—were synthesized via the reaction of $AgNO_3$ and $AgNO_3$/$NaPF_6$ with the corresponding *N*-alkylethylenediamines.[210] Complex formation was monitored with ^{13}C NMR, and the dynamic properties of the liquids were studied using diffusion measurements. Treatment of the ILs with aqueous $NaBH_4$ resulted in the formation of uniform-sized Ag(0) nanoparticles in the case of [Ag(eth-hex-en)$_2$][NO_3] in contrast to [Ag(hex-en)$_2$][PF_6], where nanoparticles were not formed. The ^{13}C spectral analysis revealed the key role of the terminal alkyl chain in this process.[210]

In situ formation of mixed phosphine−imidazolydine palladium complexes was monitored by Welton and co-workers using ^{31}P NMR (Scheme 11).[211] Addition of aryl bromide to the mixture of $Pd(PPh_3)_4$/NaCl in [BMIM][BF_4], followed by treatment with an aqueous solution of Na_2CO_3, led to the mixed complex **11.2**. The intermediate complex **11.1** and the product **11.2** were detected directly in the IL by ^{31}P NMR. In a similar way, the product **11.2** was prepared using $PdCl_2$/$Pd(OAc)_2$+PPh_3 as a source of palladium, and the intermediate complex **11.3** was also detected with ^{31}P NMR.[211]

Scheme 11. NMR Detection of Formation of Pd Imidazolydine Complex[211]

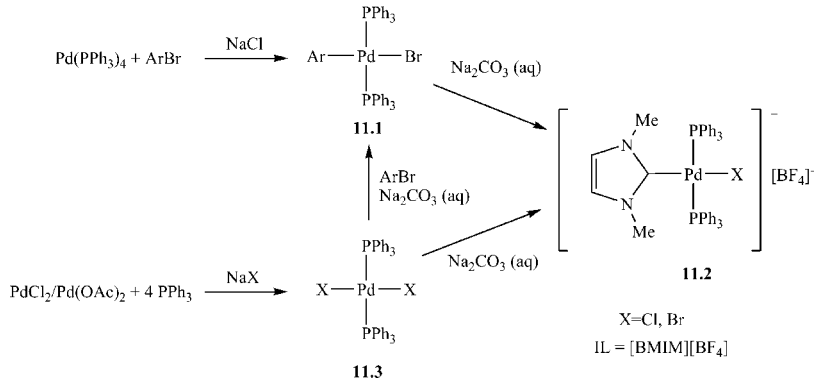

Scheme 12. Coordination of IL to the Rh Complex and Subsequent Reaction with Hydrogen[216]

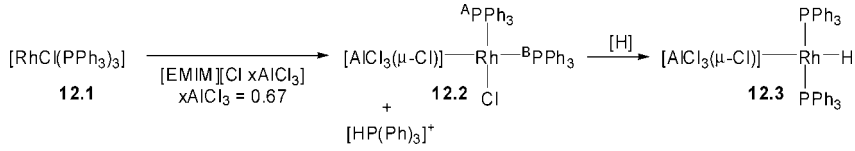

The initiation of the Pd/phospine catalyst in ILs in Suzuki cross-coupling reactions was studied by Welton and co-workers.[212] Several $[Pd(PPh_3)_2(C_4C_xIm)_nX_m]^+$ complexes (where $n = 1, 2$ and $m = 2, 1$; $x = 1$ or 4) were detected by ^{31}P NMR ($\delta(^{31}P) = 21.8 - 24.2$ ppm), and the mechanisms of their formation and decomposition were discussed. The ^{31}P NMR evidence for the palladium imidazolylidene complexes obtained was independently confirmed by electrospray ionization (ESI^+)-MS.

Conte and co-workers carried out a $^{31}P\{^1H\}$ NMR study to detect the actual presence of the $[Pt(dppb)(\mu-OH)]_2(BF_4)_2]$ catalyst in the IL [BMIM][Tf_2N] before the catalytic reaction of the Baeyer−Villiger oxidation of cyclohexanone with H_2O_2.[213] Although the Pt complex was reported to be only sparingly soluble in the IL phase, it was detected with $^{31}P\{^1H\}$ NMR because of its characteristic signal, $\delta(^{31}P) = 4.7$ ppm, $^1J(^{195}Pt, ^{31}P) = 3550$ Hz. Analysis of the initial reaction mixture was performed in the native IL phase. After completion of the reaction, the final composition of the crude reaction mixture was further examined by dissolving the IL phase in $CDCl_3$.[213]

Müller and co-workers carried out an NMR study of supported metal catalysts of a hydroamination reaction containing the IL [EMIM][Tf_2N].[214] High-resolution ^1H NMR spectra recorded for the supported catalysts revealed line widths similar to the values observed in regular $CDCl_3$ solutions. NMR data for the supported IL showed hindered rotation around the $N-C_{Ethyl}$ bond due to interaction of the nitrogen atom with the support, whereas free rotation around the $N-C_{Me}$ bond was retained. It is important to note that the ^1H and ^{31}P NMR characterization of supported Pd and Zn catalysts was carried out without the use of an additional solvent, which clearly could have broken the native structure of the supported catalyst.[214]

The formation of a symmetrical Rh−hydride complex was reported in [BMIM][SbF_6] using ^{31}P NMR. The structure was assigned the formula $[H_2Rh(PPh_3)_2(Solv)_n]^+$ ($\delta = 40.6$ ppm, $^1J(^{103}Rh, ^{31}P) = 103$ Hz).[215] The complex was considered as a possible intermediate for Rh-catalyzed hydrogenation, isomerization, and hydroformylation reactions.

Dissolution of the Wilkinson complex **12.1** in an acidic IL [EMIM][$AlCl_4$] was studied by Mann and Guzman using $^{31}P\{^1H\}$, ^{31}P, and $^{31}P\{^1H\}$-COSY NMR (Scheme 12).[216] After rigorous analysis, the authors concluded that the observed signals in the ^{31}P NMR spectrum belonged to the complex **12.2**. The $[AlCl_4]^-$ anion was suggested to be coordinated to the transition metal center through the bridging Cl^- ligand ($\delta(^{31}P)_A = 49$ ppm, $^1J(^{103}Rh,^{31}P) = 201$ Hz; $\delta(^{31}P)_B = 51$ ppm, $^1J(^{103}Rh,^{31}P) = 216$ Hz; $^2J(^{31}P,^{31}P) = 37$ Hz). Upon reaction with hydrogen, a new ^{31}P signal appeared at ($\delta(^{31}P) = 59$ ppm) as well as a high-field ^1H NMR signal ($\delta(^1H) = -17.4$ ppm). Analysis of the $^1J(^{103}Rh,^{31}P)$, $^1J(^{103}Rh,^1H)$, and $^2J(^{31}P,^1H)$ coupling constants, carried out in a selective ^{31}P decoupling NMR experiment, provided evidence for the formation of the hydride complex **12.3**.[216] It was also reported that the complex **12.3** formed in the IL from **12.2** on standing, although in this case the source of the hydrogen was not clearly understood (probably from traces of residual water). The study raised an important feature of the stabilization of low oxidation state Rh(I) complexes by ILs, which may play an important role in the hydrogenation reaction in IL media. For comparison, high oxidation state Rh(III) species are easily formed due to the oxidative addition of H_2 in regular solvents.[217]

The mechanism of the catalytic dimerization/hydrogeneation reaction of alkynes was modeled by Joó, Oro, and co-workers following a sequence of stoichiometric steps using [BMIM][BF_4] as the solvent.[218] The ^{31}P NMR monitoring of the reaction of the iridium complex **13.1** with alkynes indicated sequential formation of the alkenyl hydride **13.2** and the butadiene complex **13.3** (Scheme 13). The isomeric distributions of **13.2** and **13.3** were successfully determined. Recording the ^{31}P NMR spectra under off-resonance decoupling conditions resulted in simplification of the phosphorus spectrum by eliminating small $^nJ(^{31}P,^1H)$ spin−spin couplings presented in the $P(iPr)_3$ ligand (∼2−3 Hz). Meanwhile, the larger $^2J(^{31}P,^1H)$ spin−spin couplings due to the hydride protons (∼19−21 Hz) remained unchanged in the spectrum. This technique can be useful for the identification of hydride complexes of the transition metals with bound phosphine ligands.[218] The stoichiometric reaction was a model of the catalytic cycle involving alkyne insertion into the metal−hydrogen bond and C−C reductive elimination. The role of NMR monitoring for studying the last C−C bond-forming step, which is of primary importance in transition metal catalysis,[219] proved an important one.

Scheme 13. Sequence of Stoichiometric Reactions Studied by NMR Monitoring in [BMIM][BF_4] (Adapted with Permission from Ref 218; Copyright 2003 Wiley-VCH Verlag GmbH & Co. KgaA)

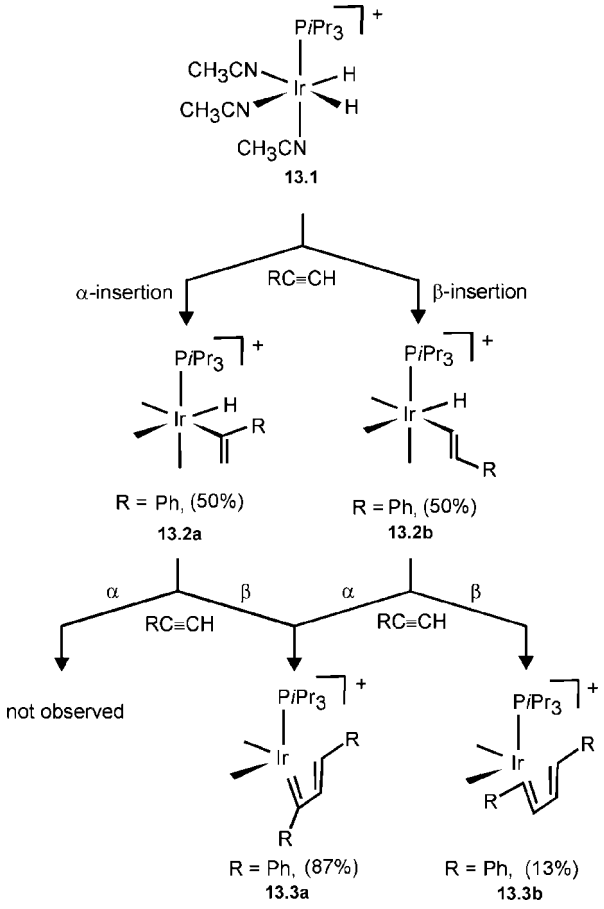

^{2}H NMR was utilized by Finke and co-workers to provide evidence for N-heterocyclic carbene formation involving iridium nanoclusters.[220] Under a D_2 atmosphere, deuterium incorporation into the imidazolium cation was observed at the 2-, 4-, and 5-positions (fast) as well as at the 8-position (slow). The proposed reaction mechanism involves C−H oxidative addition to the metal, H/D scrambling, and C−D reductive elimination. The NMR study indicated that Ir(0) nanoclusters react with the imidazolium-based ILs to form surface-attached carbenes.[220]

High-pressure NMR monitoring of the Rh-catalyzed hydroformylation of 1-octene with H_2/CO was reported by Dupont, van Leeuwen, and co-workers.[221] Reaction of the catalyst precursor Rh(acac)$(CO)_2$ with 1 equiv of the bidentate phosphine ligand in [BMIM][PF_6] resulted in the formation of a hydride complex HRh(diphosphine)$(CO)_2$. The ligand was coordinated in bis-equatorial fashion (^{31}P NMR). However, NMR monitoring under hydroformylation conditions showed the existence of a dynamic equilibrium between the Rh complexes with bis-equatorial and equatorial-apical diphosphine coordination. The conclusions drawn from this high-pressure NMR study were independently confirmed by a high-pressure IR study. The study also reported NMR evidence for the possible formation of a dimeric Rh species.[221]

Mehnert and co-workers have carried out a high-pressure ^{13}C and ^{31}P NMR study of the Rh-catalyzed hydroformylation of hexene-1 with H_2/^{13}CO in [BMIM][BF_4] and showed the presence of an equilibrium between two types of metal species.[222] At 1 bar of H_2/^{13}CO pressure, the [HRh(CO)(phosphine)$_3$] complex was detected, whereas at a higher pressure of 138 bar, signals assigned to the [HRh$(CO)_2$(phosphine)$_2$] complex were observed. After depressurizing the IL sample, the [HRh(CO)(phosphine)$_3$] signals were detected again. The use of ^{13}C labeled carbon monoxide played an important role in increasing the sensitivity of the ^{13}C NMR. Unfortunately, the study was carried out with 5 wt % of D_2O added to the IL, and the influence of this additive is difficult to rationalize.[222]

High-pressure ^{1}H NMR in an IL was utilized to investigate the mechanism of styrene hydrogenation catalyzed by metal cluster catalysts.[223] In particular, the tetranuclear cluster $[H_3Os_4(CO)_{12}]^-$ was observed in [BMIM][BF_4] by ^{1}H NMR, $\delta(^1H) = -14.8$ ppm (symmetric structure with three equivalent protons). The possible substitution of one of the CO ligands by the substrate (styrene) resulted in the formation of a new metal species whose signals were observed at a higher field, $\delta(^1H) = -20.0$ ppm.[223]

2.9. Ionic Liquids Stability and Recycling

The stability of the IL [BMIM][PF_6] under UV irradiation (254 nm) was investigated using ^{13}C NMR of the neat samples and comparing the results to those from other physical chemical methods.[224] It was concluded that [BMIM][PF_6] in its pure form can be considered as being resistant to UV irradiation and thus useful as a solvent for photochemical reactions.

Stability of the [BMIM][BF_4] IL toward hydrolysis was confirmed by ^{11}B and ^{19}F NMR in the study of photoinduced oxidation in water aimed for fabrication of semiconducting nanowires.[225] Under studied conditions, no hydrolysis products were detected by NMR.

NMR analysis has been utilized by Seddon and co-workers to investigate the radiochemical stability of 1,3-dialkylimidazolium-based ILs.[226] The ILs were found to be relatively radiation-resistant and did not undergo major decomposition of the organic component.[226] The formation of small amounts of hydrogen gas was observed under electron beam irradiation of ILs, but only in moderate yields ($\sim 2.5 \times 10^{-7}$ mol J^{-1}).[227]

The stability of [EMIM][TfO] and [HexMIM][TfO] toward oxidation by ceric ammonium nitrate (CAN) was studied with ^{1}H and ^{13}C NMR.[197] It was shown that, under typical conditions used for the oxidation of organic substrates (125−150 °C, 6 h, 1:10 IL/CAN ratio), no IL decomposition products were detected. Because decomposition of the ILs was observed only at an IL/CAN ratio of 1:2 at 150 °C,[197] these results indicate reasonable IL stability against oxidation by CAN and their reliable choice as adequate solvents to carry out oxidation reactions. This example clearly emphasizes the necessity of verifying the IL stability for developing reliable synthetic procedures.

A ^{1}H and ^{19}F NMR study of the IL recycled/regenerated after performing an electrophilic nitration reaction revealed that the counterion exchange and nitration of the imidazolium ring may take place depending on the structure of the IL.[228] Careful IL and nitration system selection made it possible to achieve both aims—namely, carry out the nitration reaction and recycle the IL.

The stability of ILs under various reaction conditions and after recovery with a view to recycling was confirmed using ^{19}F NMR.[160] Identical NMR spectra were recorded both before and after reaction, as well as after recovery.

Routine characterization of the [BMIM][BF_4] and [BMIM][PF_6] by ^{1}H and ^{13}C NMR in the neat form was carried out by Dupont and co-workers as early as 1996,[229] and similar chemical shifts values were reproduced later.[230] Other ^{1}H and ^{13}C NMR characterizations include: [BMIM][$B(HSO_4)_4$][231] and [OMIM][PF_6],[232,233] ^{19}F NMR for [EMIM][BF_4],[234] ^{1}H NMR for [EMIM][Tf_2N],[235] as well other ILs.[236−243] The multinuclear NMR characterization of both pure [BMIM][Cl] and its Ph_2P-substituted form was carried out in the neat IL.[244] Characterization of the [BPy][$AlCl_4$] in the neat state by ^{1}H and ^{13}C NMR was followed by X-ray structure analysis.[245] Another useful application of NMR spectroscopy addressed the identification of ILs and analysis of their purity.[246]

The chemical stability of IL toward metallic lithium was studied using multinuclear NMR results, suggested that [BMMIM][Tf_2N] is significantly more stable than [BMIM][Tf_2N].[247] The latter decomposed with carbene species formation when exposed to Li. The ILs were also characterized by NMR diffusion experiments.[247]

3. Overview of NMR Experiments in Ionic Liquids

The previous section illustrated the possible applications of a wide range of proton and heteronuclear spectra, including 2D NMR. In the present section, an overview of the scope and limitations in dealing with high-performance NMR in native ILs systems is provided with a special emphasis on the estimation of the accuracy of NMR measurements.

3.1. ^{1}H and ^{2}H NMR Spectra

To the best of our knowledge, the first ^{1}H NMR spectrum of a neat IL was reported by Newman and co-workers in 1972 in their study of pyridinium salts.[248]

Proton NMR spectroscopy in ILs has two major limitations: (1) commonly used ILs have residual signals in the aromatic (imidazolium ring) and aliphatic (alkyl groups) regions; (2) the high viscosity and highly ionic nature of ILs makes it difficult to achieve high performance in ^{1}H NMR studies.

Indeed, in many cases, ^{1}H NMR studies in ILs is possible only if the signals of the solute and solvent do not overlap. The solute signals can be particularly difficult to detect in the case of ILs with long side chains. This is because they occupy most of the high-field part of the spectrum, while the aromatic signals occupy the low-field part of the spectrum. Routine solvent-suppression techniques are not applicable in such cases, as neither of the T1 relaxation time differences allows achievement of this aim.

A very promising approach based on DOSY filtration has been suggested by Giernoth and Bankmann.[249] The high viscosity of ILs and the resulting slow movement of the IL molecules, compared to faster-moving solute species, made it possible to filter out the signals of the ILs. The greater the difference in size and diffusion constants between the solute and the IL, the better is the filtration performance. This method may be useful not only for reconstruction of the solvent-signal-free NMR spectrum but also for monitoring chemical reactions directly in ILs.[249]

Another approach to dealing with the problem involves preparation of specially designed ILs. To simplify the ^{1}H spectrum of the IL and avoid overlapping of the signals, the protic [HMIM][HBr_2] IL was prepared.[42] Compared to the widely used [BMIM]-based ILs, the replacement of the Bu group by hydrogen removed four multiplets from the high-field part of the ^{1}H NMR spectrum.[42] [TMSu]$^+$-based ILs were suggested as convenient solvents for doing NMR studies, because in their ^{1}H NMR spectra one sharp peak (Me group only) is present, leaving the whole spectral window free.[158]

Several studies have been carried out to estimate the numerical precision and accuracy of ^{1}H NMR measurements in ILs. In a typical experimental setup, signal widths of ~3−5 Hz at half-height were observed in the ^{1}H NMR spectra of ILs at room temperature.[75] This is compared to ~0.5−1.0 Hz, which is typically the width observed in regular solution-state NMR. A resolution of ±0.0012 ppm has been reported for the ^{1}H NMR in [EMIM][Tf_2N] at 300 MHz.[53] Experimental errors within ±0.002 ppm were reported for the ^{1}H NMR of [$P(C_6H_{13})_3(C_{14}H_{29})$][Cl] at 270 MHz.[95]

One of the ways to improve the quality of the ^{1}H spectra in ILs is to increase the sample temperature. It was shown that increasing the temperature to 328−353 K significantly reduces signal widths and dramatically improves spectral resolution.[64,65,75] The main contribution to the resolution enhancement on heating comes from reducing the IL viscosity, thus facilitating molecular tumbling. Variable-temperature NMR experiments have confirmed the decrease in the viscosity of ILs on increasing the sample temperature in agreement with the Vogel−Tamman−Fulcher equation.[64,65] However, it should be pointed out that temperature dependences of line widths of ILs may be rather complicated due to several factors (including homogeneity of the external magnetic field, sample conditions, etc.). More studies are required to fully understand whether the same temperature effect will hold for the other ILs.

To increase accuracy in the determination of spectral parameters (integrals and chemical shifts), the ^{1}H NMR spectra were fitted using a nonlinear least-squares procedure.[114] The difference between the calculated and experimental spectra was reported as being <1%.

Arce and co-workers conducted an important study of the suitability of ^{1}H NMR spectroscopy for the direct analysis of liquid−liquid equilibrium data to characterize the extraction ability of ILs.[123−125] Before doing the actual measurements, the authors verified the accuracy of ^{1}H NMR in ILs for quantitative mixture analysis. Using a series of samples with known composition, the largest deviation in mole concentration determined was found to be only 0.004.[123−125] The same type of analysis carried out in $CDCl_3$ solutions showed the largest standard deviation of 0.005.[250] Thus, selecting IL as a solvent did not diminish the accuracy of the quantitative NMR measurements. Careful analysis and verification of the analytical technique, based on the ^{1}H NMR spectroscopy of native IL samples, emphasize the following important advantages of this method: (1) analysis of all components is performed using only one step of measurements; (2) experimental error is reduced; (3) only a small amount of sample is needed for the analysis. To avoid solvent−solute signal overlapping in the NMR spectrum, a high-field instrument operating at 750 MHz was utilized in the study.[123−125]

^{2}H NMR was reported as a useful technique for monitoring the removal of water and other acidic impurities from chloroaluminate ILs.[107] To achieve the aim, a specified amount of a deuterium-containing compound (i.e., DCl) was

added to the IL before purification. ^{2}H NMR has an important advantage since the spectrum contains only the signals of interest, and their disappearance (as a result of purification) can easily be followed with high precision by NMR. This is in sharp contrast with ^{1}H NMR, where traces of acidic impurities and water were rather difficult to detect due to the presence of high-intensity residual solvent signals (indeed, detection of very small signals on a background of high intensity peaks is a complicated technical task). Thus, ^{2}H NMR is a most useful alternative for ^{1}H for this purpose.[107]

The use of deuterated substrates proved particularly advantageous for performing kinetic studies with ^{2}H NMR.[194,220] Both decay and growth curves were easily obtained from a series of ^{2}H NMR spectra. A comparative kinetic study using UV/vis spectroscopy and ^{2}H NMR spectroscopy was performed in ILs, and good agreement for the determined rate constants was found.[194] This confirms a reliable accuracy of ^{2}H NMR for kinetic measurements in ILs.

3.2. Heteronuclear Spectra

Albeit in a significantly less pronounced manner, heteronuclear NMR spectroscopy also suffers from the limitations mentioned previously (see section 3.1). The probability of signal overlap is reduced due to a larger range of chemical shifts in heteronuclear spectra. In most cases, it was easier to obtain routinely acceptable spectral parameters within the same time period used for instrument adjustment (compared to ^{1}H NMR). In the present section, possible improvements and extended applications of ^{13}C, ^{14}N, ^{15}N, ^{17}O, ^{19}F, ^{27}Al, ^{31}P, and ^{35}Cl NMR are discussed. Measurements can be carried out to characterize not only neat ILs but also the other species dissolved in the ILs and the nature of solvent−solute interactions.

We start the discussion of heteronuclear spectroscopy with ^{13}C NMR, because it is a well-established tool in the structural studies of organic compounds.[251,252] The first ^{13}C NMR spectrum of a neat molten salt was reported by Osteryoung and co-workers in 1979.[154] Nowadays, the performance of ^{13}C NMR spectroscopy in various ILs has been thoroughly evaluated.

After pulse-length calibration, the ^{13}C NMR spectrum of [BMIM][Tf_2N] with a good signal-to-noise ratio was acquired with <8 scans.[75] With modern hardware equipped with a digital oversampling module, even strong signals from a solvent should not preclude the observation of solute signals.[253]

As mentioned previously, the resolution of ^{13}C NMR spectra can be dramatically improved by raising the temperature of the sample. An order of magnitude decrease in the line widths was observed on increasing the sample temperature from 313 to 363 K.[177] The ^{13}C NMR spectrum of a cellulose solution in [BMIM][Cl] at 363 K had a resolution comparable to the solution in D_2O at 298 K.[177] A resolution of ±0.017 ppm was reported for ^{13}C NMR using a 300 MHz NMR instrument (operating at 75 MHz for ^{13}C) in [EMIM][Tf_2N].[53]

To decrease the number of solvent signals and minimize the chance of overlapping solvent−solute signals, special ILs were designed: [HMIM][HBr_2] (alkyl group replaced by hydrogen)[42] and [TMSu]$^{+}$-based ILs (the only sharp solvent peak from the Me group).[158] The same approach was used to simplify the ^{1}H spectra of the IL (see also section 3.1).

The sensitivity of natural abundance ^{13}C NMR was not enough to detect minor changes caused by the decomposition of [BMIM][PF_6]. UV−vis spectroscopy was found to be a more sensitive alternative.[224] This conclusion is in line with that of another study indicating that <1% conversion of the IL could not be observed by NMR.[226] It should be noted that this concentration limit implies the decomposition of IL itself, while the other solute molecules (if signal overlapping with IL resonances is not the case) can be detected at lower concentrations.

The sensitivity of ^{13}C NMR spectroscopy in IL studies may be further increased by using ^{13}C enriched compounds. Incorporating a ^{13}C-labeled ligand into a transition metal complex not only allowed measurement of the chemical shifts but also allowed the $^{1}J(^{13}C, ^{195}Pt)$ and $^{2}J(^{13}C, ^{13}C)$ coupling constants to be measured directly in the IL.[89] ^{13}C-labeled carbon monoxide was used for obtaining accurate measurements of its solubility in several ILs.[117] Quantitative signal integration was performed using a least-squares fitting procedure.[117] As was shown in the NMR study of the oxidation of benzyl alcohol in [EMIM][TfO], utilization of a ^{13}C labeled substrate allowed the determination of side products formed in trace amounts at a much lower concentration compared to the natural abundance sample.[197]

Although ^{1}H NMR could be expected to be the easiest way to characterize the Brønsted acidity of ILs, it was shown that in some cases indirect measurements with ^{13}C NMR are more applicable. The idea was to utilize ^{13}C-labeled acetone $(CH_3)_2{}^{13}CO$ and to study the interaction of the acidic centers with the carbonyl group. The relationship between the acidic properties and the NMR chemical shifts was discussed.[164]

Despite the low sensitivity of ^{15}N nuclei, spectra in ILs were recorded using standard NMR measurements with direct detection using a 500 MHz spectrometer operating at 50.68 MHz for nitrogen-15 (1000−3000 pulses, 5 s repetition time).[54] For dilute solutions of ILs, indirect detection within a ^{1}H−^{15}N HMBC pulse sequence was applied. Chemical shift values, independently determined by both methods, were in good agreement.[54] The measurements of ^{14}N NMR spectra required a very short time due to higher sensitivity and a shorter relaxation delay.[57] Determination of ^{14}N NMR chemical shifts and line widths with reasonable precision $\delta(^{14}N) = 210 \pm 1$ ppm and $\Delta\upsilon_{1/2} = 1500 \pm 10$ Hz was accomplished within 1 min (16 pulses, 200 ms repetition time, 500 MHz NMR spectrometer).[57] However, measurements were possible only at 80 °C, because at 25 °C the signals were too broad to be detected. The drawback of ^{14}N NMR is its low resolution. Even at high temperatures, the N1 and N3 signals of the imidazolium ring remained unresolved, and a single peak was observed for both nitrogens. Either dilute solutions[57] or ^{15}N NMR measurements[54] had to be used if both nitrogen atoms needed characterization.

To increase the sensitivity of ^{17}O NMR measurements, $H_2{}^{17}O$ (20% enrichment) was utilized.[91] In this case, the ^{17}O NMR detections of oxychloroaluminum and hydroxychloroaluminum species in [EMIM][$AlCl_4$] with a good signal-to-noise ratio were acquired using a 270 MHz NMR spectrometer operating at 36.54 MHz for ^{17}O observation. ^{17}O NMR spectroscopy was also used for the study of the nature of water molecules and of oxygen-containing species in ILs. In this case, water samples enriched with ^{17}O were necessary in order to achieve the necessary sensitivity.[90] The

nature of the solvent−solute interactions was also studied using ^{27}Al NMR[61,76,146,254] and ^{11}B NMR.[71,122] A useful approach for the monitoring of oxide contamination removal by treatment of the IL with phosgene is reported.[109] In such a case, insensitive ^{17}O NMR detection of aluminum oxide species was replaced with the much more convenient ^{13}C{^{1}H} and ^{17}O detection of phosgene and carbon dioxide (see section 2.3 for reaction details).

^{19}F NMR spectroscopy is a very useful general method for studying various properties of ILs, since most of the ILs have the ^{19}F signals from the fluorine atoms of the anions ($[PF_6]^-$, $[BF_4^-]$, $[Tf_2N]^-$, $[SbF_6]^-$, $[CF_3COO]^-$, etc.). ^{19}F NMR was widely utilized for investigating cation diffusion in ILs as well as specific cation−solute interactions. A resolution of ±0.013 ppm has been reported for ^{19}F NMR in [EMIM][Tf_2N] using a 300 MHz NMR instrument (operating at 282 MHz for ^{19}F).[53] For accurate measurements of the intensity of small signals in ^{19}F NMR, solvent suppression of the residual IL peak in [BMIM][Tf_2N] was applied.[106]

Using ^{19}F and ^{13}C NMR chemical shifts of reference compounds in ILs, an empirical numeric model was developed to analyze and predict chemical reaction selectivities[189] and solubility.[117]

A few useful approaches for the enhancement of ^{27}Al spectra quality have been reported. Removal of acidic impurities from a chloroaluminate IL by the addition of $EtAlCl_2$ led to significant narrowing of the $[AlCl_4]^-$ peak in the ^{27}Al spectrum.[107] In the ^{27}Al NMR spectrum of the IL [EMIM][$AlCl_4$], a useful approach to signal selection for observing the $[AlCl_4]^-$ and $[Al_2Cl_7]^-$ signals has been reported. The narrow $[AlCl_4]^-$ signal was separated by increasing the preacquisition delay (0.033−1.0 ms).[50]

An important ^{31}P NMR spectroscopy application concerns the identification of transition metal phosphine complexes containing phosphorus ligands. Palladium phosphine complexes in ILs were identified by comparing the ^{31}P chemical shifts with independently prepared samples.[211] The ^{31}P NMR monitoring of platinum complexes was also successfully employed in several reactions involving the metal center.[89] The study reported by Mann and Guzman provides an excellent example of the application of powerful NMR methods—^{31}P{^{1}H}, ^{31}P, selective ^{31}P decoupling, and ^{31}P{^{1}H}-COSY for carrying out line assignments in the NMR spectra of native IL systems as well as identifying transition metal complexes directly in the IL.[216]

The first ^{35}Cl NMR study of neat [BMMIM][$ZnCl_3$] was reported by Santini and co-workers.[59] The chemical shifts of [BMMIM][Cl] and [BMMIM][$ZnCl_3$] were observed at $\delta(^{35}Cl) = 84$ and 800 ppm, respectively. The temperature dynamic of the sample was monitored with ^{35}Cl NMR as a function of time. The signal corresponding to [BMMIM][$ZnCl_3$] underwent a significant shift to $\delta(^{35}Cl) = 400$ ppm after 20 min, and finally to 250 ppm after 60 min (110 °C).[59] Such a large range of ^{35}Cl chemical shifts and high sensitivity to the structural environment suggests that ^{35}Cl NMR is a valuable tool for structural studies, providing that NMR spectra of sufficient signal-to-noise ratio can be obtained. In studies by Moyna, Rogers, and co-workers, a 90°−90°−90° ARING pulse sequence was used in $^{35/37}$Cl measurements to reduce artifacts in neat ILs.[58,86,180,181]

3.3. Diffusion Studies

NMR spectroscopy provides a range of techniques for studying molecular motions in liquids.[255] The main advantages are as follows: fast experiments (typically from minutes to hours of measuring time), relatively small sample volumes (~0.5−0.7 mL with a standard 5 mm NMR probe), and easy application over wide ranges of temperature and pressure. Routine NMR hardware equipped with a pulsed-field gradient is suitable for studying fast diffusion in organic solvents as well as a slower diffusion in viscous liquids.[256] However, special attention should be paid to minimizing convection effects and to maintaining temperature stabilization.[257,258] A higher quality of diffusion spectral data may be obtained with dedicated hardware. NMR probes optimized for diffusion measurements and stronger pulsed-field gradients are available. Nowadays, routine diffusion NMR measurements are used for evaluating molecular systems in organic solvents and water. Because there have been several recent reviews on the subject,[255−260] only some specific notes concerning the application of diffusion measurements in native IL systems are summarized here.

In the case of diffusion measurements in viscous samples using a BPPLED sequence, the standard sine-shaped gradients were replaced with trapezoid-ramped gradients.[44] A modified stimulated spin−echo sequence was utilized to improve diffusion coefficient measurements in ILs.[141,100] A small sample height (at 2 or 5 mm, for example) was maintained for ILs susceptible to convection in order to minimize the possible harmful influence of convection on the diffusion measurements.[68,136,138]

Saielli and co-workers have determined the diffusion coefficients of the anion and cation of [BMIM][BF_4] at various temperatures using ^{1}H and ^{19}F NMR. Subsequently, they evaluated and further developed the molecular dynamics calculations for modeling ILs.[94] An optimal computational procedure was developed for the computer simulation of the IL translational dynamics, and their reliability was analyzed by comparison with experimental data.

In an important study, Forsyth and co-workers evaluated the reliability of routinely applied diffusion measurements.[67] The data presented in their report showed that the pulsed field gradient spin echo (PGSE) method suffers from "intrinsic internal gradients". This results in up to 20% differences in diffusion coefficients measured for different signals of the same molecule. However, the pulsed field gradient stimulating echo (PGSTE) method was applied without such anomalous behavior and produced more reliable results (<1% inaccuracy). The measurements were carried out using a special diffusion probe at 300 MHz.[67] The study emphasized that routine methodology widely utilized for traditional liquid systems may not always provide acceptable results for ILs. More insight into the subject is highly desirable to reveal the origins and the full scope of this problem.

A special NMR probe has been designed by Richter and co-workers to carry out pressure- and temperature-dependent measurements of self-diffusion coefficients in ILs.[261,262] The measurements were successfully carried out for pure [BMIM][PF_6] and binary [BMIM][PF_6]/methanol systems in the temperature range 293−313 K and in the pressure range ambient to 3000 bar. The activation energies for the self-diffusion coefficients of $[BMIM]^+$ and methanol were determined as a function of mixture composition.[261]

3.4. Relaxation Measurements

A new methodology was developed by Carper and co-workers to separate dipolar and chemical shift anisotropy in a ^{13}C relaxation study of [BMIM][PF_6], [MNIM][PF_6],[263,264] and [EMIM][$BuSO_3$].[265] The ^{13}C NMR chemical shifts, chemical shift anisotropy, ^{13}C spin−lattice relaxation times, pseudorotational correlation times, corrected maximum NOE factors, dipolar relaxation rate part, and total relaxation rate for each aromatic carbon nucleus in the imidazolium ring were determined or estimated in the studies. Analysis of the NMR data indicated the presence of several phase changes in the IL over the measured temperature ranges. The molecular radii of the $[MNIM]^+$ cation determined in the study compared fairly well with DFT calculations at the B3LYP/6-311+G(2d,p) level.[263,265] Comparison of spectral data measured for [BMIM][PF_6] and [MNIM][PF_6] allowed observation of a long side chain effect on the ^{13}C rotational microdynamics of both parts of the cation (side chain and imidazolium ring).[263,264] Analysis of the ^1H relaxation data in [BMIM][BF_4] and [BMIM][PF_6] ILs showed high sensitivity of this method to identify subtle changes in the system caused by interaction with solute molecules and to reveal specific solvent−solute interactions.[176]

3.5. Nuclear Overhauser Effect Measurements

The nuclear Overhauser effect (NOE) arises due to resonance line intensity changes caused by dipolar cross-relaxation from neighboring spins with perturbed energy level populations.[266] The intensity of the signal is proportional to the inverse sixth power of the distance between the atoms, $I \approx 1/r^6$. Thus, NOE data is very useful for stereochemical assignments and provides straightforward information about intra- and intermolecular interactions.[267] Depending on the value of the correlation time, in some cases the NOE effect is unobservable.[266,267] To overcome the problem, rotating frame measurements (ROE) can be utilized. This is due to the fact that the ROE signal does not become zero when the value of the correlation time is changed. For example, NOESY experiments for the [BMMIM][Tf_2N] and [BMIM][Tf_2N] systems exhibited very weak or null cross-peaks, while the ROESY experiment led to positive NOEs irrespective of the long rotational correlation time due to the high viscosity of the IL system.[157] The advantage of rotating frame experiments and their relevance to the fact that correlation times corresponding to small or zero NOEs are possible due to IL viscosity was also discussed in another study.[268]

Intermolecular nuclear Overhauser effect (NOE) measurements provided experimental evidence for cation−cation, cation−water, and cation−anion interactions in [BMIM][BF_4].[84] The type of cation−cation interactions and the binding site of water in cation−water interactions were investigated by homonuclear NOE in the rotating frame (ROE). The quantitative analysis of the ROE factors was performed by volume integration of the cross-peaks. The cation−anion interactions were determined using a 1D $^1H\{^{19}F\}$ NOE difference experiment (3.3−3.6% enhancement was observed).[84]

By running a gated decoupling experiment, the nuclear Overhauser enhancement was determined and used for calculating the value of correlation time.[61,71] The temperature dependence of the NOE factors has also been reported for [BMIM][PF_6].[73]

3.6. Two-Dimensional NMR Spectroscopy

Two-dimensional experiments are one of the most powerful NMR methods available nowadays for routine use. Several very useful approaches were developed for studying the structure and dynamics of molecular systems in solution.[269−271] It is of much importance to rationalize the scope of existing 2D experiments for IL systems and to understand potential applications.

The utility of 2D NMR in ILs has been illustrated by several examples throughout the review. It is very important to emphasize that in most cases standard pulse sequences supplied by the NMR spectrometer can be used to acquire 2D spectra in ILs.

A homonuclear H,H−COSY experiment on a test sample with coherence selection by pulsed-field gradients was successfully recorded in [BMIM][Tf_2N].[75] A 2D ROESY experiment in [BMIM][BF_4] was performed using a pulse sequence that had been used for off-resonance ROESY with adiabatic rotation.[272]

An elegant approach was developed to distinguish intramolecular and intermolecular NOE contacts.[81] The 2D ROESY spectra (250 ms spin locking time) of the reference [EMIM][$AlCl_4$] sample was compared to the spectrum recorded for the sample with 95% fully deuterated imidazolium cations. In the former, both intramolecular and intermolecular NOE contacts are present, whereas in the latter only intermolecular NOE contacts could be recorded due to the absence of adjacent protonated molecules.[81] The comparison, therefore, made it possible to clearly identify the intramolecular and intermolecular NOEs. The distances measured from 2D NOESY experiments for [BMIM][BF_4] and [BMMIM][BF_4] showed a good correlation with available X-ray structures.[82] NMR data was found to be reliable for providing quantitative information for the assessment of the local structure of the neat IL. Moreover, NOE contacts provided important complementary information for a deeper understanding of IL structure derived from X-ray and neutron-scattering studies.[82]

It is important to point out that even a small dilution of the original mixture with THF-d_8 (up to 25% m/m) led to partial loss of the solvent−solute intermolecular contacts in the 2D ROESY spectra.[192] Further dilution (over 50% m/m) resulted in all contacts being lost. This example once again emphasizes that dilution of IL samples with a deuterated solvent may lead to a loss of structural information and, finally, to unreliable structural models.

To carry out 2D heteronuclear Overhauser effect spectroscopy (HOESY), a strategy involving twice recycling evolution and mixing times was applied to enhance the observed NOE.[83] Carper and co-workers reported that the correct determination of hydrogen−hydrogen distances in [EMIM][BF_4] and [PMIM][BF_4] requires the use of short mixing times of ≤50 ms in the 2D NOESY experiment.[273] A mixing time of >50 ms led to an increasing contribution of spin diffusion that resulted in unrealistically short hydrogen−hydrogen distances.[273]

Diffusion coefficients were determined using DOSY methodology[255−257] by collecting a series of ^1H NMR spectra, measured as a function of gradient amplitude.[61,62] DOSY NMR spectra were recorded in [BMIM][Tf_2N] and [C_{10}MIM][Tf_2N] ILs, using BPLED or STE pulse sequences.[249] Complete separation of the solvent and solute signals was observed, and the solute spectrum was reconstructed by the summation and extraction of corresponding

rows in pseudo-2D DOSY spectrum.[249] Both types of heteronuclear correlations HETCOR and gradient-selected HMQC were successfully recorded for a range of neat ILs with standard pulse sequences.[75]

4. Practical Aspects of NMR Spectroscopy in Ionic Liquids

Several important considerations need to be taken into account to accomplish accurate and reproducible NMR measurements. The present section provides the necessary information for choosing the best practical strategy for recording spectra in ILs and highlights the most important issues for spectral parameters optimization.

Nowadays, NMR superconducting magnets are remarkably improved in terms of higher stability and better homogeneity of the magnetic field. In a routine case, the lock system may not be necessary for acquiring spectral data. Therefore, in addition to sections 4.1 and 4.2 where operation with a ^{2}H or ^{19}F lock, respectively, is discussed, the possibility of deuterium-free NMR measurements is summarized in section 4.3.

4.1. Operation with a ^{2}H Lock

Routine solution-state NMR spectroscopy operates with the ^{2}H internal standard needed for a lock signal. The ^{2}H lock system is of practical importance for adjusting the magnetic field homogeneity and maintaining high stability during the measurements. For these purposes, an internal lock provided by fully deuterated organic solvents is usually employed.

At the moment, NMR studies using fully deuterated ILs as solvents are not common, because of their high cost. Nevertheless, experimental procedures for the preparation of such perdeuterated ILs have been reported.[274,275]

Another possibility for providing the internal lock standard is dilution of the IL with a deuterated organic solvent. Although this approach was utilized in some studies (for example, a mixture of [BMIM][Cl] and 15 wt % DMSO-d_6,[177,276] [BMIM][BF_4] and 5 wt % D_2O,[222] etc.), clearly it should be avoided to preserve a native IL system.

The external lock standard may be provided in two different ways: (1) the IL solution in the inner part of the NMR tube is surrounded by the lock standard and (2) the IL solution is in the outer part of the NMR tube with the lock standard in a capillary. Important advantages of the first option are the possibility of sealing the inner tube with the IL to avoid contact with air and moisture and a slightly better resolution due to the narrower outer diameter of the IL sample. The easiest practical way is to provide the external lock standard in a capillary (second option), and this has been used in numerous studies discussed in this review.

Unfortunately, in several of the studies, the use of two concentric tubes was mentioned without the authors specifying whether the IL was placed into the inner or outer tube. This information should be necessarily provided in the experimental descriptions for better reproducibility and comparison of the NMR measurements (see section 4.7 below).

4.2. Operation with a ^{19}F Lock

^{19}F stabilization is an alternative for the deuterium-based lock system. It has the important advantage for NMR spectroscopic studies in ILs that most of them contain fluorine in the anion ($[PF_6]^-$, $[BF_4]^-$, $[Tf_2N]^-$, $[SbF_6]^-$, $[CF_3COO]^-$, etc.). Therefore, the measurements can be performed in regular ILs without any additional modifications. This approach has been tested for some ILs and has allowed recording of high-resolution NMR spectra.[75] However, fluorine-based stabilization requires a special ^{19}F lock channel, which, although available as an option, is in most cases not installed by default.

4.3. Operation without a Lock

In many applications, NMR measurements can be successfully performed without lock stabilization in the unlocked "sweep-off" mode. This is the fastest way to obtain spectra in ILs, since it does not require any additional manipulation with the sample and may even exclude magnetic field homogeneity adjustment. Strictly speaking, the necessity of the lock system can be checked by calibration of the drift of the magnetic field for a particular NMR machine. For routine measurements involving 200−600 MHz NMR machines, operations without lock are well worth trying without such calibration. It should be noted, however, that in the case of spectral measurements using high magnetic fields (750 MHz or higher), time-consuming experiments, or those involving pulsed-field gradients, the importance of a lock system stabilization should be addressed more carefully.

For several ILs, the application of the unlocked (sweep-off) mode has been reported.[106,133,175,189,195] On some routine NMR spectrometers, the sweep-off mode was the only available choice for recording ^{2}H NMR spectra to avoid artifacts caused by a lock system, which also operates at a ^{2}H resonance frequency (see, for example, ref 92). It was also particularly important for high-pressure NMR, where an external standard in a capillary is technically difficult to use.[114]

It would appear that several studies listed in the present review have actually been carried out without lock under unlocked conditions. Unfortunately, this was not explicitly mentioned in the experimental procedures description.

4.4. Key Parameters for High-Performance NMR

The following most important issues need to be addressed for high-performance NMR in ILs: (1) shimming, (2) pulse calibration, (3) probe tuning/matching, and (4) selecting a proper temperature.

Various algorithms for shimming have been described in the literature, and most of them can be applied to ILs.[277−279] For shimming in the unlocked mode, the approaches summarized in the No-D-NMR technique can be used.[280]

Ionic media are strong absorbers of radiofrequency radiation. It was reported that 90° pulses in ILs were ∼1.5 times longer than in regular organic solvents.[75] For some IL systems, NMR spectra recorded with 90° (ref 175) or 45° (refs 54 and 95) flip angles were reported. Pulse calibration is recommended before the NMR measurements in ILs to achieve high sensitivity and to measure correct integral values. Because of absorption of radiofrequency radiation by ILs, higher values of pulse power and lock power may be required.[75]

Probe tuning and matching strongly depends on the solvent properties. Nevertheless, standard probes seem to be flexible enough for reliable tuning and matching. With one exception,

where a special probe adjusted for ILs was used,[75] all the experiments discussed in the present review were performed on standard hardware. Other parameters can be further optimized to achieve high-quality NMR spectra in ILs as described in the excellent study by Giernoth and co-workers.[75]

Selecting a proper temperature is an important issue. Most of the measurements discussed in the present review were carried out at ambient temperature. However, as previously mentioned, it has been established that recording NMR spectra at higher temperatures can significantly increase the resolution and result in narrow lines in the spectrum. Such behavior would naturally be expected in viscous liquid systems (although, depending on the system, the contribution of other factors cannot be excluded). Thus, temperature ranges of 80−140 °C are not uncommon.[57,141,144] For example, line sharpening of the NMR signal with increased sample temperature has been illustrated: whereas the signal in the neat [(SiC_3)MIM][Cl] IL was resolved at 80 °C, no signals were detected at 25 °C.[57] Sample temperatures as high as 300 °C were also reported for NMR measurements.[54] Unfortunately, the authors did not specify the hardware configuration for temperature stabilization, since operation at such harsh temperatures may cause damage to some routine hardware.

ILs are not expected to suffer during the NMR measurements at high temperature because of negligible vapor pressure and good thermal stability (unless some decomposition involving solute molecules or impurities takes place). However, care should be taken about using capillary inserts (acetone-d_6, etc.), which need to be verified for their stability against development of internal pressure.

Because temperature effects can be quite large, for precise measurements a uniform sample temperature should be maintained. In some studies, a rather long temperature equilibration time of 12−24 h was reported for keeping the sample in the probe before each measurement.[72,141] A slow temperature change of 1 K min^{-1} with 30 min equilibration at each temperature was also utilized.[141] It should be noted that, with standard air-flow methods for temperature stabilization of the sample inside the NMR probe, the time interval needed to reach a uniform sample temperature depends largely on the sample volume. This is necessary to remove temperature gradients in the horizontal and vertical directions. For a better reproducibility of the NMR measurements, sample volume, temperature, the type of NMR machine, and the IL should be unambiguously specified in the experimental part (unfortunately, these details were not specified in the above-mentioned studies).

4.5. Important Notes on Sample Preparation

Ultrasonic treatment of the samples was applied to ensure complete dissolution of the substrates in the IL prior to NMR analysis.[200] This approach may be particularly useful to facilitate dissolution of metal complexes. Notably, it was reported recently that ultrasonic treatment of the sample directly in an NMR tube may lead to better spectra quality for heterogeneous samples and for samples containing metal species.[281] The use of ultrasonic treatment for degassing IL binary mixtures has also been reported.[85] The IL itself was found to be stable to ultrasonic irradiation (50 kHz, 120 W, 60 min).[162]

Another important issue concerns achieving uniform homogeneity in the sample volume. It was reported that establishing a solvent−solute equilibrium may require a long period of time (i.e., several days); until the equilibrium point is reached, several changes in the NMR spectra may take place.[150] A possible way to avoid this would involve rigorous stirring at high temperatures, followed by cooling down to the appropriate point and then conducting the necessary NMR measurements. The study of water effects on ILs has also required several days of equilibration prior to NMR measurements to ensure reaching the equilibrium state of the sample.[100] Samples used for the construction of a phase diagram in water/[BMIM][BF_4] system were stored for seven days at 25 °C before the measurements.[169] It was reported that a white crystalline solid precipitate was formed at the bottom of the NMR tube in some cases after a week of storage (assumed to be a product of tetrafluoroborate anion hydrolysis in water). Although formation of the precipitate did not introduce significant changes into the NMR measured parameters,[169] care should be taken to control native samples during long periods of storage. Undoubtedly, the nature of this problem needs to be further clarified in more detail, taking into account that the procedure for sample equilibration may not always be the same for all ILs.

To achieve better results in diffusion experiments, a special sample tube was used with the magnetic susceptibility matched to the sample, thus affording good magnetic homogeneity over the whole sample volume.[136]

NMR measurements were carried out for [BMIM][CH_3SO_3] and [BMIM][Cl] at room temperature in a supercooled liquid state (both ILs have melting points higher than room temperature).[112] In these supercooled IL variable-temperature experiments, for safety reasons a thick glass tube was used instead of a regular NMR tube. The latter may break in case of spontaneous solidification.[112]

It was shown that regular NMR hardware is suitable for studying quasi-solidified composite IL samples. The sample preparation procedure required centrifugal treatment (∼3000 rpm for several minutes) to avoid the inclusion of air bubbles into the sample.[282]

4.6. High-Resolution Magic Angle Spinning (HRMAS) NMR Spectroscopy

Poletti, Caneva, and co-workers have reported a comparative study of the performance of HRMAS NMR for the investigation of ILs.[283] The study illustrated the potential of this technique for the direct analysis of IL solutions. The following findings are worth summarizing:[283]

(a) Better resolution: line widths at a half-maximum height in ^{1}H HRMAS NMR with an internal lock (with acetone-d_6 added) were 25−40% lower than conventional 5-mm liquid probes with external lock (acetone-d_6 in a coaxial capillary). Some of the line width values in the HRMAS spectra were close to those observed in dilute solutions of $CDCl_3$. Figure 14 shows an example of a series of ^{1}H spectra of methyl 2,3,4,6-tetra-*O*-benzyl-α-D-glucopyranoside recorded in ILs using both techniques; the higher resolution in the HRMAS spectra is evident.

(b) Acceptable concentration range: HRMAS NMR does not need large solute concentrations. A routinely used amount of ∼0.2 M was shown to be enough for practical applications.

(c) The possibility for reaction monitoring: for example, acetylation of *p*-methoxybenzyl alcohol was studied in the HRMAS rotor using ^{1}H NMR. Time-dependent intensity changes of the signals belonging to reactants and product were successfully observed (Figure 15).

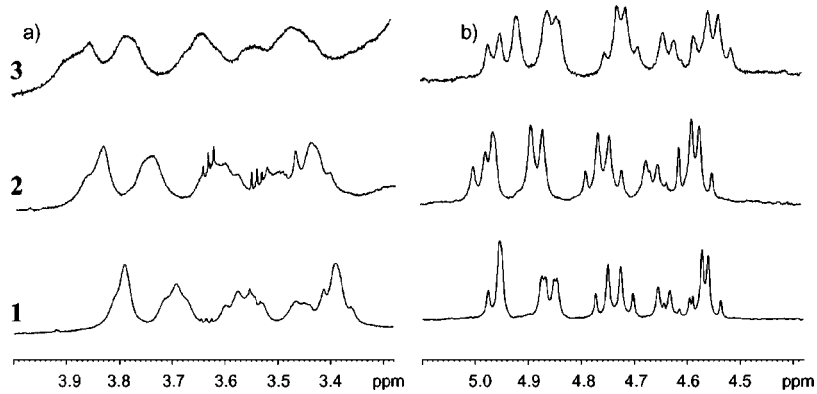

Figure 14. 500 MHz ^{1}H NMR spectra (303 K) of methyl 2,3,4,6-tetra-*O*-benzyl-α-D-glucopyranoside recorded in a standard 5-mm NMR tube with an external lock (a) and HRMAS NMR spectrum with an internal lock (b); **1**, [BMIM][PF_6]; **2**, [HexMIM][PF_6]; **3**, [OMIM][PF_6]. Reproduced with permission from ref 283. Copyright 2007 The Royal Society of Chemistry.

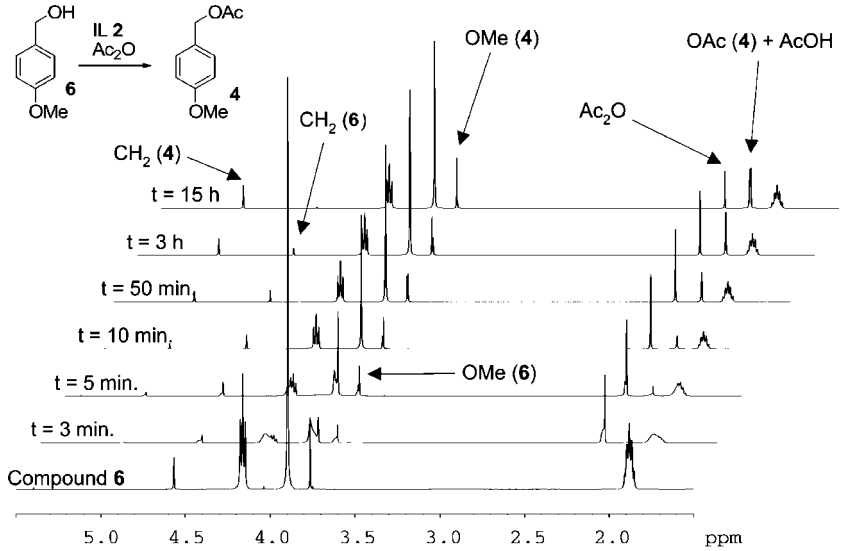

Figure 15. ^{1}H HRMAS NMR monitoring of the acetylation reaction in [HMIM][PF_6] (500 MHz, 303 K). Reproduced with permission from ref 283. Copyright 2007 The Royal Society of Chemistry.

(d) More accurate chemical shift values: although the issue is not completely clear at the moment (see section 4.7), reported results provide evidence that HRMAS NMR suffers less from the high magnetic susceptibility of ILs.

The main disadvantage of the reported study was the presence of deuterated solvent as the internal lock standard. Although only 6% of acetone-d_6 was added,[283] it was still a modification of the native IL system. Further studies are required in order to evaluate the performance of HRMAS NMR without the influence of added deuterated solvents.

The applications of HRMAS NMR for both ^{1}H and ^{13}C NMR analysis of ILs immobilized on silica,[57] as well as multinuclear ^{13}C, ^{29}Si, and ^{31}P MAS NMR characterizations of heterogeneous catalysts based on IL-modified solid supports,[284,285] have also been reported.

4.7. Referencing Procedure and the Influence of Magnetic Susceptibility

Accurate determination of NMR chemical shifts requires a consistent referencing procedure. For liquid-phase samples, two methods are routinely used: (a) an internal reference, where the reference compound is added directly to the solution under study (or a signal of a solute component with a known chemical shift is used as a reference) and (b) an external reference, where the solution under study and the reference are positioned separately, for example, in different coaxial tubes. The advantages and disadvantages of these (and other) referencing methods have already been discussed.[286]

Where ILs are concerned, the accuracy of the chemical shift referencing requires special attention irrespective of the method used.

(a) An internal referencing procedure provides the desired accuracy only in the absence of intermolecular interactions between the reference compound and the solvent (or other solute components). This effect can be minimized by reliable choice of the reference compound, taking into account solubility, miscibility, and concentration. Special note should be made concerning the primary reference compounds—TMS (tetramethylsilane) and DSS (sodium 3-(trimethylsilyl)propane-1-sulfonate; $Me_3Si-(CH_2)_3-SO_3^-Na^+$)—as suggested by IUPAC regulations.[286] The solubility of TMS in native IL systems is questionable and should be verified before use. The ionic nature of DSS means that it can interact with ILs and hence change the native system in an unpredictable manner. If the interactions

are strong enough, they may change the chemical shifts of the DSS. Anyway, even if DSS dissolved in the IL may still give correct chemical shift references, it is more advisible to avoid direct interaction with ILs to preserve native system properties.

(b) An external referencing procedure does not suffer from the above-mentioned problem since the reference compound and studied system are isolated from each other, but it still requires a special correction to be applied. This is due to differences in the bulk magnetic susceptibilities between sample and reference.

These effects are all well recognized for solutions composed of regular organic solvents or water.[286,287] In some cases (^{1}H and ^{13}C NMR) bulk magnetic susceptibility effects can be of the same order of magnitude as the chemical shift differences usually used to derive structural information.[286,287] Several methods were developed to overcome this problem and to carry out high-precision measurements while using an external referencing approach (see, for example, refs 288−290).

Because of the clearly different natures of ILs and organic solvents (the reference compound is dissolved in the latter), one might expect noticeable deviations due to bulk susceptibility in the case of the external referencing procedure. Of course, this mostly concerns the accuracy in referencing the exact chemical shift values. The correction is not needed to describe relative trends in measured chemical shifts ($\Delta\delta$).

To date, no systematic studies are available for the characterization of the influence of the bulk magnetic susceptibility effect in ILs on the accuracy of chemical shift measurements. Some studies have mentioned that the bulk magnetic susceptibility effect could be a source of inaccurate chemical shift determination in ILs.[216,218] In a few studies, correction of the observed chemical shifts for the volume susceptibility effect was carried out, but the values of the corrections and their influence on the determination of structural information were not discussed in detail.[53,95] Comparison of the ^{15}N NMR chemical shifts of [BMIM][BF_4], measured with the external referencing procedure in neat IL, and in diluted solutions in organic solvents or water, revealed small differences for both nitrogen atoms $\delta(^{15}N) = -198 \pm 2$ ppm and $\delta(^{15}N) = -210 \pm 2$ ppm. In fact, these differences may also include contributions from solvent and concentration effects.[54]

It was shown that in theory the magic-angle spinning (MAS) technique can be free from bulk magnetic susceptibility problems.[286] The chemical shifts of H-2 protons of [BMIM][PF_6], [HexMIM][PF_6], and [OMIM][PF_6] measured with HRMAS NMR and internal referencing were $\delta = 8.43-8.47$ ppm.[283] The measurements carried out in the ILs using a conventional probe with external referencing resulted in high-field shifted values $\delta = 7.28-7.41$ ppm. Thus, the approximate deviation of 1 ppm in the ^{1}H chemical shifts could have originated from the bulk susceptibility problem. However, these HRMAS NMR measurements were carried out with 6% acetone-d_6 added to the IL as an internal reference, and the influence of the additive cannot be completely ruled out.[283]

It should be noted that the contribution of paramagnetic metal centers could be another source of line broadening and chemical shift deviation in ILs.[291]

5. Concluding Remarks

As shown in this review, significant progress has been made in recent years in the development of reliable NMR methodology for studying native ILs systems, including both neat ILs and their mixtures with other compounds of interest. A summary of chemical applications of NMR spectroscopy in ILs is provided in Table 1. In spite of some initial bias, NMR measurements in ILs have been carried out with high accuracy and good sensitivity on routinely available hardware, providing that the necessary spectral parameter adjustments were made. The information about NMR experiments discussed in this review is summarized in Table 2. NMR strategies for operation in native ILs systems are given in Table 3.

Several enlightening examples discussed in the text have clearly emphasized that native IL systems possess unique properties that can be easily altered even by a very minor change in the composition. Where NMR studies are concerned, there is an important difference between systems involving ILs and regular solvents: while adding deuterium-containing cosolvents and internal standards to the latter is a common NMR practice, utilizing the same approach in the former case may lead to noticeably different results. Thus, as the studies reviewed in the present article strongly suggest, any modification of the samples for the purpose of NMR measurements should be avoided. Whenever possible, measurements should be carried out for native ILs samples.[292] Otherwise, there is a risk of altering the characteristics of the sample and overlooking some intriguing property of the IL system.

NMR spectroscopy has been established as a flexible and convenient tool not only for homogeneous IL systems but also for the investigation of heterogeneous and multiphase systems (Table 1). Separate NMR spectra from the different phases were successfully recorded and characterized for each part of the multiphase systems. Such spectral studies afford a comprehensive treatment of these complicated systems.[293]

Careful sample preparation is another important concern, which distinguishes ILs from regular NMR solvents. For better reproducibility of the NMR measurements, the sample preparation procedure should be specified. If an external referencing method is used (Table 3), the geometry parameters of the NMR sample should be indicated (diameters of external and internal tubes, sample height, etc.). The rather slow reorganization of IL systems, a possible result of bulk magnetic susceptibility and the pronounced sensitivity of ILs aggregation to various experimental conditions, unambiguously suggests that careful description of sample preparation and temperature control during the measurements cannot be neglected.

From the examples presented in this review, we can conclude that a wide range of powerful homonuclear, heteronuclear, and two-dimensional NMR methods were successfully applied to native IL systems (Table 2). Further growth in the field of native IL NMR is anticipated as the technique becomes more widely known. The wider use of the structural and mechanistic NMR studies identified in this review is expected, as well as the emergence of many more applications.

Table 1. Application of NMR Spectroscopy in Native IL Systems[a]

type of NMR study	ionic liquids
reaction monitoring and reaction mechanism	[BMIM][$AlCl_4$],[203] [BMIM][BF_4],[117,189,198,212,218,220] [BMIM][Br],[198] [BMIM][CF_3COO],[114,189] [BMIM][CF_3SO_3],[114] [BMIM][Cl],[191,198,208] [BMIM][ClO_4],[198] [BMIM][PF_6],[89,114,117,118,189,198,220,283] [BMIM][SbF_6],[114,215] [BMIM][Tf_2N],[106,114,117,189,193,200,220,249] [BMPyrr][Tf_2N][114] [BPy][BF_4],[196,194] [BPy][Tf_2N],[114] [C_{10}MIM][Tf_2N][249] [EMIM][$AlCl_4$],[190,195,216] [EMIM][BF_4],[194,196] [EMIM][Tf_2N],[197,199] [EMIM][TfO],[197] [EPy][BF_4][194,196] [HexMIM][BF_4],[114,117] [HexMIM][PF_6],[283] [HMIM][HBr_2],[42] [Me_3NH][$AlCl_4$],[201] [Me_4N][F],[175] [OMIM][BF_4],[114] [OMIM][PF_6],[283] [$P(C_6H_{13})_3(C_{14}H_{29})$][$PF_3(C_2F_5)_3$],[114] [$P(C_6H_{13})_3(C_{14}H_{29})$][$Tf_2N$],[207] [$(SiC_3)$MIM][Cl][203]
transition metal complexes	[BMIM][BF_4],[211,212,218,220,222] [BMIM][PF_6][89,209,221,220] [BMIM][SbF_6],[215] [BMIM][Tf_2N],[213,220] [EMIM][$AlCl_4$][216] [EMIM][Tf_2N][214]
catalytic reactions	[BMIM][BF_4],[117,222,223] [BMIM][CF_3COO],[114] [BMIM][CF_3SO_3],[114] [BMIM][PF_6],[114,117] [BMIM][SbF_6][114] [BMIM][Tf_2N],[114,117,213] [BMMIM][Tf_2N],[114] [BMPyrr][Tf_2N],[114] [BPy][BF_4],[194,196] [BPy][Tf_2N][114] [EMIM][BF_4],[194,196] [EPy][BF_4],[194,196] [HexMIM][BF_4],[114,117] [MBMIM][Tf_2N],[192] [OMIM][BF_4],[114] [$P(C_6H_{13})_3(C_{14}H_{29})$][$PF_3(C_2F_5)_3$][114]
kinetic studies, determination of equilibrium constants and thermodynamic parameters	[BMIM][BF_4],[132,170,220] [BMIM][$N(CN)_2$],[132] [BMIM][PF_6],[220] [BMIM][Tf_2N],[106,131,189,200,220,249] [BMPy][BF_4],[131,132] [BPy][BF_4],[194] [BPy][CH_3SO_4],[131] [C_{10}MIM][Tf_2N],[249] [EMIM][$AlCl_4$],[47,91,92,133] [EMIM][BF_4],[194] [EPy][BF_4][194] [HMIM][HBr_2][42]
gas absorption (solubility of gases)	[BMIM][BF_4],[114,115,117,119,120] [BMIM][CF_3COO][114,117] [BMIM][CF_3SO_3],[114] [BMIM][Cl],[120] [BMIM][Cu_2Cl_3][119] [BMIM][PF_6],[114,117,118,120] [BMIM][SbF_6][114,117] [BMIM][Tf_2N],[114,117,120] [BMIM][TfO][120] [BMMIM][Tf_2N],[114] [BMPyrr][Tf_2N][114] [BPy][Tf_2N],[114] [EMIM][BF_4],[117] [EMIM][Tf_2N][116,117] [HexMIM][BF_4],[114,117] [HexMIM][Tf_2N][117] [$(HOCH_2CH_2)$MIM][BF_4],[115] [MMIM][BF_4][117] [MMIM][Tf_2N],[117] [OMIM][BF_4][114] [OMIM][Tf_2N][117] [$P(C_6H_{13})_3(C_{14}H_{29})$][$PF_3(C_2F_5)_3$],[114] [R][$Tf_2N$] (27 examples)[117]
solvent−solute interactions	[$(AlkOC_2)_2$IM][Tf_2N],[173] [(Allyl)MIM][Cl][181] [BMIM][$AlCl_4$],[164] [BMIM][BF_4][84,119,121,122,150,151,153,156,167−171,176,211,220] [BMIM][Cl],[177,180,181] [BMIM][ClO_4],[187] [BMIM][Cu_2Cl_3][119] [BMIM][$GaCl_4$],[164] [BMIM][$InCl_4$],[164] [BMIM][PF_6],[73,74,89,121,122,156,167,176,171,220,261] [BMIM][$SnCl_3$][60] [BMIM][Tf_2N],[140,145,150,151,153,156,157,189,220] [BMMIM][Tf_2N],[140,157] [BMPy][Tf_2N],[149] [BMPyrr][BF_4][152] [BMPyrr][Tf_2N],[142] [BPy][$AlBr_4$],[154] [BPy][$AlCl_4$][146,154] [EMIM][$(MeO)RPO_2$] (R = H, Me, MeO),[179] [EMIM][$AlCl_4$],[78,90,92,195] [EMIM][BF_4][71,121,122,138] [EMIM][$HCl_2/AlCl_4$],[155] [EMIM][OAc],[181] [EMIM][Tf_2N][156] [HBIM][BF_4],[160−162] [HexMIM][PF_6],[156] [HIM][Tf_2N][66] [MBMIM][Tf_2N],[192] [Me_4N][F],[175] [MEIM][$AlCl_4$][76] [MEIM][$EtAlCl_2/AlCl_3$/Cl],[76] [MEIM][$EtAlCl_3$][61] [MEIM][$EtAlCl_3$],[76] [MMIM][PF_6],[156] [MPPyrr][TF_2N][141] [OMIM][BF_4],[174] [Ph_2P][$GaCl_4$],[241] [$R^1{}_3R^2N$][Tf_2N],[143] [TMSu][HBr_2/AlX_3] (X = Cl, Br)[158]
water effect and water/protons removal	[BMIM][BF_4],[84,89,103] [BMIM][Cl],[86,99] [BMIM][Tf_2N],[100,106,189] [BPy][$AlCl_4$][107] [C_{10}MIM][Br],[96] [C_{10}MIM][NO_3],[96] [choline][Tf_2N],[104] [EMIM][$AlCl_4$],[90,91,107,109,110] [HBet][Tf_2N],[98] [$P(C_6H_{13})_3(C_{14}H_{29})$][Cl][95]
self-diffusion and transport properties	[BMIM][$(C_nF_{2n+1})_2N$],[68] [BMIM][BF_4],[68,153] [BMIM][CF_3COO],[68] [BMIM][CF_3SO_3],[68] [BMIM][PF_6],[68,72,105,261] [BMIM][Tf_2N][65,70,140,145,153] [BMMIM][Tf_2N],[137,140,247] [BMPyrr][Tf_2N][67,70,142] [BPy][BF_4],[64] [BPy][Tf_2N],[64,70] [DEME][Tf_2N][135] [EMIM][BF_4],[64,71,138] [EMIM][Tf_2N],[64,65,67] [HBenzIM][Tf_2N],[144] [HexMIM][PF_6][72] [HexMIM][Tf_2N],[65] [HIM][Tf_2N],[66] [Me_3BuN][Tf_2N][70] [MEIM][$AlCl_4$],[62,63] [MEIM][$EtAlCl_3$],[61] [MMIM][Tf_2N][65] [MPPyrr][$N(CN)_2$],[67] [MPPyrr][TF_2N],[141] [MPPyrr][Tf_2N],[67] [NpMIM][BF_4],[79] [NpMIM][Tf_2N],[79] [OMIM][PF_6],[72] [OMIM][Tf_2N],[65] [$P(C_6H_{13})_3(C_{14}H_{29})$] [$Tf_2N$],[67] [SiMIM][$BF_4$],[79] [SiMIM][$Tf_2N$][79]
extraction and separations	[BMIM][BF_4],[121,122,132] [BMIM][Cl],[123,124] [BMIM][$N(CN)_2$],[132] [BMIM][PF_6],[121,122,134] [BMIM][Tf_2N],[131] [BMIM][TfO],[123,124] [BMPy][BF_4],[131,132] [BPy][CH_3SO_4],[131] [EMIM][$AlCl_4$],[133] [EMIM][BF_4],[121,122] [EMIM][$EtSO_4$],[126] [EMIM][HSO_4],[125] [EMIM][$MeSO_3$],[127] [EMIM][Tf_2N][128,130]

Table 1. Continued

type of NMR study	ionic liquids
ILs structure and properties[b]	[BMMIM][BF_4],[82] [BMIM][Br],[80] [BEIM][CF_3SO_3][54] [BMIM][$(C_2F_5SO_2)_2N$],[68] [BMIM][$AlEt_xCl_{4-x}$] ($x = 1-3$)[48] [BMIM][BF_4],[54,68,82] [BMIM][CF_3COO],[68] [BMIM][CF_3SO_3],[68] [BMIM][CH_3COO],[54] [BMIM][CH_3SO_3],[54] [BMIM][Cl],[58] [BMIM][PF_6],[54,68,263,264] [BMIM][$SnCl_3$],[60] [BMIM][X] ([X] = [ICl_2]$^-$, [I_2Cl]$^-$, [Br_3]$^-$, [IBr_2]$^-$),[44,45] [BMMIM][PF_6],[54] [BMMIM][$ZnCl_3$],[59] [BDMAP][$AlCl_4$],[147] [BPy][$AlCl_4$],[51,147] [EMIM][$(C_2F_5SO_2)_2N$],[54] [EMIM][$AlCl_4$],[50,77,78,81] [EMIM][$BuSO_3$],[265] [EMIM][BF_4],[273] [EMIM][CF_3SO_3][54] [EMIM][$EtSO_3$],[54] [EMIM][HCl_2],[46] [EMIM][Tf_2N][53,54] [EMIM][X] ([X] =[Et_2PO_4], [CF_3COO]$^-$, [$HexSO_4$]$^-$, [$EtSO_4$], [$BuSO_4$]$^-$, [SCN]$^-$, [BF_4]$^-$, [TfO]$^-$, [$N(CN)_2$]$^-$, [Tf_2N]),[52] [HBenzIM][Tf_2N],[144] [HBIM][X] ([X] = [BF_4]$^-$, [Cl]$^-$, [Br]$^-$, [ClO_4]$^-$),[163] [HexMIM][BF_4],[54] [HMIM][HBr_2][42] [HMIM][X] ([X] = [ICl_2]$^-$, [I_2Cl]$^-$, [Br_3]$^-$, [IBr_2]$^-$)[44,45] [MMIM][CH_3SO_3],[54] [MNIM][PF_6][263,264] [NpMIM][BF_4],[79] [NpMIM][Tf_2N],[79] [PMIM][BF_4][273] [SiMIM][BF_4],[79] [SiMIM][Tf_2N][79]
stability, recycling and characterization of ILs	[BMIM][$B(HSO_4)_4$],[231] [BMIM][BF_4],[225,229,230] [BMIM][Cl],[244] [BMIM][$Co(CO)_4$],[242] [BMIM][PF_6],[224,229,230] [BMMIM][Tf_2N],[247] [EMIM][BF_4],[228] [EMIM][PF_6][228] [EMIM][Tf_2N],[235] [HBIM][BF_4],[160][OMIM][PF_6][232,233]

[a] Abbreviations used in the table: [B DMAP]$^+$ = 1-*n*-butyl-4-(dimethylamino)pyridinium; [TMSu]$^+$ = trimethylsulfonium; BenzIm = benzimidazole; [PMPyrr][$N(CN)_2$] = *N*-methyl-*N*-propylpyrrolidinium dicyanamide; [HBet]$^+$ = betainium cation ($Me_3N^+CH_2COOH$); [choline]$^+$ = (2-hydroxyethylammonium)trimethylammonium). [b] The question of IL structure is partially discussed in the studies of self-diffusion and solvent−solute interaction.

Table 2. Scope of the NMR Studies Performed in Native IL Systems[a]

type of study	ionic liquids
^{1}H	[$(AlkOC_2)_2$IM][Tf_2N],[173] [(Allyl)MIM][Cl][181] [BMIM][$(C_2F_5SO_2)_2N$)],[68] [BMIM][$AlEt_xCl_{4-x}$] ($x = 1-3$)[48] [BMIM][BF_4],[68,84,103,114,120−122,150,151,153,156,167−171,176,189,198,223] [BMIM][Br],[80,198] [BMIM][CF_3COO],[68,189,114] [BMIM][CF_3SO_3],[68,114] [BMIM][Cl][58,86,120,123,124,181,191,198] [BMIM][ClO_4],[187,198] [BMIM][$Co(CO)_4$],[242] [BMIM][PF_6][68,72,105,114,118,120−122,134,156,171,176,189,198,283] [BMIM][SbF_6],[114] [BMIM][$SnCl_3$][60] [BMIM][Tf_2N][65,70,75,100,106,114,120,140,145,150,151,153,156,157,167,189] [BMIM][TfO],[120,123,124] [BMIM][X] ([X] = [ICl_2]$^-$, [I_2Cl]$^-$, [Br_3]$^-$, [IBr_2]$^-$),[44,45] [BMMIM][PF_6][137] [BMMIM][Tf_2N],[114,140,157] [BMPy][Tf_2N][149] [BMPyrr][BF_4],[152] [BMPyrr][Tf_2N][70,114,142] [BPy][$AlBr_4$],[154] [BPy][$AlCl_4$],[107,154] [BPy][BF_4][64] [BPy][Tf_2N],[64,70,114] [choline][Tf_2N],[104] [DEME][Tf_2N],[135] [EMIM][$(MeO)RPO_2$] (R = H, Me, MeO)[179] [EMIM][$AlCl_4$],[47,92,107,190] [EMIM][BF_4][64,121,122,138] [EMIM][$EtSO_4$],[126] [EMIM][HCl_2],[46] [EMIM][HSO_4][125] [EMIM][$MeSO_3$],[127] [EMIM][OAc],[181] [EMIM][Tf_2N],[53,64,65,116,128,130,156,199,197,214,235] [EMIM][X] ([X] = [Et_2PO_4], [CF_3COO]$^-$, [$HexSO_4$]$^-$, [$EtSO_4$], [$BuSO_4$]$^-$, [SCN]$^-$, [BF_4]$^-$, [TfO]$^-$, [$N(CN)_2$]$^-$, [Tf_2N]),[52] [Et_3HN][CF_3COO],[83] [Et_3HN][CH_3COO][83] [Et_3HN][Tf_2N],[83] [HBenzIM][Tf_2N],[144] [HBet][Tf_2N][98] [HBIM][X] ([X] = [BF_4]$^-$, [Cl]$^-$, [Br]$^-$, [ClO_4]$^-$)[163] [HexMIM][BF_4],[65,114] [HexMIM][PF_6],[283] [HexMIM][PF_6],[72,156,246] [HIM][Tf_2N],[66] [HMIM][HBr_2][42] [HMIM][X] ([X] = [ICl_2]$^-$, [I_2Cl]$^-$, [Br_3]$^-$, [IBr_2]$^-$)[44,45] [Me_3BuN][Tf_2N],[70] [Me_3NH][$AlCl_4$],[201] [Me_4N][F][175] [MMIM][PF_6],[156] [MMIM][Tf_2N],[65] [MPPyrr][TF_2N][141] [NpMIM][BF_4],[79] [NpMIM][Tf_2N],[79] [OMIM][BF_4][65,114,174] [OMIM][PF_6],[72,232,233,283] [$P(C_6H_{13})_3(C_{14}H_{29})$][Cl],[95] [$P(C_6H_{13})_3(C_{14}H_{29})$][$PF_3(C_2F_5)_3$],[114] [$R^{13}R^2N$][$Tf_2N$],[143] [SiMIM][$BF_4$],[79] [SiMIM][$Tf_2N$],[79] [TMSu][$HBr_2/AlX_3$] (X = Cl, Br)[158]
^{2}H	[BMIM][BF_4],[220] [BMIM][Cl],[99] [BMIM][PF_6],[220] [BMIM][Tf_2N][220] [BPy][$AlCl_4$],[107] [BPy][BF_4][196,194] [EMIM][$AlCl_4$],[92,107,110,195] [EMIM][BF_4],[196,194] [EPy][BF_4][196,194]
^{7}Li	[BMIM][Tf_2N],[140] [BMMIM][Tf_2N],[137] [BMMIM][Tf_2N][140] [BMPyrr][Tf_2N],[142] [DEME][Tf_2N],[135] [EMIM][$AlCl_4$][133] [EMIM][BF_4],[138] [MPPyrr][TF_2N],[141] [$R^1{}_3R^2N$][Tf_2N][143]
^{11}B	[BMIM][BF_4],[122,225] [BMIM][Cl],[208] [BMIM][PF_6],[122] [EMIM][BF_4][71,122]

Table 2. Continued

type of study	ionic liquids
^{13}C and DEPT	[(Allyl)MIM][Cl],[181] [BMIM][$AlCl_4$],[164] [BMIM][BF_4],[117,121,222] [BMIM][Br],[80] [BMIM][CF_3SO_3][117] [BMIM][Cl],[177,180,181,191] [BMIM][$Co(CO)_4$][242] [BMIM][$GaCl_4$],[164] [BMIM][$InCl_4$],[164] [BMIM][PF_6],[73,74,89,117,118,121,224,263,264] [BMIM][SbF_6][189,117] [BMIM][Tf_2N],[75,117,189,200] [BMMIM][$ZnCl_3$],[59] [BMPy][Tf_2N],[149] [BMPyrr][Tf_2N][142] [BDMAP][$AlCl_4$],[147] [BPy][$AlBr_4$],[154] [BPy][$AlCl_4$][147,154] [EMIM][(MeO)RPO_2] (R = H, Me, MeO),[179] [EMIM][$AlCl_4$],[50,109] [EMIM][BF_4],[71,117,121] [EMIM][$BuSO_3$],[265] [EMIM][OAc],[181] [EMIM][Tf_2N][53,117] [EMIM][TfO],[197] [EMIM][X] ([X] = [Et_2PO_4], [CF_3COO]$^-$, [$HexSO_4$]$^-$, [$EtSO_4$], [$BuSO_4$]$^-$, [SCN]$^-$, [BF_4]$^-$, [TfO]$^-$, [$N(CN)_2$]$^-$, [Tf_2N]),[52] [HBIM][BF_4][160−162] [HexMIM][BF_4],[117] [HexMIM][Tf_2N],[117] [HMIM][HBr_2][42] [Me_4N][F],[175] [MEIM][$AlCl_4$],[62,63] [MEIM][$EtAlCl_3$][61] [MMIM][BF_4],[117] [MMIM][Tf_2N],[117] [MNIM][PF_6][263,264] [OMIM][PF_6],[232,233] [OMIM][Tf_2N],[117] [P(C_6H_{13})$_3$($C_{14}H_{29}$)][Tf_2N],[207] [R][Tf_2N] (27 examples)[117]
^{15}N, ^{14}N	[(SiC_3)BIM][Cl],[57] [(SiC_3)MIM][Cl],[57] [BEIM][CF_3SO_3][54] [BMIM][BF_4],[54] [BMIM][CH_3COO],[54] [BMIM][CH_3SO_3][54] [BMIM][PF_6],[54] [BMMIM][PF_6],[54] [EMIM][($C_2F_5SO_2$)$_2$N][54] [EMIM][CF_3SO_3],[54] [EMIM][$EtSO_3$],[54] [EMIM][Tf_2N][54] [Et_3HN][CF_3COO],[83] [Et_3HN][CH_3COO],[83] [Et_3HN][Tf_2N][83] [HexMIM][BF_4],[54] [MMIM][CH_3SO_3][54]
^{17}O	[EMIM][$AlCl_4$][90,91,109,110]
^{19}F	[BMIM][($C_2F_5SO_2$)$_2$N)],[68] [BMIM][BF_4][68,119,122,153,169,225] [BMIM][CF_3COO],[68] [BMIM][CF_3SO_3],[68] [BMIM][PF_6],[68,72,105,122] [BMIM][Tf_2N][65,70,100,106,140,153] [BMMIM][Tf_2N],[140] [BMPy][Tf_2N],[149] [BMPyrr][Tf_2N][70] [BPy][BF_4],[64] [BPy][Tf_2N],[64,70] [DEME][Tf_2N][135] [EMIM][BF_4],[64,122,138] [EMIM][Tf_2N],[53,64,65,197] [Et_3HN][CF_3COO],[83] [Et_3HN][CH_3COO][83] [Et_3HN][Tf_2N],[83] [HBenzIM][Tf_2N],[144] [HBIM][BF_4][160] [HexMIM][PF_6],[72] [HexMIM][Tf_2N],[65] [HIM][Tf_2N][66] [Me_3BuN][Tf_2N],[70] [Me_4N][F],[175] [MMIM][Tf_2N][65] [MPPyrr][Tf_2N],[141] [NpMIM][BF_4],[79] [NpMIM][Tf_2N][79] [OMIM][PF_6],[72] [OMIM][Tf_2N],[65] [P(C_6H_{13})$_3$($C_{14}H_{29}$)][Tf_2N],[207] [$R^{13}R^2N$][Tf_2N],[143] [SiMIM][BF_4],[79] [SiMIM][Tf_2N][79]
^{23}Na	[BMIM][BF_4][169]
^{27}Al	[BMIM][$AlCl_4$],[203] [BMIM][Cl],[191] [BPy][$AlCl_4$][51,107,146] [EMIM][$AlCl_4$],[50,107] [Me_3NH][$AlCl_4$],[201] [MEIM][$AlCl_4$][76] [MEIM][$EtAlCl_2$/$AlCl_3$/Cl],[76] [MEIM][$EtAlCl_3$],[61,76,254] [(SiC_3)MIM][Cl][203]
^{29}Si	[BMIM][$AlCl_4$],[203] [(SiC_3)MIM][Cl][203]
^{31}P	[BMIM][BF_4],[122,211,218,222] [BMIM][BF_4],[212] [BMIM][Cu_2Cl_3],[119] [BMIM][PF_6],[89,122,209,221] [BMIM][SbF_6],[215] [BMIM][Tf_2N],[145,213] [BMMIM][Tf_2N][137] [EMIM][$AlCl_4$],[216] [EMIM][BF_4],[122] [EMIM][Tf_2N][214] [P(C_6H_{13})$_3$($C_{14}H_{29}$)][Tf_2N],[207] [Ph_2P][$GaCl_4$][241]
^{35}Cl, ^{37}Cl	[(Allyl)MIM][Cl],[181] [BMIM][Cl],[58,86,180,181] [BMMIM][$ZnCl_3$][59]
^{119}Sn	[BMIM][$SnCl_3$][60]
^{133}Cs	[BMIM][BF_4],[132] [BMIM][$N(CN)_2$],[132] [BMIM][Tf_2N],[131] [BMPy][BF_4],[131,132] [BPy][CH_3SO_4][131]
diffusion measurements	[(Allyl)MIM][Cl],[181] [BMIM][(C_nF_{2n+1})$_2$N),[68] [BMIM][BF_4],[68,153,169] [BMIM][CF_3COO],[68] [BMIM][CF_3SO_3],[68] [BMIM][Cl],[181] [BMIM][PF_6][68,105] [BMIM][Tf_2N],[65,70,100,140,153] [BMIM][X] ([X] = [ICl_2]$^-$, [Br_3]$^-$, [IBr_2]$^-$),[44,45] [BMMIM][Tf_2N],[137,140,247] [BMPyrr][Tf_2N],[67,70,142] [BPy][BF_4],[64] [BPy][Tf_2N][64,70] [DEME][Tf_2N],[135] [EMIM][BF_4],[64,71,138] [EMIM][Tf_2N],[64,65,67] [Et_3HN][CF_3COO],[83] [Et_3HN][CH_3COO],[83] [Et_3HN][Tf_2N],[83] [HBenzIM][Tf_2N][144] [HexMIM][Tf_2N],[65] [HIM][Tf_2N],[66] [Me_3BuN][Tf_2N][70] [MMIM][Tf_2N],[65] [MPPyrr][$N(CN)_2$],[67] [MPPyrr][Tf_2N],[67,141] [NpMIM][BF_4],[79] [NpMIM][Tf_2N],[79] [OMIM][Tf_2N],[65] [P(C_6H_{13})$_3$($C_{14}H_{29}$)][Tf_2N],[67] [$R^1{}_3R^2N$][Tf_2N],[143] [SiMIM][BF_4],[79] [SiMIM][Tf_2N][79]
relaxation studies	[(Allyl)MIM][Cl],[181] [BMIM][Br],[80] [BMIM][BF_4],[176] [BMIM][Cl],[181] [BMIM][PF_6],[73,176,263,264] [BMIM][Tf_2N],[75] [BPy][$AlCl_4$],[51] [EMIM][$AlCl_4$],[77,78] [EMIM][BF_4],[71] [EMIM][$BuSO_3$],[265] [EMIM][OAc],[181] [MEIM][$AlCl_4$],[76] [MEIM][$EtAlCl_2$/$AlCl_3$/Cl],[76] [MEIM][$EtAlCl_3$][61,76] [MNIM][PF_6],[263,264] [NpMIM][BF_4],[79] [NpMIM][Tf_2N][79] [SiMIM][BF_4],[79] [SiMIM][Tf_2N][79]

Table 2. Continued

type of study	ionic liquids
variable-temperature NMR	[BMIM][(C_nF_{2n+1})$_2$N)],[68] [BMIM][BF_4],[68,132,170,171] [BMIM][Br],[80] [BMIM][CF_3COO],[68] [BMIM][CF_3SO_3],[68] [BMIM][Cl],[177,180] [BMIM][$N(CN)_2$],[132] [BMIM][PF_6],[68,73,89,118,171,263,264] [BMIM][Tf_2N][70,75,131,140,145,200] [BMMIM][Tf_2N],[140] [BMMIM][$ZnCl_3$],[59] [BMPy][BF_4],[131,132] [BMPyrr][Tf_2N],[70] [BPy][$AlCl_4$],[51,146] [BPy][BF_4],[64] [BPy][CH_3SO_4],[131] [BPy][Tf_2N],[64,70] [choline][Tf_2N],[104] [DEME][Tf_2N],[135] [EMIM][$AlCl_4$],[50,92,133] [EMIM][BF_4],[64,71,138] [EMIM][$BuSO_3$],[265] [EMIM][$EtSO_4$],[126] [EMIM][HCl_2][46] [EMIM][Tf_2N],[53,64,128,130] [HBet][Tf_2N],[98] [HMIM][HBr_2][42] [Me_3BuN][Tf_2N],[70] [Me_3NH][$AlCl_4$],[201] [MEIM][$AlCl_4$][76] [MEIM][$EtAlCl_3$/$AlCl_3$/Cl],[76] [MEIM][$EtAlCl_3$],[76] [MNIM][PF_6],[263,264] [MPPyrr][TF_2N],[141] [NpMIM][BF_4][79] [NpMIM][Tf_2N],[79] [P(C_6H_{13})$_3$($C_{14}H_{29}$)][Cl],[95] [Ph_2P][$GaCl_4$],[241] [SiMIM][BF_4],[79] [SiMIM][Tf_2N][79] [TMSu][HBr_2/AlX_3] (X = Cl, Br)[158]
high-pressure MR	[BMIM][BF_4],[114,115,117,119,120,222,223] [BMIM][CF_3COO][114] [BMIM][CF_3SO_3],[114] [BMIM][Cl],[120] [BMIM][Cu_2Cl_3][119] [BMIM][PF_6],[114,117,120,221,261] [BMIM][SbF_6],[114] [BMIM][Tf_2N],[114,117,120] [BMIM][TfO][120] [BMMIM][Tf_2N],[114] [BMPyrr][Tf_2N],[114] [BPy][Tf_2N][114] [EMIM][Tf_2N],[116] [HexMIM][BF_4],[114,117] [($HOCH_2CH_2$)MIM][BF_4],[115] [OMIM][BF_4],[114] [P(C_6H_{13})$_3$($C_{14}H_{29}$)][PF_3(C_2F_5)$_3$][114]
NOE measurements	[BMIM][BF_4],[84] [BMIM][Br],[80] [BMIM][PF_6][73,74,263,264] [EMIM][BF_4],[71] [EMIM][$BuSO_3$],[265] [MEIM][$EtAlCl_3$][61] [MNIM][PF_6][263,264]
2D DOSY	[BMIM][Tf_2N],[249] [C_{10}MIM][Tf_2N],[249] [MEIM][$AlCl_4$][62,63] [MEIM][$EtAlCl_3$][61]
2D ROESY and 2D NOESY	[BMIM][BF_4],[82,84,153,167,168] [BMIM][Tf_2N][153,157,167] [BMMIM][BF_4],[82] [BMMIM][Tf_2N],[157] [EMIM][$AlCl_4$][81] [EMIM][BF_4],[273] [MBMIM][Tf_2N],[192] [PMIM][BF_4][273]
2D HOESY	[BMIM][BF_4],[153] [BMIM][Tf_2N],[153] [Et_3HN][CF_3COO][83] [Et_3HN][CH_3COO],[83] [Et_3HN][Tf_2N],[83] [$R^1{}_3R^2N$][Tf_2N][143]
2D COSY	[BMIM][Cl],[191] [BMIM][Tf_2N][75]
2D $^{31}P\{^1H\}$-COSY	[EMIM][$AlCl_4$][216]
2D HMQC	[BMIM][Tf_2N][75]
solid-state NMR[b]	[BMIM][$AlCl_4$],[203] [BMIM][Cl],[208] [BMIM][PF_6],[283] [BMIM][Tf_2N],[145] [HexMIM][PF_6],[283] [OMIM][PF_6],[283] [P(C_6H_{13})$_3$($C_{14}H_{29}$)][Tf_2N],[207] [(SiC_3)BIM][Cl][57] [(SiC_3)MIM][Cl][57,203]

[a] For some abbreviations, see footnote *a* to Table 1. [b] For the studies of supported systems, see section 2.7 (see also refs 31 and 32).

Table 3. Overview of NMR Techniques Used for Spectra Registration[a,b]

lock nuclei	details	ionic liquids
^2H	external lock standard in a capillary	[($AlkOC_2$)$_2$IM][Tf_2N],[173] [(Allyl)MIM][Cl][181] [BEIM][CF_3SO_3],[54] [BMIM][$AlCl_4$][164] [BMIM][BF_4][54,84,122,132,150,151,153,156,167,168,218] [BMIM][CH_3COO],[54] [BMIM][CH_3SO_3][54] [BMIM][Cl],[58,123,124,177,180,181] [BMIM][$GaCl_4$],[164] [BMIM][$InCl_4$],[164] [BMIM][$N(CN)_2$][132] [BMIM][PF_6][54,89,122,156,209,283] [BMIM][$SnCl_3$],[60] [BMIM][Tf_2N][75,131,150,151,153,156,157,167,200,249] [BMIM][TfO],[123,124] [BMMIM][PF_6][54] [BMMIM][Tf_2N],[157] [BMMIM][$ZnCl_3$][59] [BMPy][BF_4],[131,132] [BMPy][Tf_2N][149] [BMPyrr][BF_4],[152] [BDMAP][$AlCl_4$][147] [BPy][$AlBr_4$][154] [BPy][$AlCl_4$][147,154] [BPy][BF_4],[194,196] [BPy][CH_3SO_4][131] [C_{10}MIM][Tf_2N],[249] [EMIM][($C_2F_5SO_2$)$_2$N][54] [EMIM][$AlCl_4$],[47,92,216] [EMIM][BF_4],[71,122,196,194,273] [EMIM][$BuSO_3$][265] [EMIM][CF_3SO_3],[54] [EMIM][$EtSO_3$][54] [EMIM][$EtSO_4$],[126] [EMIM][HSO_4][125] [EMIM][$MeSO_3$],[127] [EMIM][OAc][181] [EMIM][Tf_2N],[128,156] [EMIM][X] ([X] = [Et_2PO_4], [CF_3COO]$^-$, [$HexSO_4$]$^-$, [$EtSO_4$], [$BuSO_4$]$^-$, [SCN]$^-$, [BF_4]$^-$, [TfO]$^-$, [$N(CN)_2$]$^-$, [Tf_2N]),[52] [EPy][BF_4][194,196] [HexMIM][BF_4],[54] [HexMIM][PF_6][156] [HexMIM][PF_6],[283] [HMIM][HBr_2][42] [Me_3NH][$AlCl_4$],[201] [MMIM][$MeSO_3$][54] [MMIM][PF_6],[156] [OMIM][PF_6][283] [PMIM][BF_4],[273] [TMSu][HBr_2/AlX_3] (X = Cl, Br)[158]
	external lock with IL surrounded by lock standard	[BMIM][($C_2F_5SO_2$)$_2$N],[68] [BMIM][$AlEt_xCl_{4-x}$] (x = 1 - 3),[48] [BMIM][BF_4],[68] [BMIM][CF_3COO],[68] [BMIM][CF_3SO_3][68] [BMIM][PF_6],[68,72,105,263,264] [EMIM][HCl_2][46] [EMIM][Tf_2N],[130,199] [HBenzIM][Tf_2N][144] [HexMIM][PF_6],[72] [HIM][Tf_2N],[66] [MBMIM][Tf_2N],[192] [MNIM][PF_6],[263,264] [OMIM][PF_6][72]
	internal lock by dilution of IL with lock standard[c]	[BMIM][BF_4],[222] [BMIM][Cl],[177,276] [BMIM][PF_6],[283] [EMIM][Tf_2N],[116] [HexMIM][PF_6],[283] [OMIM][PF_6][283]
^{19}F	internal lock using special hardware	[BMIM][BF_4],[75] [BMIM][PF_6],[75] [BMIM][Tf_2N],[75] [EMIM][BF_4],[75] [EMIM][PF_6][75]
No Lock	Unlocked or "sweep-off" mode	[BMIM][BF_4],[114,189,225] [BMIM][CF_3COO],[114,189] [BMIM][CF_3SO_3],[114] [BMIM][PF_6],[114,189] [BMIM][SbF_6],[114] [BMIM][Tf_2N],[106,114,189] [BMMIM][Tf_2N],[114] [BMPyrr][Tf_2N],[114] [BPy][Tf_2N],[114] [EMIM][$AlCl_4$],[92,133,195] [HexMIM][BF_4],[114] [Me_4N][F],[175] [OMIM][BF_4],[114] [P(C_6H_{13})$_3$($C_{14}H_{29}$)][PF_3(C_2F_5)$_3$][114]

[a] Only those studies where the utilized NMR technique was explicitly mentioned are listed in this table. [b] For some abbreviations, see footnote *a* to Table 1. [c] Only a few selected examples were present for comparative purpose; in general, this approach is not recommended to study native IL systems (see text).

6. Abbreviations

ARING	acoustic ringing (cancellation pulse sequence)
BPLED	bipolar longitudinal eddy current delay
COSY	correlation spectroscopy
DEPT	distortionless enhancement by polarization transfer
DOSY	diffusion ordered spectroscopy
GIAO	gauge-including atomic orbitals
HETCOR	heteronuclear correlation
HMBC	heteronuclear multiple bond correlation
HMQC	heteronuclear multiple quantum correlation
HOESY	heteronuclear Overhauser effect spectroscopy
HRMAS	high-resolution magic angle spinning
LED	longitudinal eddy current delay
NOE	nuclear Overhauser effect
NOESY	nuclear Overhauser effect spectroscopy
PGSE	pulsed field gradient spin echo
PGSTE	pulsed field gradient stimulated echo
ROESY	rotating frame Overhauser effect spectroscopy
STE	stimulated echo

7. References

(1) Welton, T. *Chem. Rev.* **1999**, *99*, 2071.
(2) Sheldon, R. *Chem. Commun.* **2001**, 2399.
(3) Earle, M. J.; Seddon, K. R. *Pure Appl. Chem.* **2000**, *72*, 1391.
(4) Dupont, J.; de Souza, R. F.; Suarez, P. A. *Chem. Rev.* **2002**, *102*, 3667.
(5) Wasserscheid, P.; Keim, W. *Angew. Chem., Int. Ed.* **2000**, *39*, 3773.
(6) Zhao, D.; Wu, M.; Kou, Y.; Min, E. *Catal. Today* **2002**, *74*, 157.
(7) Rogers, R. D.; Voth, G. A. *Acc. Chem. Res.* **2007**, *40*, 1077.
(8) Welton, T. *Coord. Chem. Rev.* **2004**, *248*, 2459.
(9) Zhang, Z. C. *Adv. Catal.* **2006**, *49*, 153.
(10) Olivier-Bourbigou, H.; Magna, L. *J. Mol. Catal. A: Chem.* **2002**, *182*, 419.
(11) Prvulescu, V. I.; Hardacre, C. *Chem. Rev.* **2007**, *107*, 2615.
(12) Welton, T.; Smith, P. J. *Adv. Organomet. Chem.* **2004**, *51*, 251.
(13) Gordon, C. M. *Appl. Catal., A* **2001**, *222*, 101.
(14) Haumann, M.; Riisager, A. *Chem. Rev.* **2008**, *108*, 1474.
(15) Martins, M. A. P.; Frizzo, C. P.; Moreira, D. N.; Zanatta, N.; Bonacorso, H. G. *Chem. Rev.* **2008**, *108*, 2015.
(16) Winkel, A.; Reddy, P. V. G.; Wilhelm, R. *Synthesis* **2008**, 999.
(17) Patil, M. L.; Sasai, H. *Chem. Rec.* **2008**, *8*, 98.
(18) Jain, N.; Kumar, A.; Chauhan, S.; Chauhan, S. M. S. *Tetrahedron* **2005**, *61*, 1015.
(19) Wilkes, J. S. *Green Chem.* **2002**, *4*, 73.
(20) Zhao, H.; Malhotra, S. V. *Aldrichim. Acta* **2002**, *35*, 75.
(21) Hagiwara, R.; Ito, Y. *J. Fluorine Chem.* **2000**, *105*, 221.
(22) Plaquevent, J.-C.; Levillain, J.; Guillen, F.; Malhiac, C.; Gaumont, A.-C. *Chem. Rev.* **2008**, *108*, 5035.
(23) Kragl, U.; Eckstein, M.; Kaftzik, N. *Curr. Opin. Biotechnol.* **2002**, *13*, 565.
(24) van Rantwijk, F.; Sheldon, R. A. *Chem. Rev.* **2007**, *107*, 2757.
(25) Seddon, K. R.; Stark, A.; Torres, M.-J. *Pure Appl. Chem.* **2000**, *72*, 2275.
(26) Weingartner, H. *Angew. Chem., Int. Ed.* **2008**, *47*, 654.
(27) Greaves, T. L.; Drummond, C. J. *Chem. Rev.* **2008**, *108*, 206.
(28) Hapiot, P.; Lagrost, C. *Chem. Rev.* **2008**, *108*, 2238.
(29) MacFarlane, D. R.; Forsyth, M.; Howlett, P. C.; Pringle, J. M.; Sun, J.; Annat, G.; Neil, W.; Izgorodina, E. I. *Acc. Chem. Res.* **2007**, *40*, 1165.
(30) Barrosse-Antle, L. E.; Bond, A. M.; Compton, R. G.; O'Mahony, A. M.; Rogers, E. I.; Silvester, D. S. *Chem. Asian J.* **2010**, *5*, 202.
(31) Bankmann, D.; Giernoth, R. *Prog. Nucl. Magn. Reson. Spectrosc.* **2007**, *51*, 63.
(32) Giernoth, R. In *Ionic Liquids in Chemical Analysis*; Koel, M., Ed.; CRC Press, Taylor & Francis Group: Boca Raton, FL, 2009; p 355.
(33) Plechkova, N. V.; Seddon, K. R. *Chem. Soc. Rev.* **2008**, *37*, 123.
(34) Zhao, H. *Chem. Eng. Commun.* **2006**, *193*, 1660.
(35) Anderson, J. L.; Dixon, J. K.; Brennecke, J. F. *Acc. Chem. Res.* **2007**, *40*, 1208.
(36) Han, X.; Armstrong, D. W. *Acc. Chem. Res.* **2007**, *40*, 1079.
(37) Ueki, T.; Watanabe, M. *Macromolecules* **2008**, *41*, 3739.
(38) Pinkert, A.; Marsh, K. N.; Pang, S.; Staiger, M. P. *Chem. Rev.* **2009**, *109*, 6712.
(39) Zhou, Y. *Curr. Nanosci.* **2005**, *1*, 35.
(40) Abbott, A. P.; Frisch, G.; Ryder, K. S. *Annu. Rep. Prog. Chem., Sect. A* **2008**, *104*, 21.
(41) Binnemans, K. *Chem. Rev.* **2007**, *107*, 2592.
(42) Driver, G.; Johnson, K. E. *Green Chem.* **2003**, *5*, 163.
(43) Johansson, K. M.; Izgorodina, E. I.; Forsyth, M.; MacFarlane, D. R.; Seddon, K. R. *Phys. Chem. Chem. Phys.* **2008**, *10*, 2972.
(44) Bagno, A.; Butts, C.; Chiappe, C.; D'Amico, F.; Lord, J. C. D.; Pieraccini, D.; Rastrelli, F. *Org. Biomol. Chem.* **2005**, *3*, 1624.
(45) Bortolini, O.; Bottai, M.; Chiappe, C.; Conte, V.; Pieraccini, D. *Green Chem.* **2002**, *4*, 621.
(46) Campbell, J. L. E.; Johnson, K. E.; Torkelson, J. R. *Inorg. Chem.* **1994**, *33*, 3340.
(47) Campbell, J. L. E.; Johnson, K. E. *Inorg. Chem.* **1993**, *32*, 3809.
(48) Chauvin, Y.; Tiggelen, F. D. M.-V.; Olivier, H. *J. Chem. Soc., Dalton Trans.* **1993**, 1009.
(49) Dailey, B. P.; Shoolery, J. N. *J. Am. Chem. Soc.* **1955**, *77*, 3977.
(50) Wilkes, J. S.; Frye, J. S.; Reynolds, G. F. *Inorg. Chem.* **1983**, *22*, 3870.
(51) Matsumoto., T.; Ichikawa, K. *J. Am. Chem. Soc.* **1984**, *106*, 4316.
(52) Begel, S.; Illner, P.; Kern, S.; Puchta, R.; van Eldik, R. *Inorg. Chem.* **2008**, *47*, 7121.
(53) Fujii, K.; Soejima, Y.; Kyoshoin, Y.; Fukuda, S.; Kanzaki, R.; Umebayashi, Y.; Yamaguchi, T.; Ishiguro, S.; Takamuku, T. *J. Phys. Chem. B* **2008**, *112*, 4329.
(54) Lyčka, A.; Dolecek, R.; Simunek, P.; Machacek, V. *Magn. Reson. Chem.* **2006**, *44*, 521.
(55) Marek, R.; Lyčka, A.; Kolehmainen, E.; Sievänen, E.; Toušek, J. *Curr. Org. Chem.* **2007**, *11*, 1154.
(56) Bifulco, G.; Dambruoso, P.; Gomez-Paloma, L.; Riccio, R. *Chem. Rev.* **2007**, *107*, 3744.
(57) Brenna, S.; Posset, T.; Furrer, J.; Blümel, J. *Chem.—Eur. J.* **2006**, *12*, 2880.
(58) Remsing, R. C.; Wildin, J. L.; Rapp, A. L.; Moyna, G. *J. Phys. Chem. B* **2007**, *111*, 11619.
(59) Lecocq, V.; Graille, A.; Santini, C. C.; Baudouin, A.; Chauvin, Y.; Basset, J. M.; Arzel, L.; Bouchub, D.; Fenetc, B. *New J. Chem.* **2005**, *29*, 700.
(60) Illner, P.; Zahl, A.; Puchta, R.; Hommes, N. E.; Wasserscheid, P.; van Eldik, R. *J. Organomet. Chem.* **2005**, *690*, 3567.
(61) Larive, C. K.; Lin, M.; Kinnear, B. S.; Piersma, B. J.; Keller, C. E.; Carper, W. R. *J. Phys. Chem. B* **1998**, *102*, 1717.
(62) Carper, W. R.; Mains, G. J.; Piersma, B. J.; Mansfield, S. L.; Larive, C. K. *J. Phys. Chem.* **1996**, *100*, 4724.
(63) Larive, C. K.; Lin, M.; Piersma, B. J.; Carper, W. R. *J. Phys. Chem.* **1995**, *99*, 12409.
(64) Noda, A.; Hayamizu, K.; Watanabe, M. *J. Phys. Chem. B* **2001**, *105*, 4603.
(65) Tokuda, H.; Hayamizu, K.; Ishii, K.; Susan, M. A. B. H.; Watanabe, M. *J. Phys. Chem. B* **2005**, *109*, 6103.
(66) Noda, A.; Susan, M. A. B. H.; Kudo, K.; Mitsushima, S.; Hayamizu, K.; Watanabe, M. *J. Phys. Chem. B* **2003**, *107*, 4024.
(67) Annat, G.; MacFarlane, D. R.; Forsyth, M. *J. Phys. Chem. B* **2007**, *111*, 9018.
(68) Tokuda, H.; Hayamizu, K.; Ishii, K.; Susan, M. A. B. H.; Watanabe, M. *J. Phys. Chem. B* **2004**, *108*, 16593.
(69) Tokuda, H.; Tsuzuki, S.; Susan, M. A. B. H.; Hayamizu, K.; Watanabe, M. *J. Phys. Chem. B* **2006**, *110*, 19593.
(70) Tokuda, H.; Ishii, K.; Susan, M. A. B. H.; Tsuzuki, S.; Hayamizu, K.; Watanabe, M. *J. Phys. Chem. B* **2006**, *110*, 2833.
(71) Huang, J.-F.; Chen, P.-Y.; Sun, I.-W.; Wang, S. P. *Inorg. Chim. Acta* **2001**, *320*, 7.
(72) Umecky, T.; Kanakubo, M.; Ikushima, Y. *J. Mol. Liq.* **2005**, *119*, 77.
(73) Antony, J. H.; Mertens, D.; Dölle, A.; Wasserscheid, P.; Carper, W. R. *ChemPhysChem* **2003**, *4*, 588.
(74) Carper, W. R.; Wahlbeck, P. G.; Antony, J. H.; Mertens, D.; Dölle, A.; Wasserscheid, P. *Anal. Bioanal. Chem.* **2004**, *378*, 1548.
(75) Giernoth, R.; Bankmann, D.; Schlörer, N. *Green Chem.* **2005**, *7*, 279.
(76) Keller, C. E.; Carper, W. R. *Inorg. Chim. Acta* **1993**, *210*, 203.
(77) Carper, W. R.; Pflug, J. L.; Elias, A. M.; Wilkes, J. S. *J. Phys. Chem.* **1992**, *96*, 3828.
(78) Keller, C. E.; Carper, W. R. *J. Phys. Chem.* **1994**, *98*, 6865.
(79) Chung, S. H.; Lopato, R.; Greenbaum, S. G.; Shirota, H.; Castner, E. W.; Wishart, J. F. *J. Phys. Chem. B* **2007**, *111*, 4885.
(80) Imanari, M.; Tsuchiya, H.; Seki, H.; Nishikawa, K.; Tashiro, M. *Magn. Reson. Chem.* **2009**, *47*, 67.
(81) Mantz, R. A.; Trulove, P. C.; Carlin, R. T.; Osteryoung, R. A. *Inorg. Chem.* **1995**, *34*, 3846.
(82) Mele, A.; Romanò, G.; Giannone, M.; Ragg, E.; Fronza, G.; Raos, G.; Marcon, V. *Angew. Chem., Int. Ed.* **2006**, *45*, 1123.
(83) Judeinstein, P.; Iojoiu, C.; Sanchez, J.-Y.; Ancian, B. *J. Phys. Chem. B* **2008**, *112*, 3680.

(84) Mele, A.; Tran, C. D.; De Paoli Lacerda, S. H. *Angew. Chem., Int. Ed.* **2003**, *42*, 4364.
(85) Zhao, Y.; Gao, S.; Wang, J.; Tang, J. *J. Phys. Chem. B* **2008**, *112*, 2031.
(86) Remsing, R. C.; Liu, Z.; Sergeyev, I.; Moyna, G. *J. Phys. Chem. B* **2008**, *112*, 7363.
(87) Martins, C. T.; Sato, B. M.; El Seoud, O. A. *J. Phys. Chem. B* **2008**, *112*, 8330.
(88) Singh, T.; Kumar, A. *J. Phys. Chem. B* **2007**, *111*, 7843.
(89) Rangits, G.; Petõcz, G.; Berente, Z.; Kollár, L. *Inorg. Chim. Acta* **2003**, *353*, 301.
(90) Zawodzinski, T. A., Jr.; Osteryoung, R. A. *Inorg. Chem.* **1987**, *26*, 2920.
(91) Zawodzinski, T. A., Jr.; Osteryoung, R. A. *Inorg. Chem.* **1990**, *29*, 2842.
(92) Trulove, P. C.; Sukumaran, D. K.; Osteryoung, R. A. *Inorg. Chem.* **1993**, *32*, 4396.
(93) Palomar, J.; Ferro, V. R.; Gilarranz, M. A.; Rodriguez, J. J. *J. Phys. Chem. B* **2007**, *111*, 168.
(94) Bagno, A.; D'Amico, F.; Saielli, G. *J. Phys. Chem. B* **2006**, *110*, 23004.
(95) Dwan, J.; Durant, D.; Ghandi, K. *Cent. Eur. J. Chem.* **2008**, *6*, 347.
(96) Firestone, M. A.; Rickert, P. G.; Seifert, S.; Dietz, M. L. *Inorg. Chim. Acta* **2004**, *357*, 3991.
(97) Firestone, M. A.; Dzielawa, J. A.; Zapol, P.; Curtiss, L. A.; Seifert, S.; Dietz, M. L. *Langmuir* **2002**, *18*, 7258.
(98) Nockemann, P.; Thijs, B.; Parac-Vogt, T. N.; Van Hecke, K.; Van Meervelt, L.; Tinant, B.; Hartenbach, I.; Schleid, T.; Ngan, V. T.; Nguyen, M. T.; Binnemans, K. *Inorg. Chem.* **2008**, *47*, 9987.
(99) Yasaka, Y.; Wakai, C.; Matubayasi, N.; Nakahara, M. *J. Phys. Chem. A* **2007**, *111*, 541.
(100) Rollet, A.-L.; Porion, P.; Vaultier, M.; Billard, I.; Deschamps, M.; Bessada, C.; Jouvensal, L. *J. Phys. Chem. B* **2007**, *111*, 11888.
(101) Ma, K.; Shahkhatuni, A. A.; Somashekhar, B. S.; Gowda, G. A. N.; Tong, Y. Y.; Khetrapal, C. L.; Weiss, R. G. *Langmuir* **2008**, *24*, 9843.
(102) Shahkhatuni, A. A.; Ma, K.; Weiss, R. G. *J. Phys. Chem. B* **2009**, *113*, 4209.
(103) Moreno, M.; Castiglione, F.; Mele, A.; Pasqui, C.; Raos, G. *J. Phys. Chem. B* **2008**, *112*, 7826.
(104) Nockemann, P.; Binnemans, K.; Thijs, B.; Parac-Vogt, T. N.; Merz, K.; Mudring, A.-V.; Menon, P. C.; Rajesh, R. N.; Cordoyiannis, G.; Thoen, J.; Leys, J.; Glorieux, C. *J. Phys. Chem. B* **2009**, *113*, 1429.
(105) Umecky, T.; Kanakubo, M.; Ikushima, Y. *Fluid Phase Equilib.* **2005**, *288*−*289*, 329.
(106) Creary, X.; Willis, E. D.; Gagnon, M. *J. Am. Chem. Soc.* **2005**, *127*, 18114.
(107) Zawodzinski, T. A., Jr.; Carlin, R. T.; Osteryoung, R. A. *Anal. Chem.* **1987**, *59*, 2639.
(108) Abdul-Sada, A. K.; Avent, A. G.; Parkington, M. J.; Ryan, T. A.; Seddon, K. R.; Welton, T. *J. Chem. Soc., Chem. Commun.* **1987**, 1643.
(109) Abdul-Sada, A. K.; Avent, A. G.; Parkington, M. J.; Ryan, T. A.; Seddon, K. R.; Welton, T. *J. Chem. Soc., Dalton Trans.* **1993**, 3283.
(110) Noël, M. A. M.; Trulove, P. C.; Osteryoung, R. A. *Anal. Chem.* **1991**, *63*, 2892.
(111) Kovacs, H.; Moskau, D.; Spraul, M. *Prog. Nucl. Magn. Reson. Spectrosc.* **2005**, *46*, 131.
(112) Yasaka, Y.; Wakai, C.; Matubayasi, N.; Nakahara, M. *Anal. Chem.* **2009**, *81*, 400.
(113) Anthony, J. L.; Maginn, E. J.; Brennecke, J. F. *J. Phys. Chem. B* **2002**, *106*, 7315.
(114) Dyson, P. J.; Laurenczy, G.; Ohlin, C. A.; Vallance, J.; Welton, T. *Chem. Commun.* **2003**, 2418.
(115) Yang, X.; Yan, N.; Fei, Z.; Crespo-Quesada, R. M.; Laurenczy, G.; Kiwi-Minsker, L.; Kou, Y.; Li, Y.; Dyson, P. J. *Inorg. Chem.* **2008**, *47*, 7444.
(116) Solinas, M.; Pfaltz, A.; Cozzi, P. G.; Leitner, W. *J. Am. Chem. Soc.* **2004**, *126*, 16142.
(117) Ohlin, C. A.; Dyson, P. J.; Laurenczy, G. *Chem. Commun.* **2004**, 1070.
(118) Ruta, M.; Laurenczy, G.; Dyson, P. J.; Kiwi-Minsker, L. *J. Phys. Chem. C* **2008**, *112*, 17814.
(119) Tempel, D. J.; Henderson, P. B.; Brzozowski, J. R.; Pearlstein, R. M.; Cheng, H. *J. Am. Chem. Soc.* **2008**, *130*, 400.
(120) Pomelli, C. S.; Chiappe, C.; Vidis, A.; Laurenczy, G.; Dyson, P. J. *J. Phys. Chem. B* **2007**, *111*, 13014.
(121) Zhang, S.; Zhang, Z. C. *Green Chem.* **2002**, *4*, 376.
(122) Su, B.-M.; Zhang, S.; Zhang, Z. C. *J. Phys. Chem. B* **2004**, *108*, 19510.
(123) Arce, A.; Rodríguez, O.; Soto, A. *Ind. Eng. Chem. Res.* **2004**, *43*, 8323.
(124) Arce, A.; Rodríguez, O.; Soto, A. *J. Chem. Eng. Data* **2004**, *49*, 514.
(125) Arce, A.; Rodríguez, O.; Soto, A. *Chem. Eng. Sci.* **2006**, *61*, 6929.
(126) Arce, A.; Pobudkowska, A.; Rodríguez, O.; Soto, A. *Chem. Eng. J.* **2007**, *133*, 213.
(127) Arce, A.; Marchiaro, A.; Rodríguez, O.; Soto, A. *AIChE J.* **2006**, *52*, 2089.
(128) Arce, A.; Earle, M. J.; Rodríguez, H.; Seddon, K. R. *Green Chem.* **2007**, *9*, 70.
(129) Selvan, M. S.; McKinley, M. D.; Dubois, R. H.; Atwood, J. L. *J. Chem. Eng. Data* **2000**, *45*, 841.
(130) Tsuda, R.; Kodama, K.; Ueki, T.; Kokubo, H.; Imabayashi, S.-i.; Watanabe, M. *Chem. Commun.* **2008**, 4939.
(131) Vendilo, A. G.; Rönkkömäki, H.; Hannu-Kuure, M.; Lajunen, M.; Asikkala, J.; Petrov, A. A.; Krasovsky, V. G.; Chernikova, E. A.; Oksman, P.; Lajunen, L. H. J.; Popov, K. I. *Russ. J. Coord. Chem.* **2008**, *34*, 635.
(132) Vendilo, A. G.; Rönkkömäki, H.; Hannu-Kuure, M.; Lajunen, M.; Asikkala, J.; Chernikova, E. A.; Lajunen, L. H. J.; Tuomi, T.; Popov, K. I. *Mendeleev Commun.* **2009**, *19*, 196.
(133) Gerhard, A.; Cobranchi, D. P.; Garland, B. A.; Highley, A. M.; Huang, Y.-H.; Konya, G.; Zahl, A.; van Eldik, R.; Petrucci, S.; Eyring, E. M. *J. Phys. Chem.* **1994**, *98*, 7923.
(134) Huang, H.-L.; Wang, H. P.; Wei, G.-T.; Sun., I.-W.; Huang, J.-F.; Yang, Y. W. *Environ. Sci. Technol.* **2006**, *40*, 4761.
(135) Hayamizu, K.; Tsuzuki, S.; Seki, S.; Ohno, Y.; Miyashiro, H.; Kobayashi, Y. *J. Phys. Chem. B* **2008**, *112*, 1189.
(136) Hayamizu, K.; Tsuzuki, S.; Seki, S. *J. Phys. Chem. A* **2008**, *112*, 12027.
(137) Lee, S.-Y.; Yong, H. H.; Lee, Y. J.; Kim, S. K.; Ahn, S. *J. Phys. Chem. B* **2005**, *109*, 13663.
(138) Hayamizu, K.; Aihara, Y.; Nakagawa, H.; Nukuda, T.; Price, W. S. *J. Phys. Chem. B* **2004**, *108*, 19527.
(139) Aihara, Y.; Sugimoto, K.; Price, W. S.; Hayamizu, K. *J. Chem. Phys.* **2000**, *113*, 1981.
(140) Saito, Y.; Umecky, T.; Niwa, J.; Sakai, T.; Maeda, S. *J. Phys. Chem. B* **2007**, *111*, 11794.
(141) Nicotera, I.; Oliviero, C.; Henderson, W. A.; Appetecchi, G. B.; Passerini, S. *J. Phys. Chem. B* **2005**, *109*, 22814.
(142) Frömling, T.; Kunze, M.; Schönhoff, M.; Sundermeyer, J.; Roling, B. *J. Phys. Chem. B* **2008**, *112*, 12985.
(143) Le, M. L. P.; Alloin, F.; Strobel, P.; Leprêtre, J.-C.; del Valle, C. P.; Judeinstein, P. *J. Phys. Chem. B* **2010**, *114*, 894.
(144) Nakamoto, H.; Noda, A.; Hayamizu, K.; Hayashi, S.; Hamaguchi, H.; Watanabe, M. *J. Phys. Chem. C* **2007**, *111*, 1541.
(145) Kim, J.-D.; Hayashi, S.; Onoda, M.; Sato, A.; Nishimura, C.; Mori, T.; Honma, I. *Electrochim. Acta* **2008**, *53*, 7638.
(146) Gray, J. L.; Maciel, G. E. *J. Am. Chem. Soc.* **1981**, *103*, 7147.
(147) Cheek, G. T.; Osteryoung, R. A. *Inorg. Chem.* **1982**, *21*, 3581.
(148) Trulove, P. C.; Carlin, R. T.; Osteryoung, R. A. *J. Am. Chem. Soc.* **1990**, *112*, 4567.
(149) Brausch, N.; Metlen, A.; Wasserscheid, P. *Chem. Commun.* **2004**, 1552.
(150) D'Anna, F.; Frenna, V.; Pace, V.; Noto, R. *Tetrahedron* **2006**, *62*, 1690.
(151) D'Anna, F.; Frenna, V.; La Marca, S.; Noto, R.; Pace, V.; Spinelli, D. *Tetrahedron* **2008**, *64*, 672.
(152) D'Anna, F.; La Marca, S.; Noto, R. *J. Org. Chem.* **2008**, *73*, 3397.
(153) Nama, D.; Kumar, P.G. A.; Pregosin, P. S.; Geldbach, T. J.; Dyson, P. J. *Inorg. Chim. Acta* **2006**, *359*, 1907.
(154) Robinson, J.; Bugle, R. C.; Chum, H. L.; Koran, D.; Osteryoung, R. A. *J. Am. Chem. Soc.* **1979**, *101*, 3776.
(155) Zawodzinski, T. A., Jr.; Osteryoung, R. A. *Inorg. Chem.* **1988**, *27*, 4383.
(156) Holbrey, J. D.; Reichert, W. M.; Nieuwenhuyzen, M.; Sheppard, O.; Hardacre, C.; Rogers, R. D. *Chem. Commun.* **2003**, 476.
(157) Gutel, T.; Santini, C. C.; Pádua, A. A. H.; Fenet, B.; Chauvin, Y.; Lopes, J. N. C.; Bayard, F.; Gomes, M. F. C.; Pensado, A. S. *J. Phys. Chem. B* **2009**, *113*, 170.
(158) Ma, M.; Johnson, K. E. *J. Am. Chem. Soc.* **1995**, *117*, 1508.
(159) Smith, G. P.; Dworkin, A. S.; Pagni, R. M.; Zing, S. P. *J. Am. Chem. Soc.* **1989**, *111*, 5075.
(160) Gholap, A. R.; Venkatesan, K.; Daniel, T.; Lahoti, R. J.; Srinivasan, K. V. *Green Chem.* **2004**, *6*, 147.
(161) Gholap, A. R.; Chakor, N. S.; Daniel, T.; Lahoti, R. J.; Srinivasan, K. V. *J. Mol. Catal. A: Chem.* **2006**, *245*, 37.
(162) Venkatesan, K.; Pujari, S. S.; Lahoti, R. J.; Srinivasan, K. V. *Ultrason. Sonochem.* **2008**, *15*, 548.
(163) Nadaf, R. N.; Siddiqui, S. A.; Daniel, T.; Lahoti, R. J.; Srinivasan, K. V. *J. Mol. Catal. A: Chem.* **2004**, *214*, 155.
(164) Angueira, E. J.; White, M. G. *J. Mol. Catal. A: Chem.* **2007**, *277*, 164.

(165) Li, N.; Zhang, S.; Zheng, L.; Wu, J.; Li, X.; Yu, L. *J. Phys. Chem. B* **2008**, *112*, 12453.
(166) Gao, Y.; Zhang, J.; Li, X.; Yu, L. *ChemPhysChem* **2006**, *7*, 1554.
(167) Gao, Y.; Li, N.; Li, X.; Zhang, S.; Zheng, L.; Bai, X.; Yu, L. *J. Phys. Chem. B* **2009**, *113*, 123.
(168) Gao, Y.; Li, N.; Zhang, S.; Zheng, L.; Li, X.; Dong, B.; Yu, L. *J. Phys. Chem. B* **2009**, *113*, 1389.
(169) Murgia, S.; Palazzo, G.; Mamusa, M.; Lampis, S.; Monduzzi, M. *J. Phys. Chem. B* **2009**, *113*, 9216.
(170) Inoue, T. *J. Colloid Interface Sci.* **2009**, *337*, 240.
(171) Inoue, T.; Misono, T. *J. Colloid Interface Sci.* **2009**, *337*, 247.
(172) Gayet, F.; Kalamouni, C. E.; Lavedan, P.; Marty, J.-D.; Brûlet, A.; de Viguerie, N. L. *Langmuir* **2009**, *25*, 9741.
(173) Riisager, A.; Fehrmann, R.; Berg, R. W.; van Hal, R.; Wasserscheid, P. *Phys. Chem. Chem. Phys.* **2005**, *7*, 3052.
(174) Singh, T.; Kumar, A. *J. Phys. Chem. B* **2008**, *112*, 4079.
(175) Yonker, C. R.; Linehan, J. C. *J. Supercrit. Fluids* **2004**, *29*, 257.
(176) Shiddiky, M. J. A.; Torriero, A. A. J.; Zhao, C.; Burgar, I.; Kennedy, G.; Bond, A. M. *J. Am. Chem. Soc.* **2009**, *131*, 7976.
(177) Moulthrop, J. S.; Swatloski, R. P.; Moyna, G.; Rogers, R. D. *Chem. Commun.* **2005**, 1557.
(178) Brendler, E.; Fischer, S.; Leipner, H. *Cellulose* **2002**, 1 (and references therein).
(179) Fukaya, Y.; Hayashi, K.; Wada, M.; Ohno, H. *Green Chem.* **2008**, *10*, 44.
(180) Remsing, R. C.; Swatloski, R. P.; Rogers, R. D.; Moyna, G. *Chem. Commun.* **2006**, 1271.
(181) Remsing, R. C.; Hernandez, G.; Swatloski, R. P.; Massefski, W. W.; Rogers, R. D.; Moyna, G. *J. Phys. Chem. B* **2008**, *112*, 11071.
(182) Youngs, T. G. A.; Hardacre, C.; Holbrey, J. D. *J. Phys. Chem. B* **2007**, *111*, 13765.
(183) Sievers, C.; Valenzuela-Olarte, M. B.; Marzialetti, T.; Musin, I.; Agrawal, P. K.; Jones, C. W. *Ind. Eng. Chem. Res.* **2009**, *48*, 1277.
(184) Byrne, N.; Wang, L.-M.; Belieres, J.-P.; Angell, C. A. *Chem. Commun.* **2007**, 2714.
(185) Baker, S. N.; McCleskey, T. M.; Pandey, S.; Baker, G. A. *Chem. Commun.* **2004**, 940.
(186) Fujita, K.; MacFarlane, D. R.; Forsyth, M. *Chem. Commun.* **2005**, 4804.
(187) Byrne, N.; Angell, C. A. *J. Mol. Biol.* **2008**, *378*, 707.
(188) Belieres, J.-P.; Angell, C. A. *J. Phys. Chem. B* **2007**, *111*, 4926.
(189) Vidis, A.; Ohlin, C. A.; Laurenczy, G.; Kusters, E.; Sedelmeier, G.; Dayson, P. J. *Adv. Synth. Catal.* **2005**, *347*, 266.
(190) Boon, J. A.; Levisky, J. A.; Pflug, J. L.; Wilkes, J. S. *J. Org. Chem.* **1986**, *51*, 480.
(191) Csihony, S.; Bodor, A.; Rohonczy, J.; Horváth, I. T. *J. Chem. Soc., Perkin Trans. 1* **2002**, 2861.
(192) Leclercq, L.; Suisse, I.; Agbossou-Niedercorn, F. *Chem. Commun.* **2008**, 311.
(193) Scholten, J. D.; Dupont, J. *Organometallics* **2008**, *27*, 4439.
(194) Owens, G. S.; Durazo, A.; Abu-Omar, M. M. *Chem.—Eur. J.* **2002**, *8*, 3053.
(195) Carlin, R. T.; Truelove, P. C.; Osteryoijng, R. A. *Electrochim. Acta* **1992**, *37*, 2615.
(196) Durazo, A.; Abu-Omar, M. M. *Chem. Commun.* **2002**, 66.
(197) Mehdi, H.; Bodor, A.; Lantos, D.; Horváth, I. T.; De Vos, D. E.; Binnemans, K. *J. Org. Chem.* **2007**, *72*, 517.
(198) Gholap, A. R.; Venkatesan, K.; Daniel, T.; Lahoti, R. J.; Srinivasan, K. V. *Green Chem.* **2003**, *5*, 693.
(199) Chiappe, C.; Piccioli, P.; Pieraccini, D. *Green Chem.* **2006**, *8*, 277.
(200) Goodrich, P.; Hardacre, C.; Mehdi, H.; Nancarrow, P.; Rooney, D. W.; Thompson, J. M. *Ind. Eng. Chem. Res.* **2006**, *45*, 6640.
(201) Schmidt, R.; Welch, M. B.; Anderson, R. L.; Sardashti, M.; Randolph, B. B. *Energy Fuels* **2008**, *22*, 1812.
(202) Frank, H.; Ziener, U.; Landfester, K. *Macromolecules* **2009**, *42*, 7846.
(203) Valkenberg, M. H.; deCastro, C.; Hölderich, W. F. *Top. Catal.* **2001**, *14*, 139.
(204) Li, P.; Wang, L.; Zhang, Y. *Tetrahedron* **2008**, *64*, 10825.
(205) Sievers, C.; Jiménez, O.; Knappa, R.; Lin, X.; Müller, T. E.; Türler, A.; Wierczinski, B.; Lercher, J. A. *J. Mol. Catal. A: Chem.* **2008**, *279*, 187.
(206) Fowa, K. L.; Jaenicke, S.; Müller, T. E.; Sievers, C. *J. Mol. Catal. A: Chem.* **2008**, *279*, 239.
(207) Pringle, J. M.; MacFarlane, D. R.; Forsyth, M. *Synth. Met.* **2005**, *155*, 684.
(208) Himmelberger, D. W.; Yoon, C. W.; Bluhm, M. E.; Carroll, P. J.; Sneddon, L. G. *J. Am. Chem. Soc.* **2009**, *131*, 14101.
(209) Rangits, G.; Berente, Z.; Kégl, T.; Kollár, T. *J. Coord. Chem.* **2005**, *58*, 869.
(210) Iida, M.; Baba, C.; Inoue, M.; Yoshida, H.; Taguchi, E.; Furusho, H. *Chem.—Eur. J.* **2008**, *14*, 5047.
(211) Mathews, C. J.; Smith, P. J.; Welton, T.; White, A. J. P.; Williams, D. J. *Organometallics* **2001**, *20*, 3848.
(212) McLachlan, F.; Mathews, C. J.; Smith, P. J.; Welton, T. *Organometallics* **2003**, *22*, 5350.
(213) Conte, V.; Floris, B.; Galloni, P.; Mirruzzo, V.; Scarso, A.; Sordi, D.; Strukul, G. *Green Chem.* **2005**, *7*, 262.
(214) Breitenlechner, S.; Fleck, M.; Müller, T. E.; Suppan, A. *J. Mol. Catal. A: Chem.* **2004**, *214*, 175.
(215) Chauvin, Y.; Mussmann, L.; Olivier, H. *Angew. Chem., Int. Ed.* **1995**, *34*, 2698.
(216) Mann, B. E.; Guzman, M. H. *Inorg. Chim. Acta* **2002**, *330*, 143.
(217) Collman, J. P.; Hegedus, L. S.; Norton, J. R.; Finke, R. G. *Principles and Application of Organotransition Metal Chemistry*; University Science Books: Mill Valley, CA, 1987.
(218) Navarro, J.; Sági, M.; Sola, E.; Lahoz, F. J.; Dobrinovitch, I. T.; Kathó, A.; Joó, F.; Oro, L. A. *Adv. Synth. Catal.* **2003**, *345*, 280.
(219) Ananikov, V. P.; Musaev, D. G.; Morokuma, K. Transition Metal Catalyzed Carbon−Carbon Bond Formation: The Key of Homogeneous Catalysis. In *Computational Modeling for Homogeneous and Enzymatic Catalysis: A Knowledge-Base for Designing Efficient Catalysts*; Wiley-VCH Verlag GmbH & Co. KGaA: Weinheim, Germany, 2008; pp 131−148.
(220) Ott, L. S.; Cline, M. L.; Deetlefs, M.; Seddon, K. R.; Finke, R. G. *J. Am. Chem. Soc.* **2005**, *127*, 5758.
(221) Silva, S. M.; Bronger, R. P. J.; Freixa, Z.; Dupont, J.; van Leeuwen, P. W. N. M. *New J. Chem.* **2003**, *27*, 1294.
(222) Mehnert, C. P.; Cook, R. A.; Dispenziere, N. C.; Mozeleski, E. J. *Polyhedron* **2004**, *23*, 2679.
(223) Zhao, D.; Dyson, P. J.; Laurenczy, G.; McIndoe, J. S. *J. Mol. Catal. A: Chem.* **2004**, *214*, 19.
(224) Yang, Q.; Dionysiou, D. D. *J. Photochem. Photobiol. A* **2004**, *165*, 229.
(225) Zhao, C.; Bond, A. M. *J. Am. Chem. Soc.* **2009**, *131*, 4279.
(226) Allen, D.; Baston, G.; Bradley, A. E.; Gorman, T.; Haile, A.; Hamblett, I.; Hatter, J. E.; Healey, M. J. F.; Hodgson, B.; Lewin, R.; Lovell, K. V.; Newton, B.; Pitner, W. R.; Rooney, D. W.; Sanders, D.; Seddon, K. R.; Sims, H. E.; Thiedd, R. C. *Green Chem.* **2002**, *4*, 152.
(227) Tarábek, P.; Liu, S.; Haygarth, K.; Bartels, D. M. *Radiat. Phys. Chem.* **2009**, *78*, 168.
(228) Laali, K. K.; Gettwert, V. J. *J. Org. Chem.* **2001**, *66*, 35.
(229) Suarez, P. A. Z.; Dullius, J. E. L.; Einloft, S.; de Souza, R. F.; Dupont, J. *Polyhedron* **1996**, *15*, 1217.
(230) Suarez, P. A. Z.; Einloft, S.; Dullius, J. E. L.; de Souza, R. F.; Dupont, J. *J. Chim. Phys.* **1998**, *95*, 1626.
(231) Wasserscheid, P.; Sesing, M.; Korth, W. *Green Chem.* **2002**, *4*, 134.
(232) Zuo, Y.; Liu, Y.; Chen, J.; Li, D. Q. *Ind. Eng. Chem. Res.* **2008**, *47*, 2349.
(233) Zuo, Y.; Chen, J.; Li, D. *Sep. Purif. Technol.* **2008**, *63*, 684.
(234) Fuller, J.; Carlin, R. T.; Osteryoung, R. A. *J. Electrochem. Soc.* **1997**, *144*, 3881.
(235) Zhang, Z. X.; Zhou, H. Y.; Yang, L.; Tachibana, K.; Kamijima, K.; Xud, J. *Electrochim. Acta* **2008**, *53*, 4833.
(236) Schneider, S.; Hawkins, T.; Rosander, M.; Mills, J.; Brand, A.; Hudgens, L.; Warmoth, G.; Vij, A. *Inorg. Chem.* **2008**, *47*, 3617.
(237) Schneider, S.; Hawkins, T.; Rosander, M.; Mills, J.; Vaghjiani, G.; Chambreau, S. *Inorg. Chem.* **2008**, *47*, 6082.
(238) Siriwardana, v.; Crossley, I. R.; J. Torriero, A. A.; Burgar, I. M.; Dunlop, N. F.; Bond, A. M.; Deacon, G. B.; MacFarlane, D. R. *J. Org. Chem.* **2008**, *73*, 4676.
(239) Zhao, C.; Burrell, G.; Torriero, A. A. J.; Separovic, F.; Dunlop, N. F.; MacFarlane, D. R.; Bond, A. M. *J. Phys. Chem. B* **2008**, *112*, 6923.
(240) Hulse, R.; Singh, R. *Int. J. Thermophys.* **2008**, *29*, 1939.
(241) Weigand, J. J.; Burford, N.; Decken, A. *Eur. J. Inorg. Chem.* **2008**, 4343.
(242) Deng, F.-G.; Hu, B.; Sun, W.; Xia, C.-G. *Dalton Trans.* **2008**, 5957.
(243) Mayrand-Provencher, L.; Lin, S.; Lazzerini, D.; Rochefort, D. *J. Power Sources* **2010**, *195*, 5114.
(244) Brauer, D. J.; Kottsieper, K. W.; Like, C.; Stelzer, O.; Waffenschmidt, H.; Wasserscheid, P. *J. Organomet. Chem.* **2001**, *630*, 177.
(245) Mahjoor, P.; Latturner, S. E. *Cryst. Growth Des.* **2009**, *9*, 1385.
(246) Astolfi, D. L.; Mayville, F. C., Jr. *Tetrahedron Lett.* **2003**, *44*, 9223.
(247) Bazito, F. F. C.; Kawano, Y.; Torresi, R. M. *Electrochim. Acta* **2007**, *52*, 6427.
(248) Newman, D. S.; Rohr, W.; Kirklin, D. *J. Electrochem. Soc.* **1972**, 797.
(249) Giernoth, R.; Bankmann, D. *Eur. J. Org. Chem.* **2005**, 4529.
(250) Arce, A.; Rodríguez, H.; Soto, A. *Chem. Eng. J.* **2006**, *115*, 219.
(251) *Carbon-13 NMR Spectroscopy*; Kalinowski, H-.O., Berger, S., Braun, S., Eds.; John Wiley & Sons: New York, 1988.
(252) *Carbon-13 NMR Chemical Shifts in Structural and Stereochemical Analysis*; Pihlaja, K., Kleinpeter, E., Eds.; John Wiley & Sons: New York, 1994.
(253) Moskau, D. *Concepts Magn. Reson. (Magn. Reson. Eng.)* **2002**, *15*, 164.

(254) Keller, C. E.; Carper, W. R.; Piersma, B. J. *Inorg. Chim. Acta* **1993**, *209*, 239.
(255) Johnson, C. S., Jr. *Prog. Nucl. Magn. Reson. Spectrosc.* **1999**, *34*, 203.
(256) Weingartner, H.; Holz, M. *Annu. Rep. Prog. Chem., Sect. C* **2002**, *98*, 121.
(257) Pregosin, P. S.; Kumar, P. G. A.; Fernández, I. *Chem. Rev.* **2005**, *105*, 2977.
(258) Pregosin, P. S. *Prog. Nucl. Magn. Reson. Spectrosc.* **2006**, *49*, 261.
(259) Macchioni, A.; Ciancaleoni, G.; Zuccaccia, C.; Zuccaccia, D. *Chem. Soc. Rev.* **2008**, *37*, 479.
(260) Cohen, Y.; Avram, L.; Frish, L. *Angew. Chem., Int. Ed.* **2005**, *44*, 520.
(261) Palmer, G.; Richter, J.; Zeidler, M. D. *Z. Naturforsch.* **2004**, *59a*, 59.
(262) Palmer, G.; Richter, J.; Zeidler, M. D. *Z. Naturforsch.* **2004**, *59a*, 51.
(263) Antony, J. H.; Dölle, A.; Mertens, D.; Wasserscheid, P.; Carper, W. R.; Wahlbeck, P. G. *J. Phys. Chem. A* **2005**, *109*, 6676.
(264) Carper, W. R.; Wahlbeck, P. G.; Dolle, A. *J. Phys. Chem. A* **2004**, *108*, 6096.
(265) Heimer, N. E.; Wilkes, J. S.; Wahlbeck, P. G.; Carper, W. R. *J. Phys. Chem. A* **2006**, *110*, 868.
(266) Neuhaus, D., Williamson, M. *The Nuclear Overhauser Effect in Structural and Conformational Analysis*; Wiley-VCH: Weinheim, Germany, 2000.
(267) Branda, T.; Cabritab, E. J.; Berger, S. *Prog. Nucl. Magn. Reson. Spectrosc.* **2005**, *46*, 159.
(268) Gerig, J. T. *Annu. Rep. NMR Spectrosc.* **2008**, *64*, 21.
(269) Friebolin, H. *Basic One- and Two-Dimensional NMR Spectroscopy*; Wiley-VCH: Weinheim, 2005.
(270) *Two Dimensional NMR-Spectroscopy: Applications for Chemists and Biochemists*; Croasmun, W. R., Carlson, R. M. K., Eds.; Wiley-VCH: New York, 1994.
(271) Martin, G. E., Zektzer, A. S. *Two-Dimensional NMR Methods for Establishing Molecular Connectivity*; Wiley-VCH: Weinheim, 1988.
(272) Desvaux, H.; Berthault, P.; Birlirakis, N.; Goldman, M.; Piotto, M. *J. Magn. Reson., A* **1995**, *113*, 47.
(273) Heimer, N. E.; Del Sesto, R. E.; Carper, W. R. *Magn. Reson. Chem.* **2004**, *42*, 71.
(274) Hardacre, C.; Holbrey, J. D.; McMath, J. S. E. *Chem. Commun.* **2001**, 367.
(275) Hardacre, C.; McMath, J. S. E.; Nieuwenhuyzen, M.; Bowron, D. T.; Soper, A. K. *J. Phys.: Condens. Matter* **2003**, *15*, S159.
(276) Fort, D. A.; Swatloski, R. P.; Moyna, P.; Rogers, R. D.; Moyna, G. *Chem. Commun.* **2006**, 714.
(277) Miner, V. W., Conover, W. W. Shimming of Superconducting Magnets. In *Encyclopedia of Nuclear Magnetic Resonance*; Grant, D. M., Harris, R. K., Eds.; John Wiley & Sons: Chichester, U.K., 1996; Vol. 7, pp 4340−4356.
(278) Chmurny, G. N.; Hoult, D. I. *Concepts Magn. Reson.* **1990**, *2*, 131.
(279) Sukumar, S.; Johnson, M. O.; Hurd, R. E.; Van Zijl, P. C. M. *J. Magn. Reson.* **1997**, *125*, 159.
(280) Hoye, T. R.; Eklov, B. M.; Ryba, T. D.; Voloshin, M.; Yao, L. J. *Org. Lett.* **2004**, *6*, 953.
(281) Ananikov, V. P.; Beletskaya, I. P. *Russ. Chem. Bull. Int. Ed.* **2008**, *57*, 754.
(282) Ueno, K.; Hata, K.; Katakabe, T.; Kondoh, M.; Watanabe, M. *J. Phys. Chem. B* **2008**, *112*, 9013.
(283) Rencurosi, A.; Lay, L.; Russo, G.; Prosperi, D.; Poletti, L.; Caneva, E. *Green Chem.* **2007**, *9*, 216; see also the electronic supporting information.
(284) Yamaguchi, K.; Yoshida, C.; Uchida, S.; Mizuno, N. *J. Am. Chem. Soc.* **2005**, *127*, 530.
(285) Valkenberg, M. H.; deCastro, C.; Hölderich, W. F. *Green Chem.* **2002**, *4*, 88.
(286) Harris, R. K.; Becker, E. D.; de Menezes, S. M. C.; Goodfellow, R.; Granger, P. *Pure Appl. Chem.* **2001**, *73*, 1795.
(287) Bagno, A.; Rastrelli, F.; Saielli, G. *Prog. Nucl. Magn. Reson. Spectrosc.* **2005**, *47*, 41.
(288) Momoki, K.; Fukuzawa, Y. *Anal. Sci.* **1994**, *10*, 53.
(289) Momoki, K.; Fukuzawa, Y. *Anal. Chem.* **1990**, *62*, 1665.
(290) Mizuno, K.; Kimura, Y.; Morichika, H.; Nishimura, Y.; Shimada, S.; Maeda, S.; Imafuji, S.; Ochi, T. *J. Mol. Liq.* **2000**, *85*, 139.
(291) Friedman, R. A.; Malawer, E. G.; Wong, Y. W.; Sundheim, B. R. *J. Am. Chem. Soc.* **1980**, *102*, 925.
(292) Although the statement "neat IL sample" is often cited in the literature, it should be applied for pure IL samples only. If some reagents, reactants, products, gases, salts, etc. are dissolved in the IL, the statement "native IL system" should be preferably used. Similarly, the study "under native NMR conditions" is a preferred notation for multicomponent IL systems.
(293) It should be noted that conventional NMR measurements in organic solvents are also feasible if the content of the phases is the only question of interest (see section 2.5).

CR9000644